Vol. 67 • No. 4

April 2024

Microwave Journal

horizon house

Founded in 1958

mwjournal.com

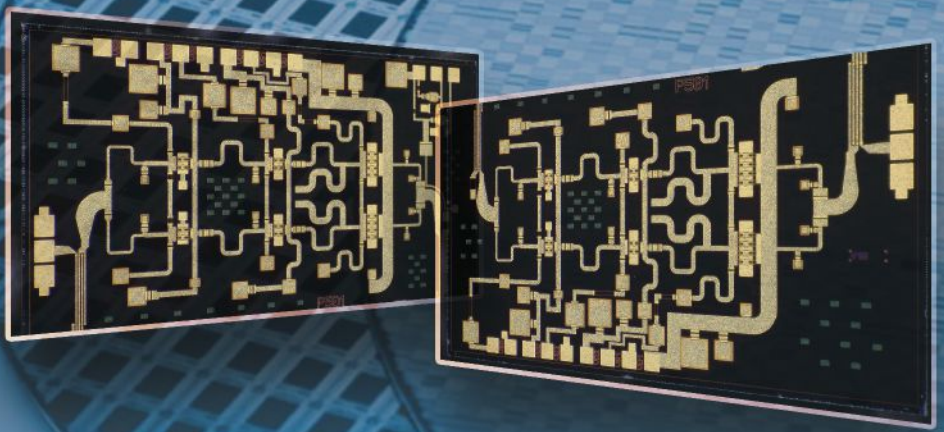

Miller MMIC is a global provider of RF semiconductor solutions with expertise in GaAs and GaN processes. We offer a diverse range of products tailored to various wireless applications. Our product lineup encompasses a wide array of offerings, including Low Noise Amplifiers, Distributed Amplifiers, Power Amplifiers, Driver Amplifiers, RF Switches, RF PIN Diode Switches, and numerous other voltage- and digitally-controllable RF components.

RF Distributed Low Noise Amplifiers

PN	Freq Low (GHz)	Freq High (GHz)	Gain (dB)	NF(dB)	P1dB (dBm)	Voltage (VDC)	Current (mA)	Package
MMW001T	DC	20.0	17~19	1~3.5	23 @ 10GHz	8.0	145	die
MMW4FP	DC	50.00	16.00	4.00	24.00	10	200	die
MMW507	0.20	22.0	14.0	4 - 6	28.0	10.0	350	die
MMW508	DC	30.0	14.0	2.5dB @ 15GHz	24.5	10.0	200	die
MMW509	30KHz	45.0	15.0		20.0	6.0	190	die
MMW510	DC	45.0	11.0	4.5	15.5	6.0	100	die
MMW510F	DC	30.00	20.00	2.50	22.00			die
MMW511	0.04	65.0	10.0	9.0	18.0	8.0	250	die
MMW512	DC	65.0	10.0	5.0	14.5	4.5	85	die
MMW5FN	DC	67.00	14.00	2.00	19.00	4.5	81	die
MMW5FP	DC	67.00	14.00	4.00	21.00	8	140	die
MMW011	DC	12.0	14.0		30.5	12.0	350	die

Low Noise Amplifiers

PN	Freq Low (GHz)	Freq High (GHz)	Gain (dB)	NF(dB)	P1dB (dBm)	Voltage (VDC)	Current (mA)	Package
MML040	6.0	18.0	24.0	1.5	14.0	5.0	35	die
MML058	1.0	18.0	15.0	1.7	17.0	5.0	35	die
MML063	18.0	40.0	11.0	2.9	15.0	5.0	52	die
MML080	0.8	18.0	16.5/15.5	1.9/1.7	18/17.5	5.0	65/40	die
MML081	2.0	18.0	25/23	1.0/1.0	16/9.5	5.0	37/24	die
MML083	0.1	20.0	23.0	1.6	11.0	5.0	58	die

RF Driver Amplifier

PN	Freq Low (GHz)	Freq High (GHz)	Gain (dB)	NF(dB)	P1dB (dBm)	Voltage (VDC)	Current (mA)	Package
MM3006	2.0	20.0	19.5	2.5	22.0	7.0	130	die
MM3014	6.0	20.0	15.0	-	19.5	5.0	107	die
MM3017T	17.0	43.0	25.0		22.0	5.0	140	die
MM3031T	20.0	43.0	20.0		24.0	5.0	480	die
MM3051	17.0	24.0	25.0	-	25.0	5.0	220	die
MM3058	18.0	40.0	20/19.5	2.5/2.3	16/14	5/4	69/52	die
MM3059	18.0	40.0	16/16	2.5/2.3	16/15	5/4	67/50	die

GaAs Medium Power Amplifier

PN	Freq Low (GHz)	Freq High (GHz)	Gain (dB)	P1dB (dBm)	Psat (dBm)	Voltage (VDC)	Current (mA)	Package
MMP107	17.0	21.0	19.0	30.0	30.0	6.0	400	die
MMP108	18.0	28.0	14.0	31.5	31.0	6.0	650	die
MMP111	26.0	34.0	25.5	33.5	33.5	6.0	1300	die
MMP112	2.0	6.0	20.0	31.5	32.0	8.0	365	die
MMP501	20.0	44.0	15.0	27 -- 32	29 - 34	5.0	1200	die
MMP502	18.0	47.0	14.0	28.0	30.0	5.0	1500	die

PN: MMW5FP

RF GaAs MMIC DC-67GHz

P1dB vs. Frequency

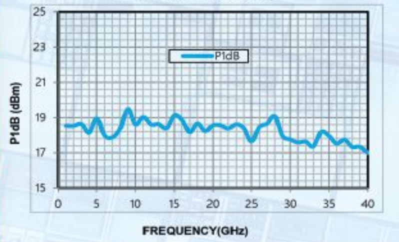

Gain vs. Frequency

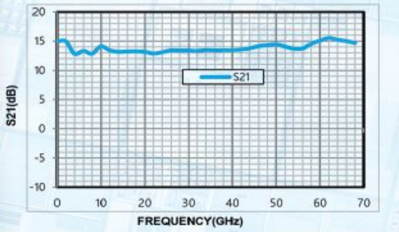

NF vs. Frequency

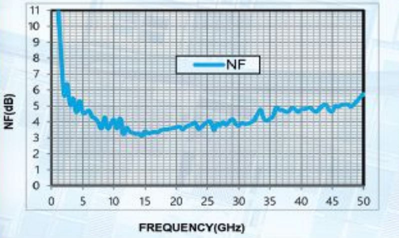

Psat vs. Frequency

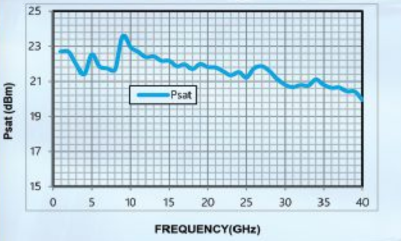

CALL US 1-833-2MILLER(264-5537)
WWW.MILLERMMIC.COM

sales@millermmic.com
support@millermmic.com

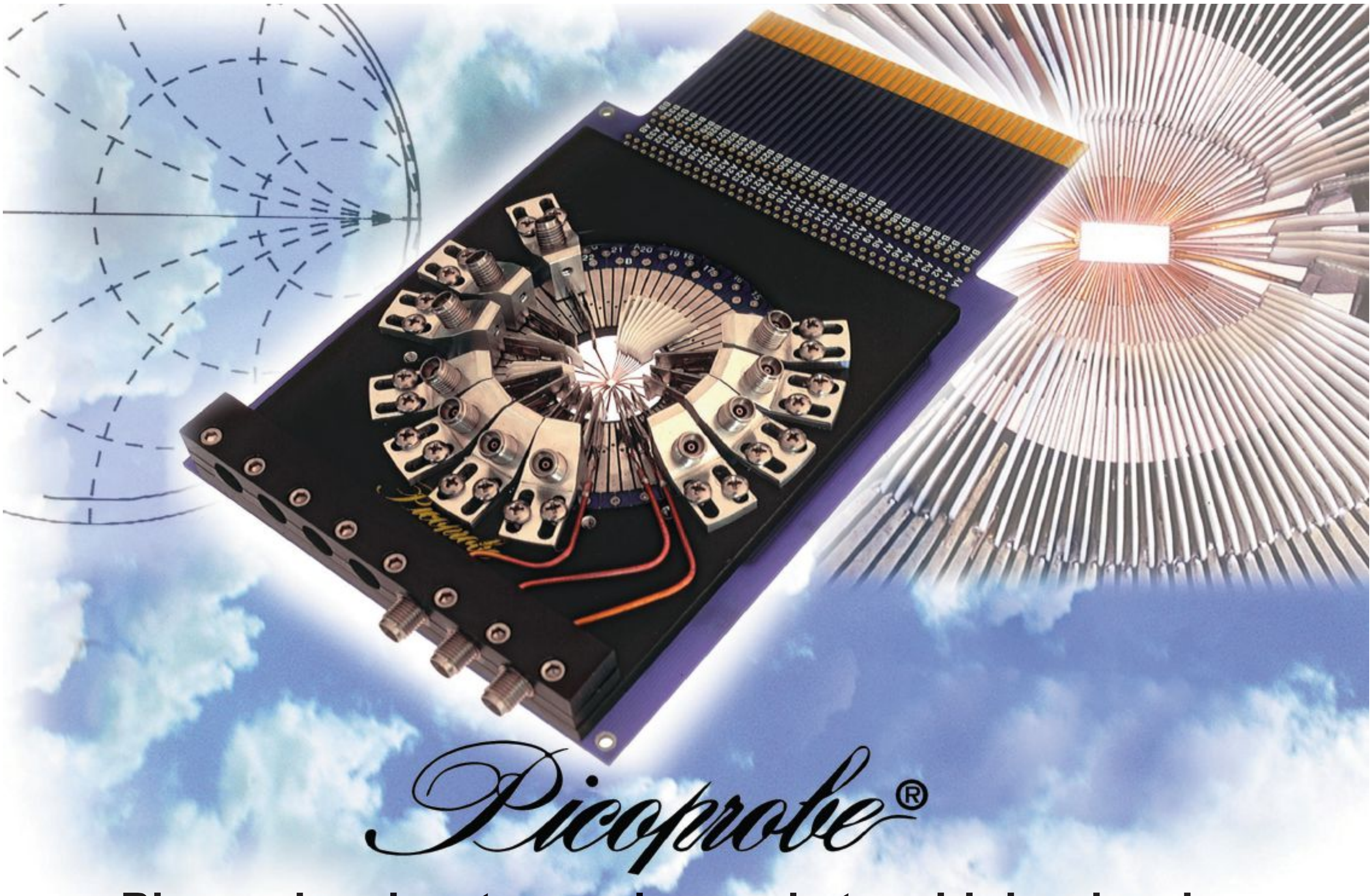

Picoprobe elevates probe cards to a higher level…

(…110 GHz to be exact.)

Since 1981, GGB Industries, Inc., has blazed the on-chip measurement trail with innovative designs, quality craftsmanship, and highly reliable products. Our line of custom microwave probe cards continues our tradition of manufacturing exceptional testing instruments.

Through unique modular design techniques, hundreds of low frequency probe needles and a variety of microwave probes with operating frequencies from DC to 40, 67, or even 110 GHz can be custom configured to your layout.

Our patented probe structures provide the precision and ruggedness you require for both production and characterization testing. And only Picoprobe® offers the lowest loss, best match, low inductance power supplies, and current sources on a single probe card.

Our proven probe card design technology allows full visibility with inking capability and ensures reliable contacts, even when probing non-planar structures.

Not only do you get all the attractive features mentioned, but you get personal, professional service, rapid response, and continuous product support--all at an affordable price so your project can be completed on time and within budget.

Typical Specs	10GHz	20GHz	40GHz
Insertion Loss	0.6 dB	0.8 dB	1.3 dB
Return Loss	22 dB	18 dB	15 dB

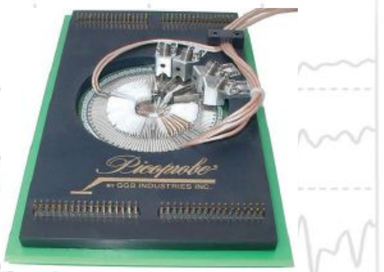

For technical assistance, custom product designs, or off-the-shelf delivery,call GGB Industries, Inc., at (239) 643-4400.

GGB INDUSTRIES, INC. • P.O. BOX 10958 • NAPLES, FL 34101

Telephone (239) 643-4400 • Fax (239) 643-4403 • E-mail email@ggb.com • www.picoprobe.com

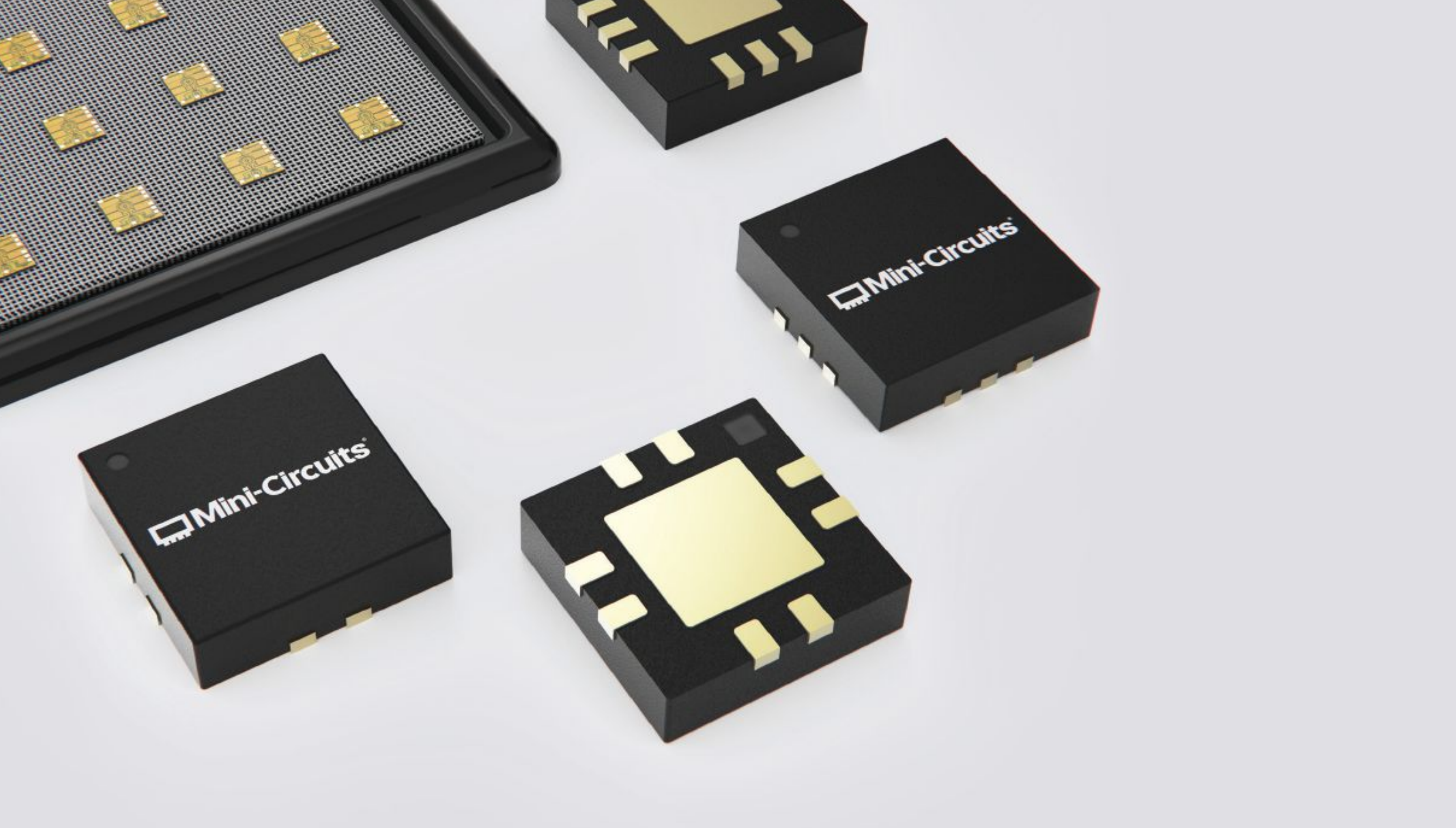

DC TO 50 GHz

MMIC Amplifiers

300+ Models Designed in House

- Wide selection of GaAs HBT and E-pHEMT designs
- Noise figure as low as 0.38 dB
- OIP3 up to +50 dBm
- Industry-leading phase noise performance
- In-house packaging assembly
- Surface mount and bare die formats
- Upscreening available

LEARN MORE

Options for Every Requirement

CATV (75Ω)

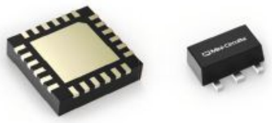

Supporting DOCSIS® 3.1
and 4.0 requirements

Dual Matched

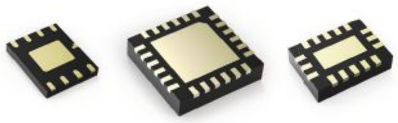

Save space in balanced and
push-pull configurations

Hi-Rel

Rugged ceramic package
meets MIL requirements for
harsh operating conditions

High Linearity

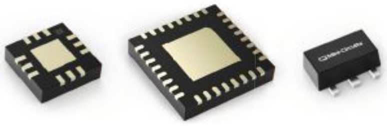

High dynamic range over wide
bandwidths up to 45 GHz

Low Noise

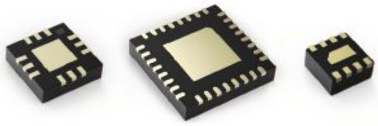

NF as low as 0.38 dB for
sensitive receiver applications

Low Additive Phase Noise

As low as -173 dBc/Hz
@ 10 kHz offset

RF Transistors

<1 dB NF with footprints as
small as 1.18 x 1.42mm

Variable Gain

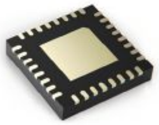

Up to 31.5 dB digital
gain control

Wideband Gain Blocks

Flat gain for broadband
and multi-band use

Mini-Circuits®


Signal & Spectrum Analyzer · 10 Hz – 30 GHz

Microwave Journal
CONTENTS

April 2024
Vol. 67 • No. 4
Amplifiers and Oscillators
mwjournal.com

Cover Feature

Technical Features

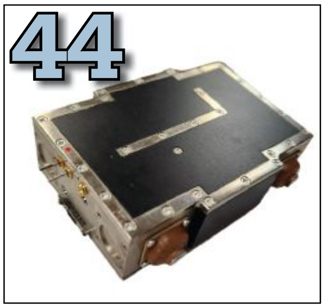

online spotlight

Look for this month's exclusive article online at mwjournal.com

Application Notes

67 YEARS OF PUBLISHING EXCELLENCE

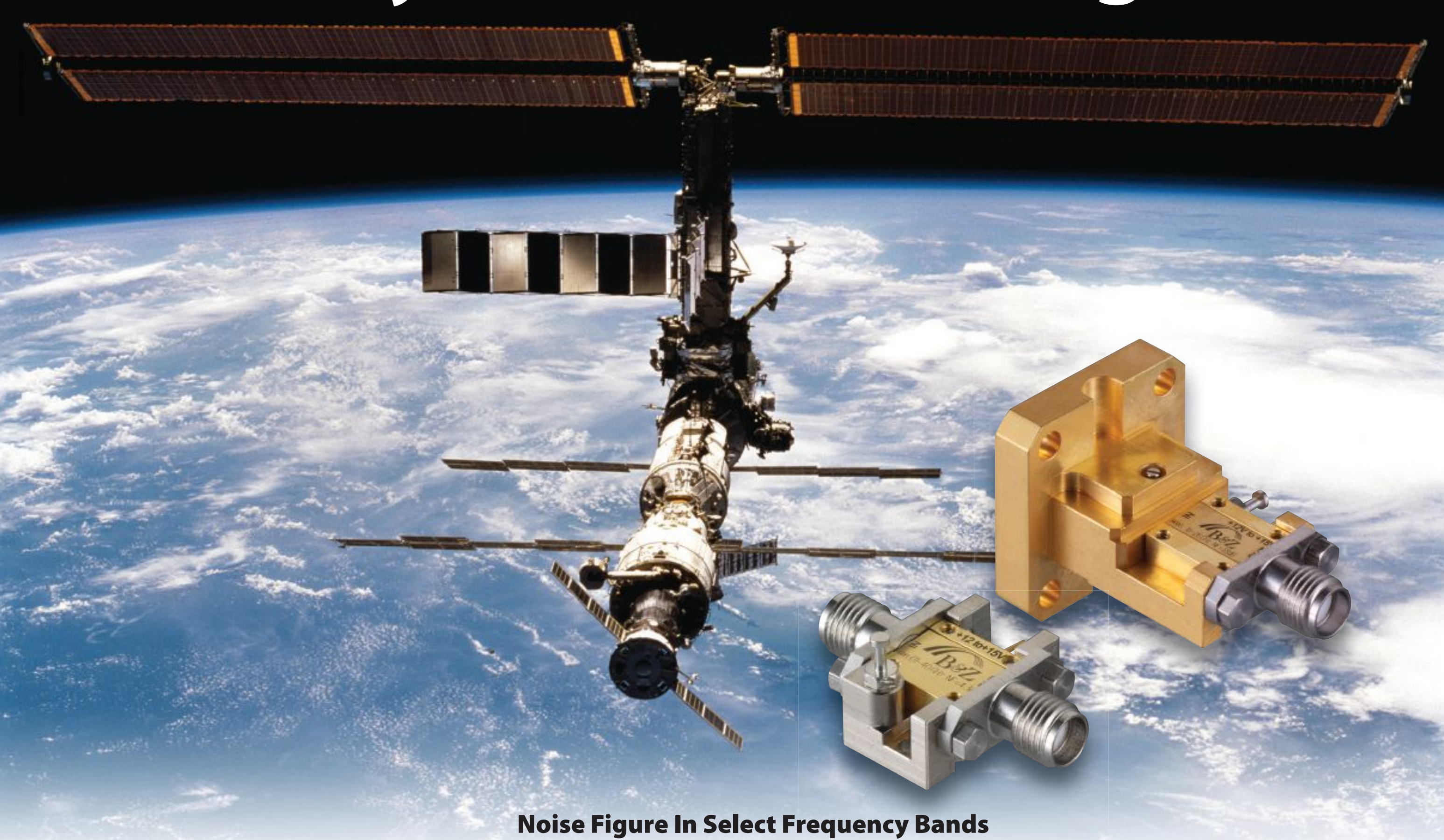

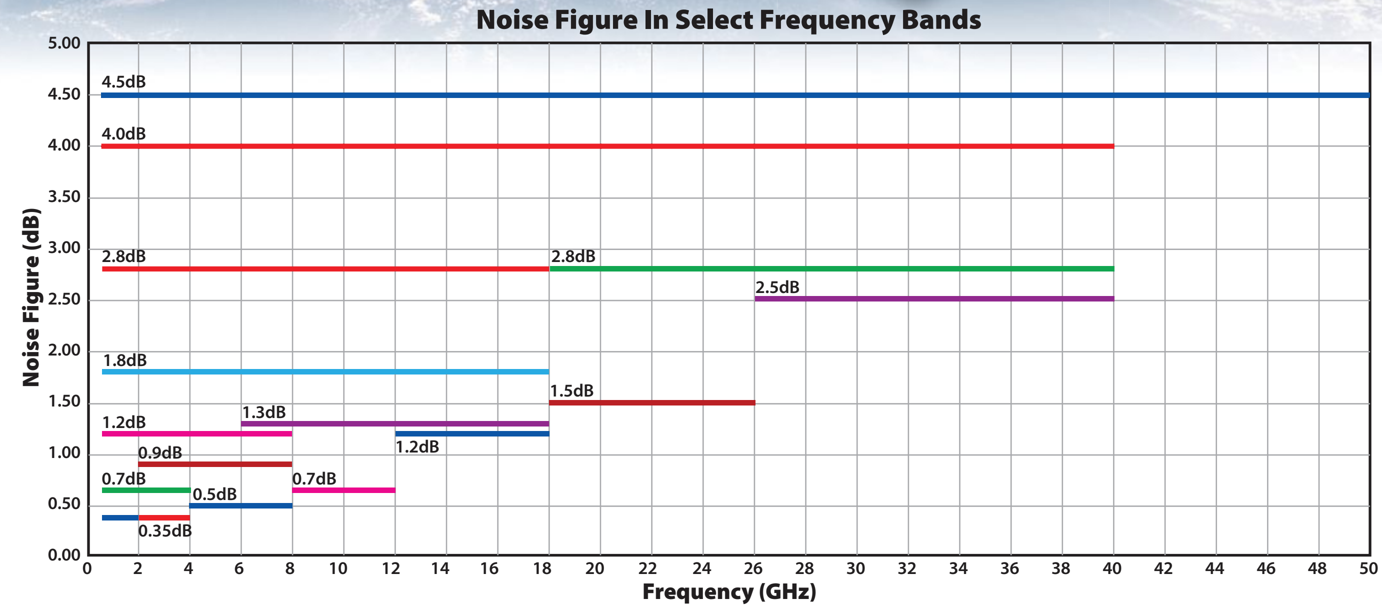
Noise Figure In Select Frequency Bands
Noise Figure (dB)
5.00
4.50
4.00
3.50
3.00
2.50
2.00
1.50
1.00
0.50
0.00
4.5dB
4.0dB
2.8dB
2.8dB
2.5dB
1.8dB
1.5dB
1.3dB
1.2dB
1.2dB
0.9dB
0.7dB
0.7dB
0.5dB
0.35dB
0 2 4 6 8 10 12 14 16 18 20 22 24 26 28 30 32 34 36 38 40 42 44 46 48 50
Frequency (GHz)

Microwave Journal CONTENTS

mwjournal.com

Product Feature

Tech Briefs

Departments

Microwave Journal (USPS 396-250) (ISSN 0192-6225) is published monthly by Horizon House Publications Inc., 685 Canton St., Norwood, MA 02062. Periodicals postage paid at Norwood, MA 02062 and additional mailing offices.

POSTMASTER: Send address corrections to Microwave Journal, PO Box 1028, Lowell, MA 01853 or e-mail mwj@e-circ.net.com. Subscription information: (978) 671-0446. This journal is issued without charge upon written request to qualified persons working in the RF & microwave industry. Other subscriptions are: domestic, $130.00 per year, two-year subscriptions, $200.00; foreign, $225.00 per year, two-year subscriptions, $400.00; back issues (if available) and single copies, $20.00 domestic and $30.00 foreign. Claims for missing issues must be filed within 90 days of date of issue for complimentary replacement.

Posted under Canadian international publications mail agreement #PM40612608

STAFF

Group Director: Carl Sheffres
Associate Publisher: Michael Hallman
Media Director: Patrick Hindle
Brand & Content Director: Jennifer DiMarco
Technical Editor: Eric Higham
Associate Technical Editor: Cliff Drubin
Editorial & Media Specialist: Kelley Roche
Associate Editor: Kaitlyn Joyner
Multimedia Staff Editor: Barbara Walsh
Electronic Marketing Manager: Chris Stanfa
Senior Digital Content Specialist: Lauren Tully
Digital Content Specialist: Vincent Carrabino
Director of Production & Distribution:
Edward Kiessling
Art Director: Janice Levenson
Graphic Designer: Ann Pierce

EUROPE

Office Manager: Nina Plesu

CORPORATE STAFF

CEO: William M. Bazzy
President: Ivar Bazzy
Vice President: Jared Bazzy

EDITORIAL REVIEW BOARD

EXECUTIVE EDITORIAL OFFICE

685 Canton Street, Norwood, MA 02062
Tel: (781) 769-9750
FAX: (781) 769-5037
e-mail: mwj@mwjournal.com

EUROPEAN EDITORIAL OFFICE

16 Sussex Street, London SW1V 4RW, England
Tel: Editorial: +44 207 596 8730 Sales: +44 207 596 8740
FAX: +44 207 596 8749

SUBSCRIPTION SERVICES

Send subscription inquiries and address changes to:
Tel: (978) 671-0446
e-mail: mwj@e-circ.net

www.mwjournal.com

Printed in the USA

PRECISION DEVICES knowles

DIELECTRIC LABORATORIES

SWAP-C Optimized Parts for RADAR SYSTEMS

Radar systems are growing into multi-function, multi-mission systems that need to be contained in the smallest possible footprint.

Knowles Precision Devices' DLI Brand of RF and Capacitor components are designed to address your SWAP-C challenges by leveraging our decades of Aerospace and Defense expertise in:

Vertical Integration | Materials Science | High Performance

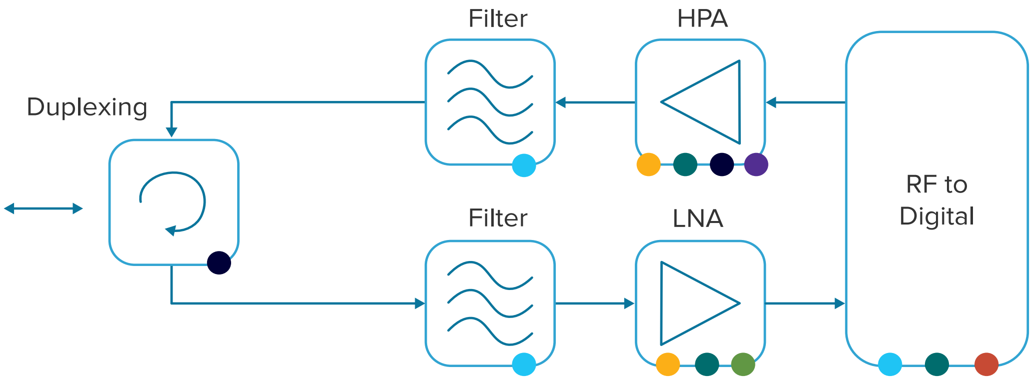

Knowles RF Components Support All Major Functions:

- ● Filter
- ● Low Noise Oscillators
- ● Bypass & Coupling Capacitors
- ● Bias Networks
- ● Hybrid Couplers
- ● Storage Capacitors
- ● Gain Equalizers

RF and Capacitor components have always played a key role in the success of radar systems as they have evolved over the years. At Knowles Precision Devices, we work closely with you to identify the filter solution you need to meet the challenges you face today.

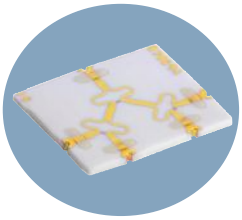

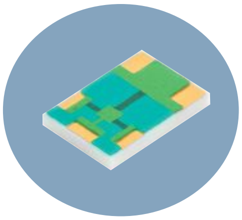

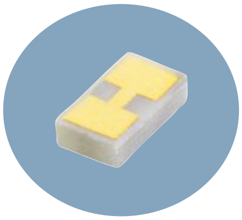

RFMW®

>> Learn more: rfmw.com/dielectric

Contact us today to explore a range of catalog and custom design options: **sales@rfmw.com**

Microwave Journal ONLINE .COM

LEARNING CENTER

BAW Filter Mastery for All: Exploring XBAW and New XP3F Technology, Leveraging Foundry Services from 2 to 20 GHz
Sponsored by: RFMW, Akoustis 5/1

Catch *Frequency Matters*, the industry update from *Microwave Journal*,
microwavejournal.com/FrequencyMatters

WHITE PAPERS

Lifecom	Unlocking Connectivity Frontiers - Exploring IoT-NTN Innovations
AMCAD Engineering Advanced Modeling for Computer-Aided Design	Power Amplifier Behavioral Modeling for System Level Simulation
COPPER MOUNTAIN TECHNOLOGIES	VNA Time Domain Processing
Mini-Circuits	Measurement of Amplifier Additive Phase Modulation Noise (APM)
ROHDE&SCHWARZ Make ideas real	Fundamentals of Radome and Bumper Material Measurements

Look for additional content from:

Coilcraft

Executive Interviews

Thomas Chen, Founder and CEO of **Swiftlink Technologies**, talks about the company, its product portfolio and differentiators along with Swiftlink Technologies' view of emerging opportunities and applications.

Chris Armstrong, Marketing Director – **North America of Siglent**, talks about the company's heritage, its product portfolio and differentiators along with future directions, emerging opportunities and applications.

Join Us Online

Follow us
@Pathindle
@MWJEric
@MWJEditor

Join us at the RF and Microwave Community

Become a fan at facebook.com/microwavejournal

Visit us @ mwjournal.com

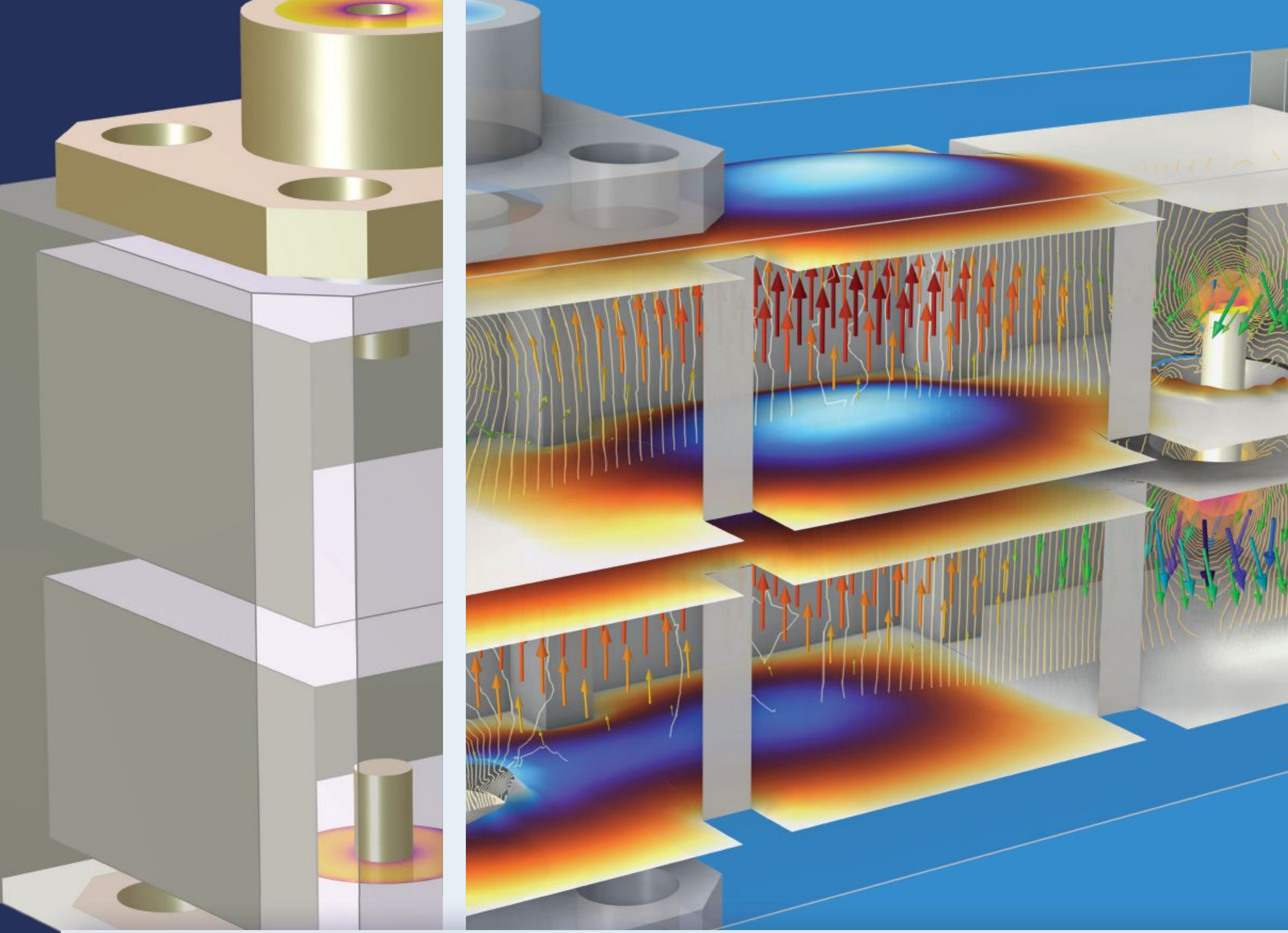

ISM RF & MW ENERGY

2.4 GHz Building Blocks

Flexible, Scalable Capabilities up to 6 kW

LEARN MORE

Signal Generator/Controller

ISC-2425-25+

Key Features:

- 30 to +25 dBm (0.1 dB steps)
- Frequency from 2.4 to 2.5 GHz (1 kHz steps)
- Closed loop and feed forward RF power control modes
- User-friendly GUI and full API

300W SSPA

ZHL-2425-250X+

Key Features:

- 300W output power
- Supports CW & pulsed signals
- 42 dB gain
- 60% efficiency
- Built-in monitoring and protection

4-Way Splitter with Phase & Amplitude Control

SPL-2G42G50W4+

Key Features:

- 2.4 to 2.5 GHz
- Drive up to 4 amplifier stages from 1 ISC-2425-25+ controller
- Precise control of amplitude and phase on each path

Coming soon

High Power 4-Way Combiner

COM-2G42G51K0+

Key Features:

- 1.2 kW power handling (sum port)
- 0.1 dB insertion loss
- 0.15 dB amplitude unbalance
- 1° phase unbalance
- 4x N-Type to 7/16 DIN

Mini-Circuits®

MARK YOUR CALENDAR

STAY CONNECTED TO COMING EVENTS

APRIL

15-16
WAMICON 2024
Clearwater Beach, Fla.
www.ieeewamicon.org

29-30
ARMMS
Thame, U.K.
www.armms.org

MAY

13-15
Space Tech Expo USA
Long Beach, Calif.
www.spacetechexpo.com

20-23
CS Mantech
Tucson, Ariz.
https://csmantech.org

JUNE


The community meeting place dedicated to Military Space.

3-4
Future Military Space Technology USA
Los Angeles, Calif.
www.smgconferences.com/defence/northamerica/milspace-usa


MILSATCOM USA 2024
Driving SATCOM innovation to Ensure Wartime Advantage

10-12
MIlSATCOM USA
Arlington, Va.
www.smgconferences.com/defence/northamerica/MilSatCom-USA

16-18
RFIC 2024
Washington, DC
https://rfic-ieee.org/

16-21
IMS2024
Washington, DC
https://ims-ieee.org

21
ARFTG-103
Washington, DC
https://arftg.org/103-conference/

24-26
Sensors Converge
Santa Clara, Calif.
www.sensorsconverge.com

JULY

9-11
IEEE COMCAS
Tel Aviv, Israel
www.comcas.org

AUGUST

5-9
IEEE EMC + SIPI
Phoenix, Ariz.
https://emc2024.org

ONLINE PANEL SERIES

6/25
New Innovations in Power Amplifiers

Call for Papers Deadlines

5/13	IEEE Phased Array
7/7	IEEE HPEC
7/7	APMC

FOR DETAILS VISIT MWJOURNAL.COM/EVENTS

COVER FEATURE
INVITED PAPER

Oscillators Enable Conversion at X-Band

Jason Breitbarth
Saetta Labs, Boulder, Colo.

Direct microwave conversion utilizing extremely high speed analog-to-digital converters (ADCs) and digital-to-analog converters (DACs), enable systems with increased bandwidth, more capabilities and better performance. X-Band DACs can drive radar arrays directly or through single-stage up-conversion, which adds near real-time beam steering and nulling capabilities. ADCs can sample microwave signals directly, improving bandwidth and real-time analysis. ADCs and DACs only exhibit phase noise contributions from the noise floor and 1/f noise. However, if maximum system performance is required, this places quite a burden on the phase noise requirements of the oscillator.

This article provides a summary of the oscillator types available for local oscillator (LO) generation, or clocking, at X-Band frequencies and above, along with the best applications for each type of oscillator. These technologies can also be combined in a multi-oscillator approach to achieve both short-term and long-term stability requirements. A phase-locked loop (PLL) is required in these system architectures but an in-depth analysis of PLLs is outside the scope of this article. A good overview of what to consider when selecting phase-locked oscillators is in the reference section.[1] The phase noise plots presented in the article come from multiple sources and vendors. They are meant to provide a qualitative comparison of high performance representative devices.

Figure 1 is a plot of the residual phase noise of a 10.24 GSPS high speed DAC with an output at 1 GHz. This phase noise profile is compared with a high-quality 100 MHz oven controlled crystal oscillator (OCXO) that is ideally multiplied to 1 GHz and a sapphire-loaded cavity oscillator (SLCO) from Saetta Labs that is ideally divided from 8 GHz to the 1 GHz output. This result is normalized to show the performance of the DAC if it were ideal. The total noise will be the RSS of the oscillator and DAC. The curves show that this new generation of DACs has exceptionally low phase noise, but a careful choice of LO generation is critical to achieve the desired performance.

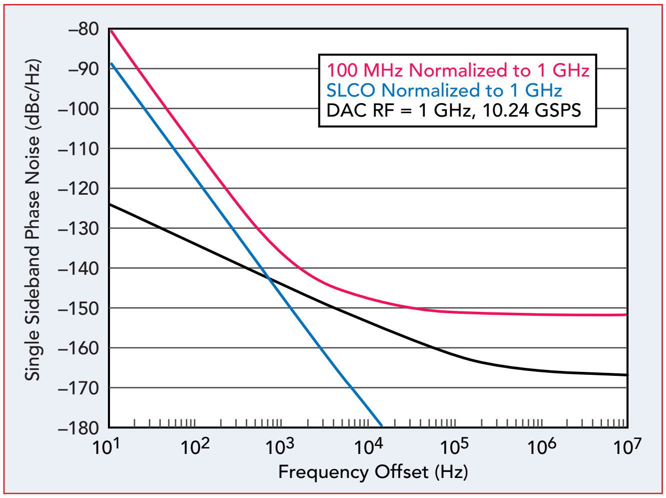

Fig. 1 Single-sideband phase noise versus frequency.

DATA COMMUNICATION SYSTEMS AND RADAR

High data rate communications systems and radar applications have significantly different phase noise requirements. Two important requirements for communications systems are long-term stability for signal acquisition and tracking, along with good phase noise performance at frequency offsets from the carrier where most of the data information is contained. Offsets in the frequency range from 20 kHz to

> 50 MHz may be of the most interest to optimize.

By contrast, radar has more stringent phase noise requirements for the low- to mid-frequency offsets. Tracking radars measure the Doppler shift of an incoming target in addition to time-of-flight ranging. Airborne targets may be traveling at rates from subsonic to hypersonic speeds. Using an 8 GHz X-Band radar as an example, a target traveling at 5x the speed of sound, or approximately 1700 m/s at sea level, has a received Doppler shift of about 95 kHz offset. A target moving at half the speed of sound has an offset of about 10 kHz and a slow-moving target or lower frequency radar, would want to be optimized for phase noise at less than 10 kHz offset.

STABILITY AND PHASE NOISE

The usefulness of an oscillator links strongly to a single performance attribute: stability. Stability is broadly categorized into short-term and long-term stability metrics. Long-term stability is described in terms of drift, measured in parts per million or parts per billion and it may also be characterized by a metric known as Allan deviation. Short-term stability is phase noise. The crossover point between categorizing stability as long-term or short-term is typically around one second. The difference between short-term and long-term stability is analogous to the differentiation between precision and accuracy.

Long-term stability is accuracy. If the frequency of an oscillator is measured every second over an hour, a day, a week or a month, the repeatability and accuracy of the frequency is typically quantified as Allan deviation. This is a measurement of stability in parts per million (ppm) or parts per billion (ppb). In most systems, this is dominated by a quartz crystal oscillator with a typical reference frequency of 10 MHz. This 10 MHz frequency may be locked to a very accurate source. This is typically accomplished with a frequency-locked loop that locks directly to an atomic clock reference or to GPS, which indirectly locks to an atomic clock.

Short-term stability is precision. It is a measure of the oscillator phase repeatability over a short period. This is measured as phase noise. Phase noise theory is another subject that cannot be addressed comprehensively in this article. Simply put, phase noise is a power spectral density at a frequency offset from the carrier relative to the carrier power. It can also be viewed as the probability of phase fluctuations from ideal.

The preceding discussion has been theoretical, but there are practical implications. A microwave LO designed to drive a DAC or an ADC must strike a balance. It is typically a combination of a high frequency oscillator with good phase noise or short-term stability phase-locked to an oscillator with good long-term stability or drift.

OSCILLATOR FUNDAMENTALS

To a first order, an oscillator fundamentally has only two components that contribute to and affect phase noise and short-term stability. These components are the amplifier and the resonator. Control tuning circuitry and thermal performance are also contributing factors, but they are second-order. Thermal performance is a significant issue for a long-term reference. Leeson's equation, shown in Equation 1, is a relatively simple equation that describes the phase noise of an oscillator based on amplifier and resonator parameters. There is an excellent summary of some of the work in this area in the reference section.[2]

$$L(f_m)=10\log\left[\overset{\substack{\text{SSB}\\ \downarrow}}{\frac{1}{2}}\left(\left(\underset{\substack{\uparrow\\ \text{20 dB/dec}\\ \text{Resonator}\\ f_m<1/2\text{ bw of Resonator}}}{\frac{f_0}{2Q_l f_m}}\right)^2+1\right)\left(\overset{\substack{\text{10 dB/dec}\\ \text{Amplifier Flicker Noise}\\ \downarrow}}{\frac{f_c}{f_m}}+1\right)\left(\underset{\substack{\uparrow\\ -177\text{ dBm-}P_s\text{+NF}\\ \text{White Noise}\\ \text{of Amplifier}}}{\frac{FkT}{P_s}}\right)\right] \qquad (1)$$

Where:[3]
f_0 is the output frequency
Q_l is the loaded quality factor
f_m is the offset from the output frequency (Hz)
f_c is the 1/f corner frequency
F is the noise factor of the amplifier
k is Boltzmann's constant in joules/kelvin
T is the absolute temperature in kelvin
P_s is the available power at the sustaining amplifier input.

Figure 2 shows a generic oscillator block diagram. The phase shifter satisfies the oscillator stability criteria of a positive feedback loop at 360 degrees. The oscillator operates in a compressed amplifier state when the open loop gain is assumed to be greater than one. From Leeson's equation, the phase noise is dominated by the Q-factor of the resonator.

Leeson's equation can be separated into independent contributions from the amplifier and the resonator, as shown in Equation 1. The two last terms, as indicated in Equation 1 apply to the amplifier. The term, FkT/P_s defines the signal-to-noise ratio of the amplifier and the noise floor. This quantity can be measured independently and under oscillation with a typical value of around 3 dB in compression.[4,5] The first term of the amplifier portion of Lesson's equation is the 1/f noise. Different technologies have different 1/f corner values, but most X-Band oscillators will use a SiGe, GaAs or InGaP HBT process with 1/f corner frequencies between 10 kHz and 100 kHz. The loop is multiplicative, so all the amplifier noise is multiplied in positive feedback with the resonator. The noise floor of an amplifier can be estimated by taking the single-sideband PM noise

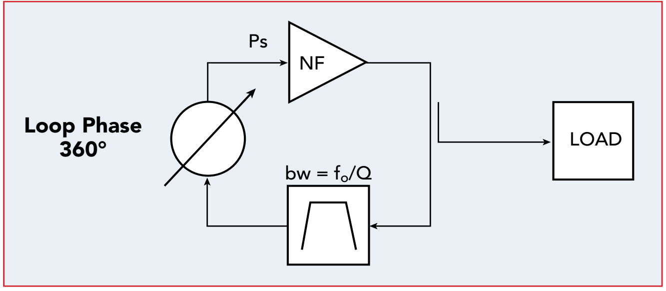

Fig. 2 **Oscillator block diagram.**

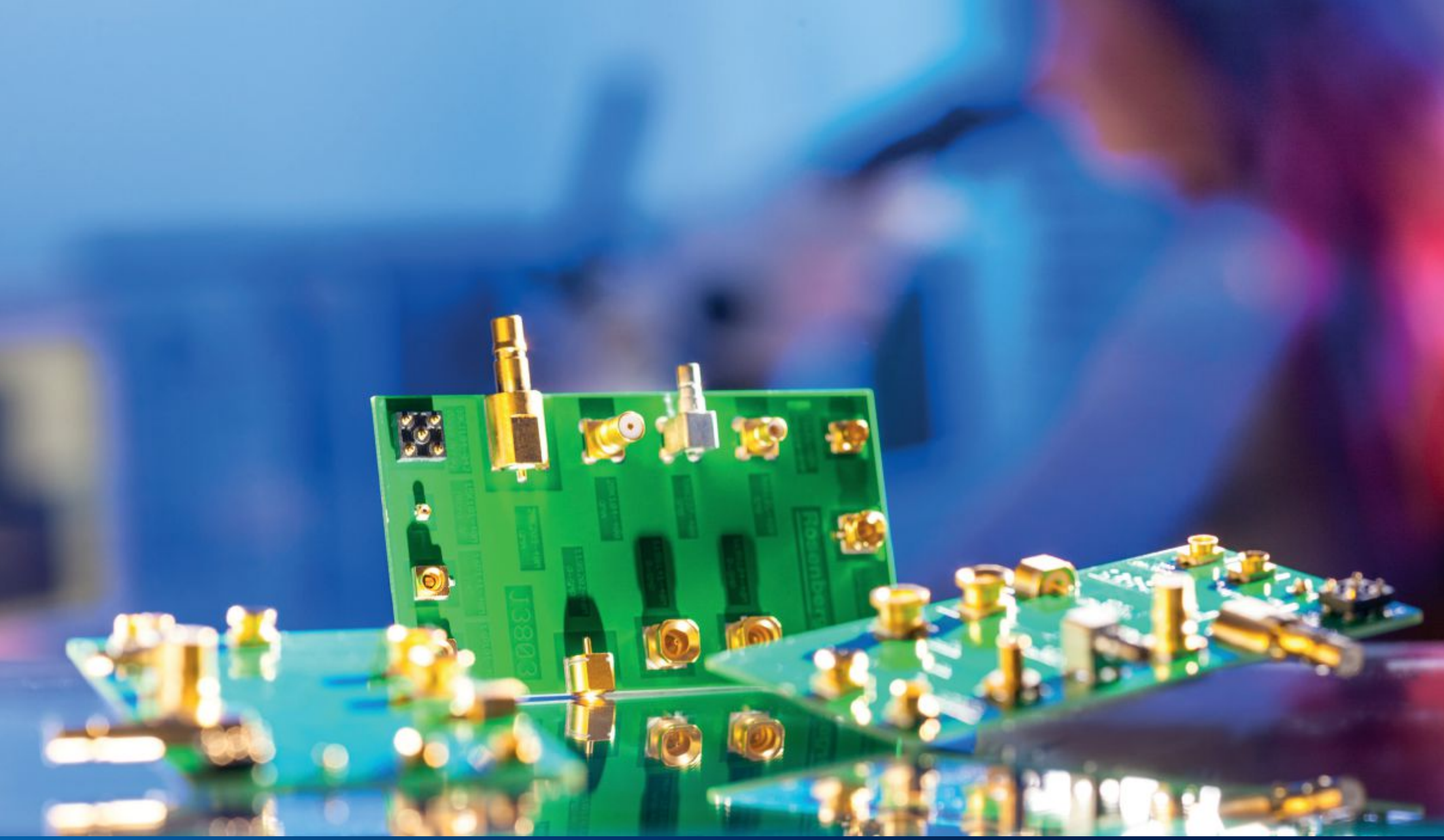

SURFACE MOUNT TECHNOLOGY

PCB Connectors

Rosenberger provides a wide range of RF coaxial connectors for PCB applications – for board-to-board- and also for cable-to-board connections.

Whether well-established standard connector series or newly developed innovative connectors – Rosenberger PCB connectors feature a lot of customer benefits:

- Minimum board-to-board distances
- Radial and axial misalignment using bullets
- Space-saving and cost-effective assembly design
- Excellent transmission quality
- Variety of back end types, e.g. SMT, edge mount, pin-in-paste, solder pin, solderless connectors as well as bullets

www.rosenberger.com

Rosenberger

floor due to thermal noise, which is -177 dBm, then subtracting the input power and adding the NF.

As an example, a medium power amplifier with 14 dB of gain, 16 dBm of output power and an NF of 5 dB results in a P_s, the input power to the amplifier in a compressed state of about 5 dBm, assuming 3 dB compression. In practice, the NF typically increases by a few dB under compression, so the assumption is that the NF increases to 8 dB. Plugging in these values (-177-5+8) yields a -174 dBc/Hz noise floor, which is the thermal noise floor in a 50 Ω system. This means that each oscillator is bound by the same amplifier condition theory and the noise floor will be similar among all oscillators.

The first term in Leeson's equation, shown in Equation 1, relates to the resonator. Resonators have a particular loaded Q-factor that depends on the technology choice and integration. The equation can be rewritten to show the $f_0/2Q_l$ term is the half bandwidth frequency of the resonator and the resonator does not affect the noise at offsets greater than this frequency. At higher offsets, the only noise contribution comes from the amplifier. At frequencies below this half bandwidth frequency, the term follows a second-order system and it can be shown as a Bode diagram increasing at 20 dB per decade.

Phase noise is a single-sideband measurement, so half the power is taken. ***Figure 3*** is Leeson's equation as a phase noise plot with the values of a typical dielectric resonator oscillator (DRO). The properties of each component of Leeson's equation are shown graphically. The amplifier is plotted separately on the bottom and then summed on a log scale with the resonator for the total phase noise. The phase noise plot identifies the 20 dB per decade phase noise characteristic of the resonator, along with the 30 dB per decade sections that result when the 1/f and resonator phase noise profiles overlap due to the multiplicative effect of the positive feedback loop. From this chart, Q, noise floor and 1/f can be estimated for any oscillator.

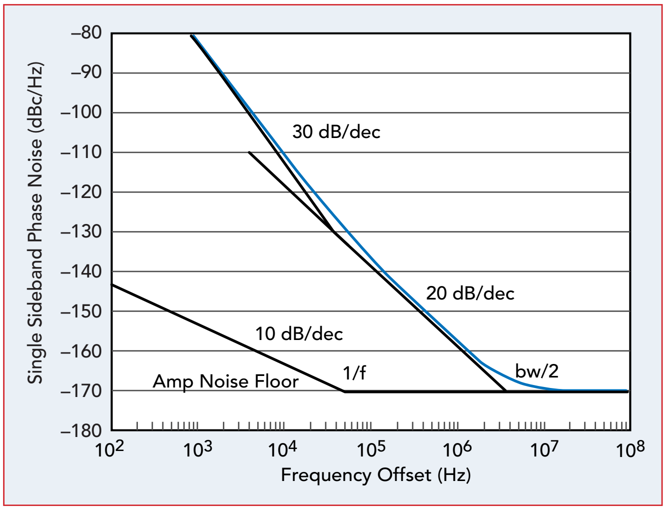

Fig. 3 **Phase noise plot of Leeson's equation.**

LOWER FREQUENCY OSCILLATORS: LONG-TERM STABILITY

Quartz Crystal Oscillators

Quartz crystals satisfy the medium- to long-term stability requirements of most microwave systems.^{6} Quartz is a bulk electroacoustic element. While crystal oscillators operate at 10 to 100 MHz, they resonate acoustically. Two properties make quartz an advantageous material: it has high Q values, typically between 10,000 in small low-cost variations to about a million in very expensive versions and quartz has a flat frequency versus temperature plateau, as shown in ***Figure 4***.

The quartz crystal resonator is cut as either AT or stress-compensated (SC). AT is the room temperature cut used in temperature-compensated crystal oscillators (TCXOs). This type of oscillator has very little frequency change versus temperature around 25°C. Additional compensation circuitry can extend this useful plateau significantly. The SC cut has a higher Q and a flat frequency-to-tempera-


3H Communication Systems
P/N: 2X2CC5300-100-8AA
S/N: 8102-1762-03 Cage: 75ET3


3H Communication Systems
P/N: CC23435-T200-5KK
S/N: 2020-N005-2233-05


3H Communication Systems
TLC6500-100-9SS-X1 SN-53021
3H Communication Systems
TLC6500-100-9SS-X1 SN-53099


3H
TLC582-U80-9SS
2015-3055 S/N: 024

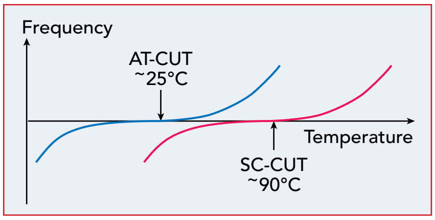

Fig. 4 **Quartz crystal oscillator frequency stability versus temperature.**

ture plateau around 90°C. Instead of temperature compensation, the SC crystal is used in an OCXO device, held at a constant temperature in an oven, to achieve even greater stability than is achievable in a TCXO.

A disadvantage of quartz-based crystal oscillators is their performance degrades at frequencies above about 100 MHz. To utilize a quartz-based oscillator in X-Band requires multiplication and this approach adds a 20log10(N) noise multiplier, where N is the frequency multiplication factor. ***Figure 5*** shows a 10 MHz and 100 MHz high-quality OCXO and their noise after ideally multiplying to 8 GHz. The 10 MHz device will almost always outperform a 100 MHz device at 1 to 100 Hz offsets. However, the 100 MHz oscillator will perform better at higher frequencies because it has been optimized for a better noise floor farther from the carrier. High performance systems may integrate and phase-lock both oscillators for the optimum phase noise and stability performance.

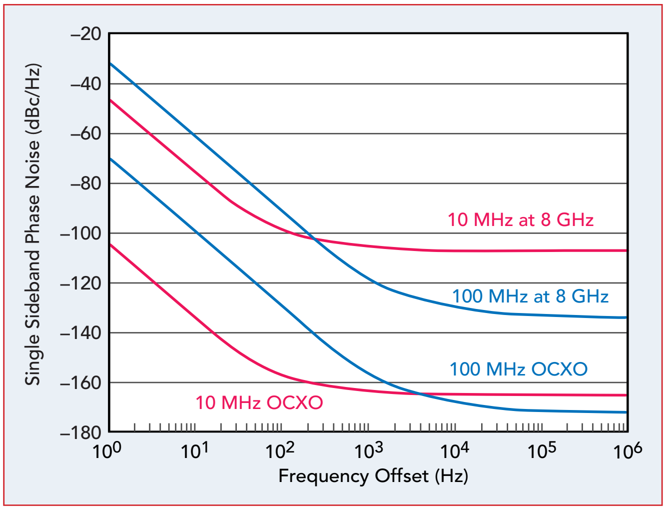

Fig. 5 **Comparison of 10 MHz and 100 MHz OCXOs at 8 GHz.**

SAW

A SAW oscillator is a surface acoustic device with a good Q-factor and small size. They operate from around 300 MHz to 2 GHz and serve as an intermediate oscillator to lock while multiplying OCXOs higher in frequency. These devices can sometimes replace a 100 MHz OCXO or a DRO. The performance of the SAW oscillator sits between the DRO and the OCXO in frequency and the material has significant size advantages. SAW oscillators require frequency multiplication for operation at X-Band and above.

X-BAND OSCILLATORS: SHORT-TERM STABILITY

Oscillators operating fundamentally at X-Band will have better phase noise than a quartz oscillator at offsets far from the carrier. ***Figure 6*** is a phase noise plot showing the quantitative performance of OCXO, voltage-controlled oscillator (VCO), DRO and SLCO designs at 8 GHz. As discussed, the Q-factor is the main performance difference in these oscillators. The Q-factors range from about 10 to 100,000, depending on the resonator technology. Size and cost are usually related to the Q-factor.

VCO

A VCO is the smallest, lowest cost and most prevalent of all the X-Band oscillators. They are typically realized as a lumped-element oscillator, either discrete or integrated on-chip. Some are embedded directly into the PLL IC for the highest level of integration. The advantages of this approach are wide tuning range, fast acquisition, low power consumption and small size. The disadvantage is a relatively low Q-factor, typically between 10 and


ERAVANT

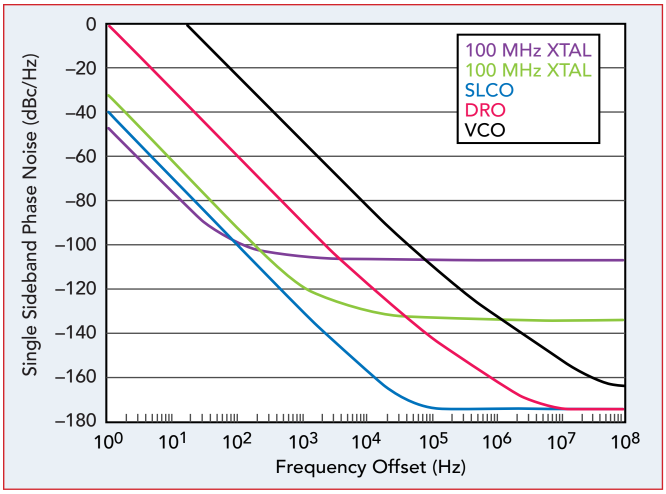

Fig. 6 **8 GHz oscillator phase noise comparison to Saetta Labs' SLCO.**

100. While this option has the lowest performance, it offers the best SWaP-C solution and the performance is often "good enough."

YIG

Yttrium iron garnet (YIG) material enables wide tuning, high Q, magnetically-tuned oscillators. The material resonates in the 3 to 10 GHz range and this range can be made wider if the material is doped. The resonance is directly proportional to a magnetic field. These oscillators have higher Q than VCOs with wide, but slow tuning. The large magnetic field results in significant power consumption and heat dissipation. These devices may be the best option when applications require a wide tuning range and better phase noise than VCOs can provide. Q-factors are in the 500 to 1000 range. YIG oscillators are significantly bigger and more expensive than VCOs and they are typically seen in higher performance systems like test equipment requiring a wide tuning range and low phase noise.

DRO

DROs are single-frequency oscillators that operate with a TM or TE electromagnetic resonance in a cylinder of high dielectric material. In a coaxial resonator oscillator (CRO), this high dielectric material is in a small coaxial cylinder. The material options range from larger dielectric pucks with high Q-factors to smaller, lower Q pucks for different applications and temperature stabilities. Unlike VCOs, they are single-frequency devices that are typically coarse-tuned mechanically and fine-tuned electrically for phase locking. DRO-based devices are about the size of a YIG but provide better phase noise performance at significantly lower operating currents. DROs are a good high performance option for architectures where fixed LOs drive ADCs and DACs. Q-factors can be around 1000, although phase noise varies greatly between manufacturers and models.

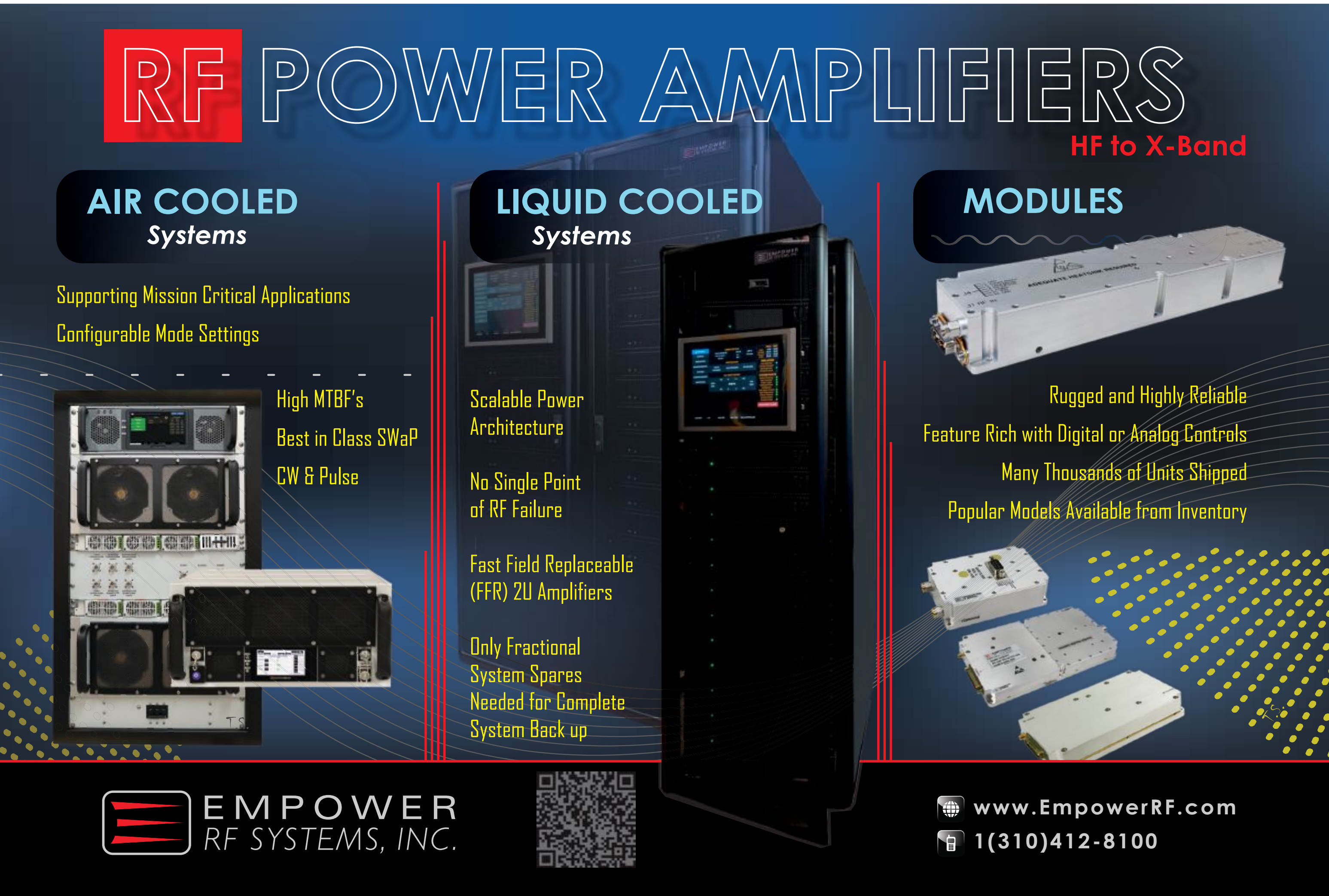

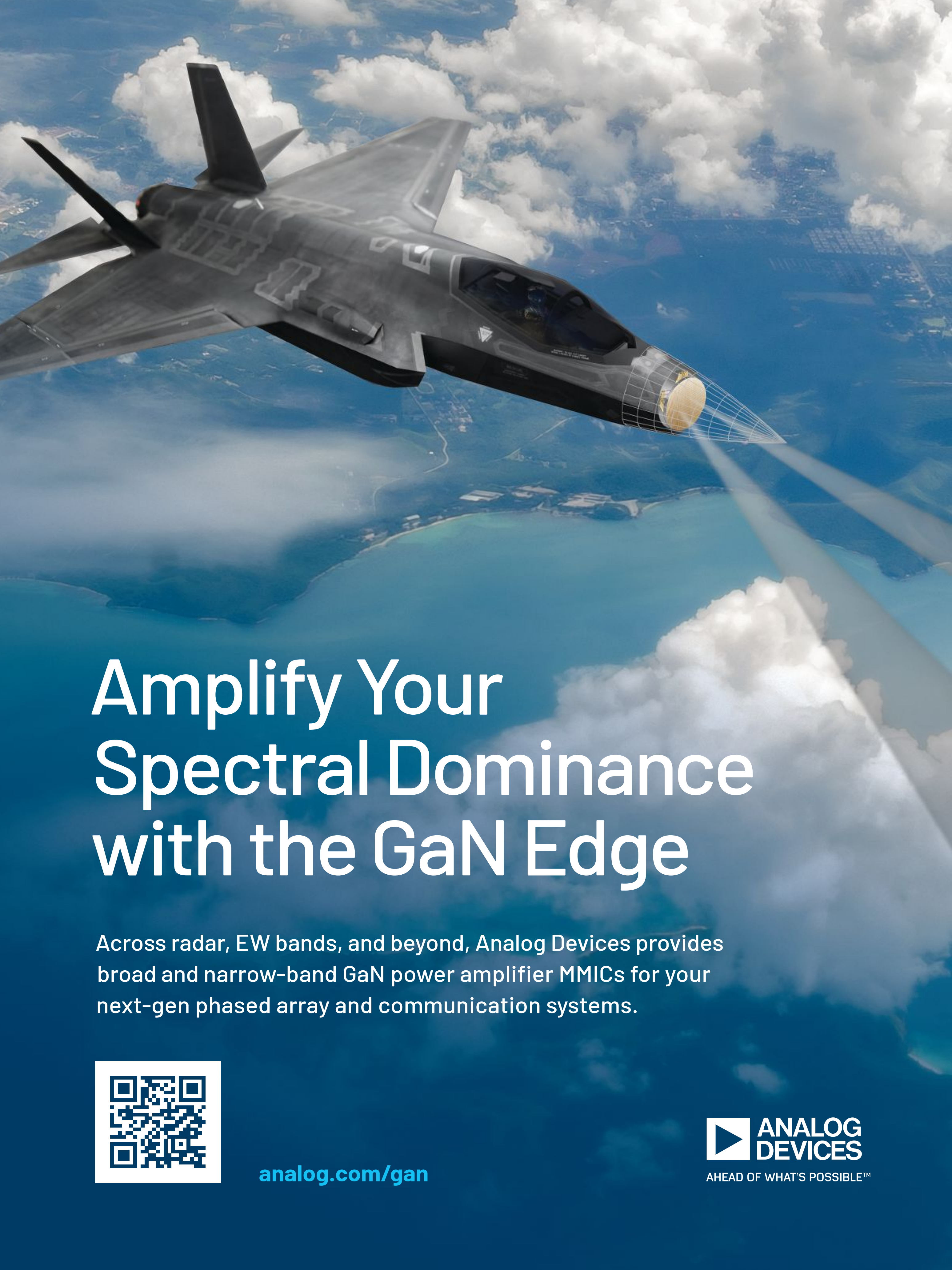

Sapphire Oscillators

Sapphire oscillators are relatively new to commercial applications. They operate as an electromagnetic device, like a DRO, but they use a different material and mode of resonance. The resonator material is sapphire and the resonance is called a whispering-gallery mode. The mode was named for the acoustic resonance in St. Paul's Cathedral in England, where the acoustic waves from a whisper travel around the perimeter of the circular hall with almost no attenuation. In a circular shape, a whispering-gallery mode can travel on the inside of two dielectric boundaries with near-perfect reflection. This removes the metallic losses inherent in DROs and cavity oscillators, improving the Q-factor from 10× to 100×. The only loss mechanism is the dielectric loss of the sapphire, which is extremely low. Sapphire oscillators have Qs around 100,000, which are like quartz but operate fundamentally at X-Band. These microwave oscillators have the lowest available noise performance but they are the largest solution and they do require power for thermal control like an OCXO. These constraints make these oscillators more expensive.

SUMMARY

Direct microwave conversion capabilities in the X-Band and above frequency range are expanding system design capabilities. The low phase noise performance of the new generation of DACs and ADCs spotlights the need for increasingly stringent clock performance requirements. In addition to improvements in materials, careful design considerations are needed to achieve the highest performance possible while still being able to accommodate SWaP-C requirements. This article has discussed oscillator phase noise and stability concerns along with the advantages and disadvantages of quartz, IC, VCO, YIG, DRO and newer SLCO technologies for designing and manufacturing oscillators that will become essential as direct conversion techniques move higher in frequency. ■

ACKNOWLEDGMENTS

Thank you to David Guidry at Texas Instruments for providing data and helpful conversations on driving high frequency DACs and ADCs.

References

1. T. Galla, "Selecting Phase-Locked Oscillators for Frequency Synthesis," *Microwave Journal*, Vol. 62, No. 9 Supplement, September 2019.
2. D. Leeson, "Oscillator Phase Noise: A 50-Year Review," *IEEE Transactions on Ultrasonics, Ferroelectrics and Frequency Control*, August 2016.
3. RF, RFIC and Microwave Theory, Design, *RFIC*, Web: www.ieee.li/pdf/essay/phase_noise_basics.pdf.
4. L. Geller, "Characterization of Additive Phase Noise in Microwave Amplifiers," *Microwave Journal*, Vol. 64, No. 1, January 2021.
5. J. Breitbarth and J. Koebel, "Additive (Residual) Phase Noise Measurement of Amplifiers, Frequency Dividers and Frequency Multipliers," *Microwave Journal*, Vol. 51, No. 6, June 2008.
6. J. Emmerich and H. Rudolph, "The Importance of Crystal Oscillators with Low Phase Noise," *Microwave Journal*, Vol. 66, No. 4, April 2023.

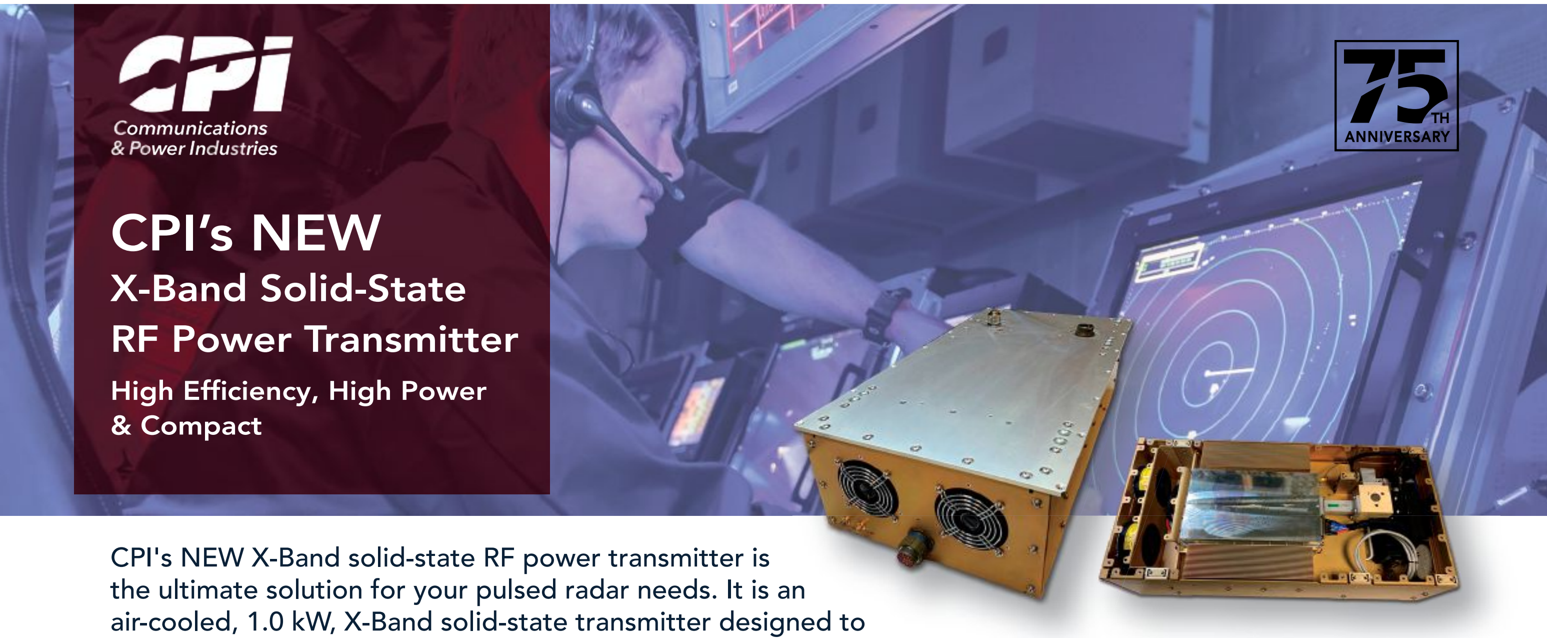

RF-LAMBDA

MADE IN USA

THE LEADER OF RF BROADBAND SOLUTIONS

EMC Broadband RF Power Amplifier

High Power Solid State

HUNDREDS IN STOCK

FAST SHIPPING

FREQUENCY UP TO 90GHZ

POWER UP TO 2KW CW

REMC06G18GG

6-18GHZ 300W

- AUTOMATIC BUILT IN SELF CALIBRATION AND BIAS ADJUSTMENT.
- OVER TEMPERATURE, CURRENT, INPUT POWER PROTECTION.
- VSWR MEASUREMENT AND OPEN CIRCUIT PROTECTION.
- USER FRIENDLY CONTROL INTERFACE.
- REMOTE ETHERNET CONTROL AND FIRMWARE UPDATE.
- HIGH POWER EFFICIENCY AND LIGHTWEIGHT.

RAMP42G47GA 42-47GHZ 8W

REMC02G06GE 2-6GHZ 500W

RAMP18G40GB-U 18-40G 20W

RAMP05M80GC 0.5-80GHZ

REMC08G11GE 8-11GHZ 400W

RF Amplifiers and Sub-Assemblies for Every Application

Delivery from Stock to 2 Weeks ARO from the catalog or built to your specifications!

- Competitive Pricing & Fast Delivery
- Military Reliability & Qualification
- Various Options: Temperature Compensation, Input Limiter Protection, Detectors/TTL & More
- Unconditionally Stable (100% tested)

ISO 9001:2000
and AS9100B
CERTIFIED

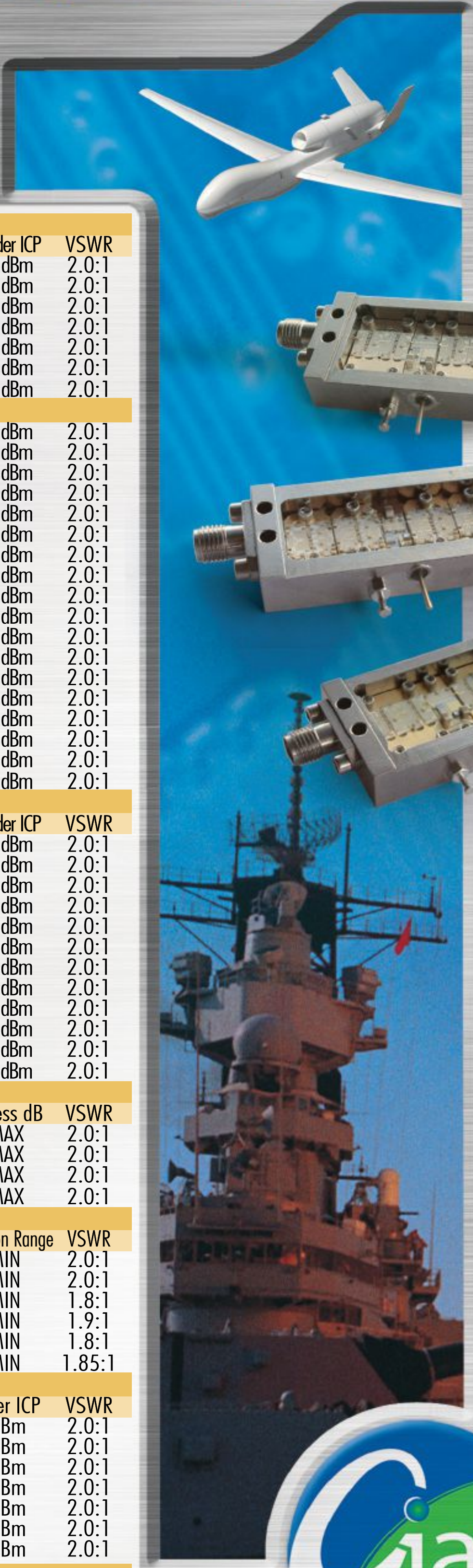

OCTAVE BAND LOW NOISE AMPLIFIERS

Model No.	Freq (GHz)	Gain (dB) MIN	Noise Figure (dB)	Power-out @ P1-dB	3rd Order ICP	VSWR
CA01-2110	0.5-1.0	28	1.0 MAX, 0.7 TYP	+10 MIN	+20 dBm	2.0:1
CA12-2110	1.0-2.0	30	1.0 MAX, 0.7 TYP	+10 MIN	+20 dBm	2.0:1
CA24-2111	2.0-4.0	29	1.1 MAX, 0.95 TYP	+10 MIN	+20 dBm	2.0:1
CA48-2111	4.0-8.0	29	1.3 MAX, 1.0 TYP	+10 MIN	+20 dBm	2.0:1
CA812-3111	8.0-12.0	27	1.6 MAX, 1.4 TYP	+10 MIN	+20 dBm	2.0:1
CA1218-4111	12.0-18.0	25	1.9 MAX, 1.7 TYP	+10 MIN	+20 dBm	2.0:1
CA1826-2110	18.0-26.5	32	3.0 MAX, 2.5 TYP	+10 MIN	+20 dBm	2.0:1

NARROW BAND LOW NOISE AND MEDIUM POWER AMPLIFIERS

Model No.	Freq (GHz)	Gain (dB) MIN	Noise Figure (dB)	Power-out @ P1-dB	3rd Order ICP	VSWR
CA01-2111	0.4 - 0.5	28	0.6 MAX, 0.4 TYP	+10 MIN	+20 dBm	2.0:1
CA01-2113	0.8 - 1.0	28	0.6 MAX, 0.4 TYP	+10 MIN	+20 dBm	2.0:1
CA12-3117	1.2 - 1.6	25	0.6 MAX, 0.4 TYP	+10 MIN	+20 dBm	2.0:1
CA23-3111	2.2 - 2.4	30	0.6 MAX, 0.45 TYP	+10 MIN	+20 dBm	2.0:1
CA23-3116	2.7 - 2.9	29	0.7 MAX, 0.5 TYP	+10 MIN	+20 dBm	2.0:1
CA34-2110	3.7 - 4.2	28	1.0 MAX, 0.5 TYP	+10 MIN	+20 dBm	2.0:1
CA56-3110	5.4 - 5.9	40	1.0 MAX, 0.5 TYP	+10 MIN	+20 dBm	2.0:1
CA78-4110	7.25 - 7.75	32	1.2 MAX, 1.0 TYP	+10 MIN	+20 dBm	2.0:1
CA910-3110	9.0 - 10.6	25	1.4 MAX, 1.2 TYP	+10 MIN	+20 dBm	2.0:1
CA1315-3110	13.75 - 15.4	25	1.6 MAX, 1.4 TYP	+10 MIN	+20 dBm	2.0:1
CA12-3114	1.35 - 1.85	30	4.0 MAX, 3.0 TYP	+33 MIN	+41 dBm	2.0:1
CA34-6116	3.1 - 3.5	40	4.5 MAX, 3.5 TYP	+35 MIN	+43 dBm	2.0:1
CA56-5114	5.9 - 6.4	30	5.0 MAX, 4.0 TYP	+30 MIN	+40 dBm	2.0:1
CA812-6115	8.0 - 12.0	30	4.5 MAX, 3.5 TYP	+30 MIN	+40 dBm	2.0:1
CA812-6116	8.0 - 12.0	30	5.0 MAX, 4.0 TYP	+33 MIN	+41 dBm	2.0:1
CA1213-7110	12.2 - 13.25	28	6.0 MAX, 5.5 TYP	+33 MIN	+42 dBm	2.0:1
CA1415-7110	14.0 - 15.0	30	5.0 MAX, 4.0 TYP	+30 MIN	+40 dBm	2.0:1
CA1722-4110	17.0 - 22.0	25	3.5 MAX, 2.8 TYP	+21 MIN	+31 dBm	2.0:1

ULTRA-BROADBAND & MULTI-OCTAVE BAND AMPLIFIERS

Model No.	Freq (GHz)	Gain (dB) MIN	Noise Figure (dB)	Power-out @ P1-dB	3rd Order ICP	VSWR
CA0102-3111	0.1-2.0	28	1.6 Max, 1.2 TYP	+10 MIN	+20 dBm	2.0:1
CA0106-3111	0.1-6.0	28	1.9 Max, 1.5 TYP	+10 MIN	+20 dBm	2.0:1
CA0108-3110	0.1-8.0	26	2.2 Max, 1.8 TYP	+10 MIN	+20 dBm	2.0:1
CA0108-4112	0.1-8.0	32	3.0 MAX, 1.8 TYP	+22 MIN	+32 dBm	2.0:1
CA02-3112	0.5-2.0	36	4.5 MAX, 2.5 TYP	+30 MIN	+40 dBm	2.0:1
CA26-3110	2.0-6.0	26	2.0 MAX, 1.5 TYP	+10 MIN	+20 dBm	2.0:1
CA26-4114	2.0-6.0	22	5.0 MAX, 3.5 TYP	+30 MIN	+40 dBm	2.0:1
CA618-4112	6.0-18.0	25	5.0 MAX, 3.5 TYP	+23 MIN	+33 dBm	2.0:1
CA618-6114	6.0-18.0	35	5.0 MAX, 3.5 TYP	+30 MIN	+40 dBm	2.0:1
CA218-4116	2.0-18.0	30	3.5 MAX, 2.8 TYP	+10 MIN	+20 dBm	2.0:1
CA218-4110	2.0-18.0	30	5.0 MAX, 3.5 TYP	+20 MIN	+30 dBm	2.0:1
CA218-4112	2.0-18.0	29	5.0 MAX, 3.5 TYP	+24 MIN	+34 dBm	2.0:1

LIMITING AMPLIFIERS

Model No.	Freq (GHz)	Input Dynamic Range	Output Power Range Psat	Power Flatness dB	VSWR
CLA24-4001	2.0 - 4.0	-28 to +10 dBm	+7 to +11 dBm	+/- 1.5 MAX	2.0:1
CLA26-8001	2.0 - 6.0	-50 to +20 dBm	+14 to +18 dBm	+/- 1.5 MAX	2.0:1
CLA712-5001	7.0 - 12.4	-21 to +10 dBm	+14 to +19 dBm	+/- 1.5 MAX	2.0:1
CLA618-1201	6.0 - 18.0	-50 to +20 dBm	+14 to +19 dBm	+/- 1.5 MAX	2.0:1

AMPLIFIERS WITH INTEGRATED GAIN ATTENUATION

Model No.	Freq (GHz)	Gain (dB) MIN	Noise Figure (dB)	Power-out @ P1-dB	Gain Attenuation Range	VSWR
CA001-2511A	0.025-0.150	21	5.0 MAX, 3.5 TYP	+12 MIN	30 dB MIN	2.0:1
CA05-3110A	0.5-5.5	23	2.5 MAX, 1.5 TYP	+18 MIN	20 dB MIN	2.0:1
CA56-3110A	5.85-6.425	28	2.5 MAX, 1.5 TYP	+16 MIN	22 dB MIN	1.8:1
CA612-4110A	6.0-12.0	24	2.5 MAX, 1.5 TYP	+12 MIN	15 dB MIN	1.9:1
CA1315-4110A	13.75-15.4	25	2.2 MAX, 1.6 TYP	+16 MIN	20 dB MIN	1.8:1
CA1518-4110A	15.0-18.0	30	3.0 MAX, 2.0 TYP	+18 MIN	20 dB MIN	1.85:1

LOW FREQUENCY AMPLIFIERS

Model No.	Freq (GHz)	Gain (dB) MIN	Noise Figure dB	Power-out @ P1-dB	3rd Order ICP	VSWR
CA001-2110	0.01-0.10	18	4.0 MAX, 2.2 TYP	+10 MIN	+20 dBm	2.0:1
CA001-2211	0.04-0.15	24	3.5 MAX, 2.2 TYP	+13 MIN	+23 dBm	2.0:1
CA001-2215	0.04-0.15	23	4.0 MAX, 2.2 TYP	+23 MIN	+33 dBm	2.0:1
CA001-3113	0.01-1.0	28	4.0 MAX, 2.8 TYP	+17 MIN	+27 dBm	2.0:1
CA002-3114	0.01-2.0	27	4.0 MAX, 2.8 TYP	+20 MIN	+30 dBm	2.0:1
CA003-3116	0.01-3.0	18	4.0 MAX, 2.8 TYP	+25 MIN	+35 dBm	2.0:1
CA004-3112	0.01-4.0	32	4.0 MAX, 2.8 TYP	+15 MIN	+25 dBm	2.0:1

CIAO Wireless can easily modify any of its standard models to meet your "exact" requirements at the Catalog Pricing.

Visit our web site at www.ciaowireless.com for our complete product offering.

Ciao wireless

Ciao Wireless, Inc. 4000 Via Pescador, Camarillo, CA 93012

Tel (805) 389-3224 Fax (805) 389-3629 sales@ciaowireless.com

DefenseNews
Cliff Drubin, Associate Technical Editor

DARPA's REMA Program to Add Mission Autonomy to Commercial Drones

Commercial drone technology is advancing rapidly, providing cost-effective and robust capabilities for a variety of civil and military missions. DARPA's Rapid Experimental Missionized Autonomy (REMA) program aims to enable a drone to autonomously continue its predefined mission when connection to the operator is lost. The program is focused on constantly providing new agnostic drone autonomy capabilities for transition in one-month intervals to outpace adversarial countermeasures. REMA progressed from program announcements to contract awards in just 70 business days.

"REMA is the demonstrator for rapid ideation and tech development," said Dr. Lael Rudd, REMA program manager. "The five performers under contract are working as a conglomerate without firewalls to create common solutions to achieve the program goals."

As small aerial vehicles play increasingly important military roles on the battlefield, REMA will render ineffective adversaries' electromagnetic countermeasures intended to disrupt communication links between operator and drone to abort missions and cause crashes.

> "Creating autonomous solutions to maximize effectiveness of stock commercial and small military drones on the battlefield."

"REMA is focused on creating autonomous solutions to maximize effectiveness of stock commercial and small military drones on the battlefield," said Dr. Rudd. "Through creating an autonomy adapter that works with all commercial drones, regardless of manufacturer and by developing mission-specific autonomy that is constantly refreshed and easy to upload prior to a mission, we aim to give drone operators the advantage in fast-paced combat operations."

The 18-month, single-phase program is divided into two technical areas: 1) A drone autonomy adapter interface and 2) mission-specific autonomy software. REMA will be able to agnostically detect the drone type when connected and apply autonomy to increase the drone's capability. REMA will be completed in development cycles starting at three-month intervals and accelerating to one-month intervals, to repeatedly provide new and improved autonomy for direct transition.

Contracts for the drone autonomy adapter interface technical area have been awarded to Anduril and RTX. Contracts for the mission-specific autonomy software technical area have been awarded to Leidos, Northrop Grumman and SoarTech.

The first development cycle, or "spiral challenge," started in December 2023, is focused on developing platforms with agnostic autonomy features.

RTX Works with AMD to Develop Next-Gen Multi-Chip Package

Raytheon, an RTX business, has been awarded a $20 million contract through the Strategic and Spectrum Missions Advanced Resilient Trusted Systems (S2MARTS) consortium to develop a next-generation multi-chip package for use in ground, maritime and airborne sensors.

Under the contract, Raytheon will package state-of-the-art commercial devices from industry partners like AMD to create a compact microelectronics package that will convert RF energy to digital information with more bandwidth and higher data rates. The integration will result in new system capabilities designed with higher performance, lower power consumption and reduced weight.

> "Collaboration will accelerate the delivery of microelectronics packaging for military systems."

"By teaming with commercial industry, we can incorporate cutting-edge technology into Department of Defense applications on a much faster timescale," said Colin Whelan, president of advanced technology at Raytheon. "Together, we will deliver the first multi-chip package that features the latest in interconnect ability, which will provide new system capabilities to our warfighters."

This multi-chip package will be created with the latest in industry-standard die-level interconnect ability, enabling individual chiplets to reach their peak performance and achieve new system capabilities in a cost-effective and high performance way. It is designed for compatibility with Raytheon's scalable sensor processing requirements.

Chiplets from commercial partners will be integrated onto a Raytheon-designed and fabricated interposer by its 3D universal packaging domestic silicon manufacturing process in Lompoc, Calif. This award will be managed by the National Security Technology Accelerator and administered by the Naval Surface Warfare Center Crane Division in Indiana.

First Flight Test for New AMRAAM-ER Variant

Raytheon, an RTX business, and Kongsberg Defence & Aerospace, with support from the Norwegian Ministry of Defense (MoD)

For More Information
Visit mwjournal.com for more defense news.

and Armed Forces, successfully completed a flight test of an updated AMRAAM®-Extended Range missile variant from a National Advanced Surface-to-Air Missile System (NASAMS). The successful flight test showcases the increased capabilities of the upgraded AMRAAM-ER.

This latest AMRAAM-ER variant is a first-of-its-kind configuration incorporating the guidance section of the AIM-120 C-8. It also incorporates a more robust 10-in. rocket motor from Nammo and a 10 in. Control actuator system from Kongsberg Defence & Aerospace, branded the Norwegian Propulsion Stack, for which the Norwegian MoD has been a collaborative partner.

"Integrating this new technology into the AMRAAM-ER ensures the advanced capabilities of the surface-launched munition for many years to come," said Paul Ferraro, president of air and space defense systems at Raytheon. "Agile software upgrades will continue to advance AMRAAM to stay ahead of evolving threats."

The testing included a test firing, during which the missile flew a preprogramed flight path to verify safe egress from the NASAMS launcher and missile performance.

NASAMS_Launch (Source: RTX)

The AMRAAM-ER is designed to be integrated with the NASAMS launcher for increased air defense protection, intercepting targets with the increased range and altitude of a non-extended range AMRAAM.

NASAMS, a highly adaptable medium-range air defense solution, is jointly developed and produced by Raytheon and Kongsberg Defence & Aerospace. Drawing on decades of experience, industrial cooperation and significant investment made by all three parties, this new cooperative arrangement will grow the capabilities of NASAMS to ensure it keeps pace with ever-evolving complex threats.

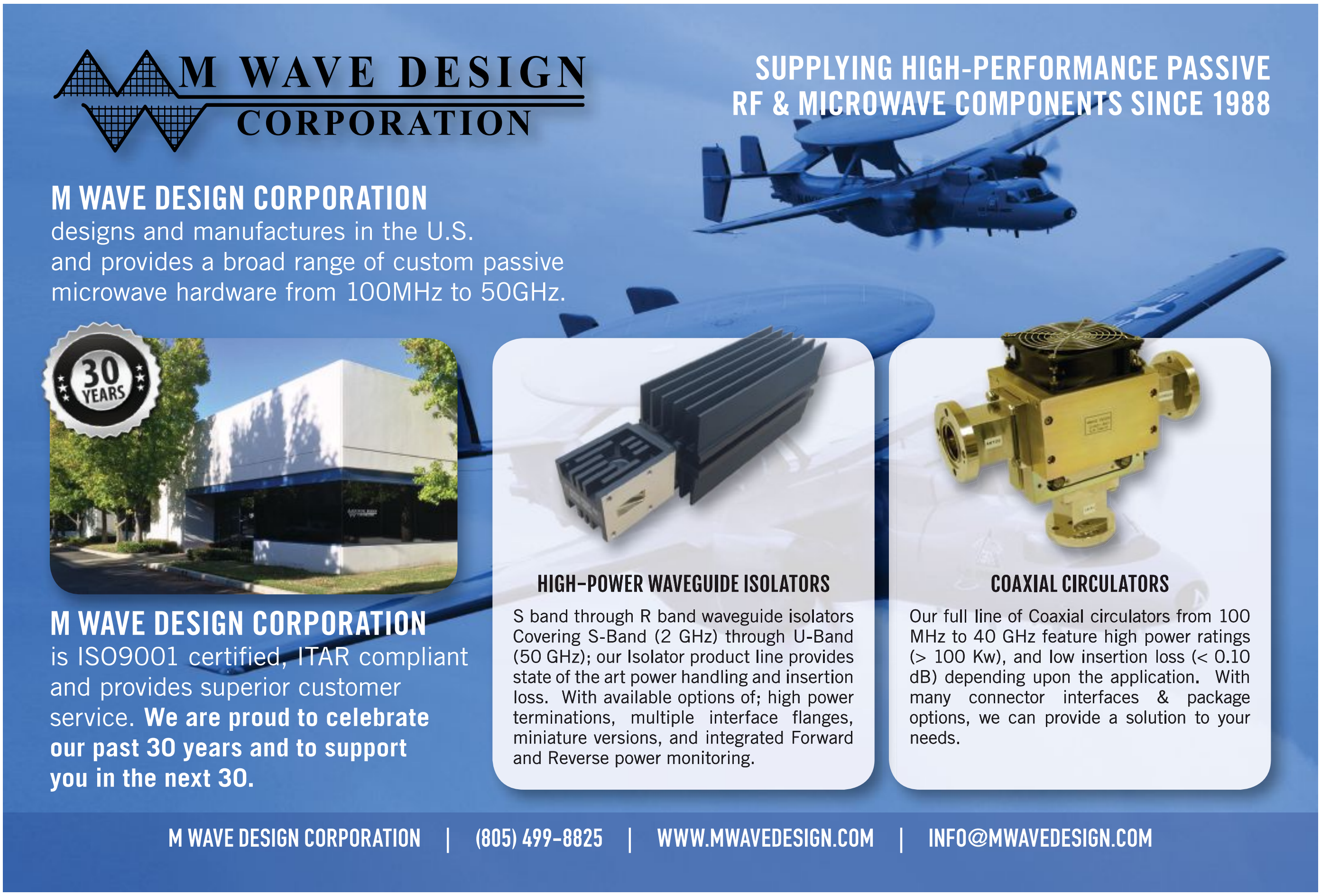

Reactel, Inc.

Reacting First to All Your Filter Needs.

Visit Reactel at Booth #814 at IMS2024 in Washington, DC and *CAPITALIZE* on over 45 years of filter-based engineering experience.

Reactel is the recognized source of filters, multiplexers and multifunction assemblies from DC to 67 GHz and offers solutions to your most challenging requirements.

Get Pantsed *at the Reactel Booth*

Visit Booth #814, and Get Pantsed at IMS! Stop in for your photo-op in the famous Maryland Filter Guy's Pants! Enter our photo contest for a grand prize, but every visitor is a winner with giveaways, treats and more!

8031 Cessna Avenue • Gaithersburg, Maryland 20879 • (301) 519-3660 • reactel@reactel.com • reactel.com

Intertek RoHS MADE IN MD *Since 1979*

DC TO 95 GHz

High-Frequency Products

For mmWave Test Applications

LEARN MORE

E-Band Amplifiers

ZVA-50953G+

E-Band Medium Power Amplifier

- 50 to 95 GHz
- +21 dBm P_{OUT} at Saturation
- 28 dB gain
- ±2.0 dB gain flatness
- Single supply voltage, +10 to +15V

ZVA-71863HP+

E-Band Medium Power Amplifier

- 71 to 86 GHz
- +24 dBm P_{OUT} at Saturation
- 38 dB gain
- ±1.5 dB gain flatness
- Single supply voltage, +10 to +15V

ZVA-71863LNX+

E-Band Low Noise Amplifier

- 71 to 86 GHz
- 4.5 dB noise figure
- 37 dB gain
- +13.8 dBm P1dB, +18 dBm P_{SAT}
- Single-supply voltage, +10 to +15V

K – V-Band Amplifiers

ZVA-35703+

Medium Power Amplifier

- 35 to 71 GHz
- +21 dBm P_{SAT}
- 17.5 dB gain
- ±1.5 dB gain flatness
- Single supply voltage, +10 to +15V

ZVA-543HP+

Medium Power Amplifier

- 18 to 54 GHz
- +29 dBm P_{SAT}
- High gain, 31 dB
- ±2.0 dB gain flatness
- Single supply voltage, +10 to +15V

ZVA-0.5W303G+

Medium Power Amplifier

- 10 MHz to 30 GHz
- 0.5W P_{OUT} at Saturation
- ±1.5 dB gain flatness
- 4.2 dB noise figure
- Single +12V bias voltage

More Products In Stock

BIAS TEES

DIGITAL STEP ATTENUATORS

I/Q MIXERS

MIXERS

MULTIPLIERS

POWER DETECTORS

SWITCHES

& MORE

Mini-Circuits®

Radar Modules and ToF Cameras for In-Cabin Sensing

With the shift toward electric vehicles, end-users are becoming less concerned about traditional differentiators like engine horsepower and are placing greater emphasis on smart interior functions. This trend is compelling automotive original equipment manufacturers to invest more effort in enhancing interior features, thereby adding greater value to their products and distinguishing them from other vehicles. IDTechEx's latest research, "In-Cabin Sensing 2024-2034: Technologies, Opportunities and Markets," compares 3D time-of-flight (ToF) cameras with mmWave radar solutions.

Driven by regulations such as Euro NCAP, driver monitoring systems (DMS) have gained significant traction and have transitioned from a luxury feature to a new norm. As of 2024, most DMS use 2D near-infrared (NIR) cameras. Due to their relatively low costs, they are anticipated to be increasingly adopted, emerging as the dominant enabling technology for DMS. For automotive OEMs to further set themselves apart from competitors, advanced features such as gesture control, child presence detection and seat belt detection are also expected to gain momentum, especially in mid- to high-end vehicles. Currently, the 3D ToF camera stands out as the most widely used technology for DMS, while some automotive OEMs, such as Volvo and Tesla, are incorporating in-cabin radar modules.

Radar has played an important role in advanced driver assistance systems for over two decades. Utilizing radio waves with a frequency-modulated continuous wave coding system, radars can accurately measure the distance and relative velocity of objects within their field of view. However, historically, radar modules have predominantly been employed for exterior sensing rather than interior applications.

As of 2023, according to Tesla's website, the in-cabin radar operates within a frequency range of 60 GHz to 64 GHz, falling within the license-free industrial, scientific and medical band. The detection distance of these radar modules typically ranges from 0.4 to 2 m, effectively covering the interior space. Though unconfirmed officially by Tesla, recent news suggests that their cybertruck is equipped with in-cabin radar modules for occupant monitoring, including functions such as child presence detection and seat belt reminders.

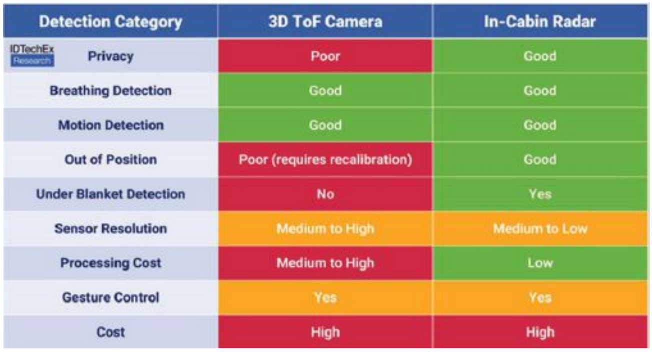

Detection Category	3D ToF Camera	In-Cabin Radar
Privacy	Poor	Good
Breathing Detection	Good	Good
Motion Detection	Good	Good
Out of Position	Poor (requires recalibration)	Good
Under Blanket Detection	No	Yes
Sensor Resolution	Medium to High	Medium to Low
Processing Cost	Medium to High	Low
Gesture Control	Yes	Yes
Cost	High	High

ToF vs. Radar (Source: IDTechEx)

Similar to radar modules, 3D ToF cameras also find application in occupant monitoring. 3D ToF cameras operate by utilizing near-infrared illuminators like LEDs or vertical cavity surface emitting lasers (VCSELs), in conjunction with image sensors. However, privacy concerns surround the use of cameras, even though some suppliers assert that they can address this issue by either blurring people's faces or storing data solely onboard.

An additional limitation of 3D ToF cameras is that, unlike in-cabin radar modules, they are unable to detect people or objects through obstacles. Furthermore, due to their reliance on computer vision technology, cameras necessitate intricate algorithms and recalibration, introducing technical complexity to their implementation. Despite these drawbacks, some suppliers are actively working to address privacy concerns and improve the overall capabilities of 3D ToF cameras for occupant monitoring in automotive applications.

As of now, 3D ToF cameras are more widely adopted for occupant monitoring systems and have advanced features compared with radar modules. However, by comparing the costs and functions of radar modules and 3D ToF cameras, IDTechEx believes there are potential opportunities for radar modules. 3D ToF cameras are adopted in the Li Auto L9, BMW iX and the new ARCFOX αS series, where radar modules are expecting adoption in Tesla and Volvo.

Global 6G Connections to Reach 290M in the First Two Years of Service

A new study from Juniper Research predicts there will be 290 million connections globally by 2030, the year after its initial expected launch in 2029.

To achieve this early growth, the report cautions operators that they must solve various technological challenges, including the issue of network interference arising from the use of the high frequency spectrum.

This use of high frequency spectrum in 6G will be the key enabling technology to provide throughput speeds 100x greater than current 5G networks. However, as cellular technologies have never used spectrum bands in this range before, the most pressing concern for operators is minimizing network interference, or the risk of interference, creating an unreliable 6G network.

To achieve this, the report urges operators to invest in reconfigurable intelligent surfaces (RIS), a technology that will mitigate the impact of interference from large obstacles, including buildings, on network services. This

For More Information

Visit mwjournal.com for more commercial market news.

is accomplished by purposefully reflecting and refracting 6G mobile signals to enable data packets to move around physical obstacles.

As 6G standards become clearer in 2025, RIS technology must become an immediate priority for development. However, the report warns that given the wide geographical areas of some 6G networks, operators must implement AI to monitor and adjust RIS configurations in real-time to maximize the technology's benefits.

Research author Alex Webb remarked, "Initial 6G coverage will occur in the most densely populated geographical areas to serve as many users as possible. Therefore, RIS technology will be key to providing a valuable 6G service to both consumer and enterprise customers in the first few years of network operation."

Distributed Antenna System Revenue to Surpass USD$36B by 2028

According to a new report from ABI Research, distributed antenna system (DAS) revenue is expected to grow at a compound annual growth rate of 20 percent from 2022 to 2028 to reach over US$36 billion. This rapid growth is driven by the rising demand for reliable in-building wireless performance across verticals such as sports venues, hospitals, airports and more.

"DAS solutions allow for increased wireless capacity and coverage and have become increasingly popular in recent years as the demand for wireless connectivity in crowded spaces grows," explained Larbi Belkhit, research analyst for 5G, 6G and Open RAN. "Reliable in-building wireless performance has become almost mandatory; therefore, this technology is expected to continue to have strong adoption growth."

In Asia-Pacific alone, DAS revenue in sports venues is expected to more than double from US$1.6 billion in 2022 to US$5.9 billion in 2028. DAS deployments in spaces like stadiums, retail and hospitals enable visitors to enjoy seamless 5G experiences. Furthermore, Active DAS revenue in Europe is expected to more than double from US$701 million in 2022 to US$1.5 billion in 2028. Active DAS is a cost-effective approach to meeting large venues' growing 5G and IoT connectivity demands.

"With neutral hosts becoming increasingly important, DAS is a key enabling technology that can allow signals to be effectively distributed across challenging indoor environments," Belkhit concluded. "The enterprise cellular market is going to see DAS as a way of meeting connectivity requirements, further driving the growth of DAS deployments and revenue opportunities in the future."

© Safran - ESO / L.Calçada / Daniel Linares - PEMA 2M

Nxbeam™

Ka / V / E - Band GaN MMIC Power

Ka

- NPA2001-DE | 26.5-29.5 GHz | 35 W
- NPA2002-DE | 27.0-30.0 GHz | 35 W
- NPA2003-DE | 27.5-31.0 GHz | 35 W
- NPA2004-DE | 25.0-28.5 GHz | 35 W
- NPA2020-DE | 24.0-25.0 GHz | 8 W
- NPA2030-DE | 27.5-31.0 GHz | 20 W
- NPA2040-DE | 27.5-31.0 GHz | 10 W

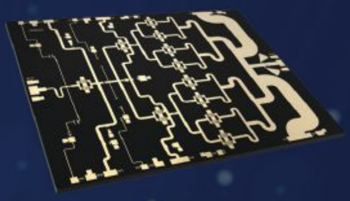

V

- NPA4000-DE | 47.0-52.0 GHz | 1.5 W
- NPA4010-DE | 47.0-52.0 GHz | 3.5 W

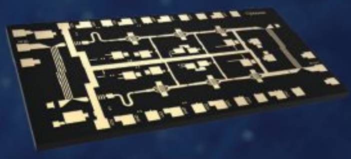

E

- NPA7000-DE | 65.0-76.0 GHz | 1 W
- NPA7010-DE | 71.0-76.0 GHz | 4 W*

* In Fabrication

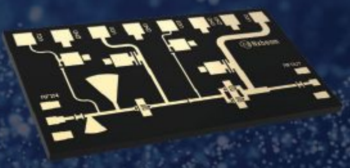

4388 Cerritos Avenue
Los Alamitos, CA 90720

www.nxbeam.com
info@nxbeam.com

Phone: 949-656-2883
info@nxbeam.com

Around the **Circuit**

Barbara Walsh, Multimedia Staff Editor

IN MEMORIAM

Kenneth L. Carr, 92, passed away peacefully on February 16, 2024, at Riverwoods in Durham, Maine. Born February 15, 1932, in Cambridge, Mass., he was the recipient of the 2022 Microwave Pioneer Award from the IEEE's Microwave Theory and Techniques Society (MTT-S) and was an IEEE life member. Carr developed electrical devices for radar systems used by the military to spot enemy submarines, land fighter planes on aircraft carriers and guide missiles. Carr also invented a device to help NASA monitor the re-entry of space capsules during Project Mercury and created an electromagnetic switch that allowed a radar system on a U.S. spy plane to take high-resolution images of Russian missile sites in Cuba.

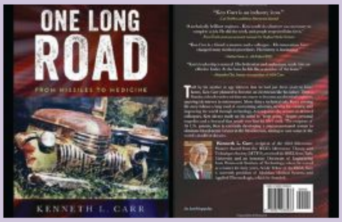

MERGERS & ACQUISITIONS

Cadence Design Systems Inc. announced it has entered into a definitive agreement to acquire **BETA CAE Systems International AG**, a leading system analysis platform provider of multi-domain, engineering simulation solutions. The addition of BETA CAE's proven technologies and talent will accelerate Cadence's Intelligent System Design™ strategy by expanding its multiphysics system analysis portfolio and enabling entry into the structural analysis segment, unlocking a multi-billion-dollar incremental TAM opportunity. Under the terms of the definitive agreement, Cadence will pay approximately $1.24 billion for the transaction, with 60 percent of the consideration to be paid in cash and 40 percent to be paid through the issuance of Cadence common stock to current BETA CAE shareholders.

Iridium Communications Inc., a leading provider of global voice and data satellite communications, announced that it had entered into an agreement to acquire **Satelles Inc.**, a leader in highly secure satellite-based time and location services that complement and protect GPS and other GNSS-reliant systems. The service, named Satellite Time and Location (STL), is an easy-to-adopt, highly secure solution that increases the efficiency and reliability of timing systems for digital infrastructure like 5G base stations, data centers and other critical infrastructure and protects against GNSS vulnerabilities using low-cost hardware that doesn't require outdoor antennas. This acquisition continues Iridium's philosophy of investing in differentiating technologies uniquely suited to its network that significantly outperform competing solutions.

COLLABORATIONS

Anritsu and **ASUS** have announced a partnership to validate the latest wireless communications standard, IEEE 802.11be (Wi-Fi 7) 320 MHz performance testing. This series of tests utilizes the Anritsu Wireless Connectivity Test Set (WLAN Tester) MT8862A in Network Mode and the ASUS ROG Phone 8 series smartphones. The IEEE 802.11be standard incorporates innovative technologies, including a 320 MHz bandwidth, 4096 QAM modulation and multiple RUs, which require comprehensive evaluation of RF performance. Anritsu's Wireless Connectivity Test Set (WLAN Tester) MT8862A is designed to measure the TRx RF performance of IEEE 802.11a/b/g/n/ac/ax/be (across 2.4 GHz, 5 GHz and 6 GHz bands) WLAN devices.

ATIS' Next G Alliance and the **6G Industry Association**, the private member of the EU Smart Networks and Services Joint Undertaking, announced the publication of the "EU-US Beyond 5G/6G Roadmap," a major first step in affirming the two regions' commitment to collaborating in the development of 6G networks. The document results from a request for the two organizations to provide an interim, joint, aligned 6G industry roadmap made during the fourth ministerial meeting of the EU-US Trade and Technology Council (TTC), which took place in Luleå, Sweden, on May 31, 2023. The collaborative input to the roadmap will be considered for inclusion in a TTC 6G "shared vision" being established by the US and EU governments.

Parallel Wireless, a leader in Open RAN and GreenRAN™ platform hardware-independent solutions, announced a partnership with **SOLiD**, a leader in distributed antenna systems for indoor mobile telecom systems, delivering greater flexibility to cellular service providers. This newly forged partnership will allow service providers to dramatically reduce their solution footprint and operating costs by reducing complexity, price, required real estate and power consumption, which can now be reduced by more than 80 percent. Deploying indoor wireless sites constitutes an intricate and costly aspect within any network operator. Across shopping malls, hospitals, underground trains or stadiums, the deployment typically spans vast and complex parameters.

OWT Global, a services and solutions provider for C5ISR, UxS and Air Domain Awareness & Defense solutions, and **Echodyne Corp.**, the radar platform company delivering high performance commercial-off-the-shelf (COTS) radars, announced a strategic relationship to develop and bring to market next-generation situational awareness solutions across OWT Global's portfolio. Echodyne's ultra-low size, weight and power radars offer electronically scanned array performance at COTS price points that radically expands situational awareness capabilities across deployed forces and assets. Integrated into OWT Global's advanced intelligent sensing as a service platform, the precision radar data improves end-to-end system performance.

For More Information

For up-to-date news briefs, visit mwjournal.com

DUAL or SINGLE LOOP
SYNTHESIZER & PLO MODULES

Up to 30 GHz*

Features:

- Proprietary digital Integer and Fractional PLL technology
- Lowest digital noise floor available -237 dBc/Hz figure of merit
- Output frequencies from 100 MHz locked crystal to 30 GHz
- Available with reference clean up dual loop, or single loop for very low noise reference
- Parallel fixed band stepping or SPI interface synthesized up to octave bandwidths
- Reference input range 1 MHz to 1.5 GHz
- Dual RF output or reference sample output available
- +12 dBm standard output power +16 dBm available
- Standard module size 2.25 X 2.25 X 0.5 Inches (LxWxH)
- Standard operating temperature -10 to 60 °C, -40 to +85 °C available

Applications:

- SATCOM, RADAR, MICROWAVE RADIO

16 - 30 GHz with added x2 module < 1" in height.

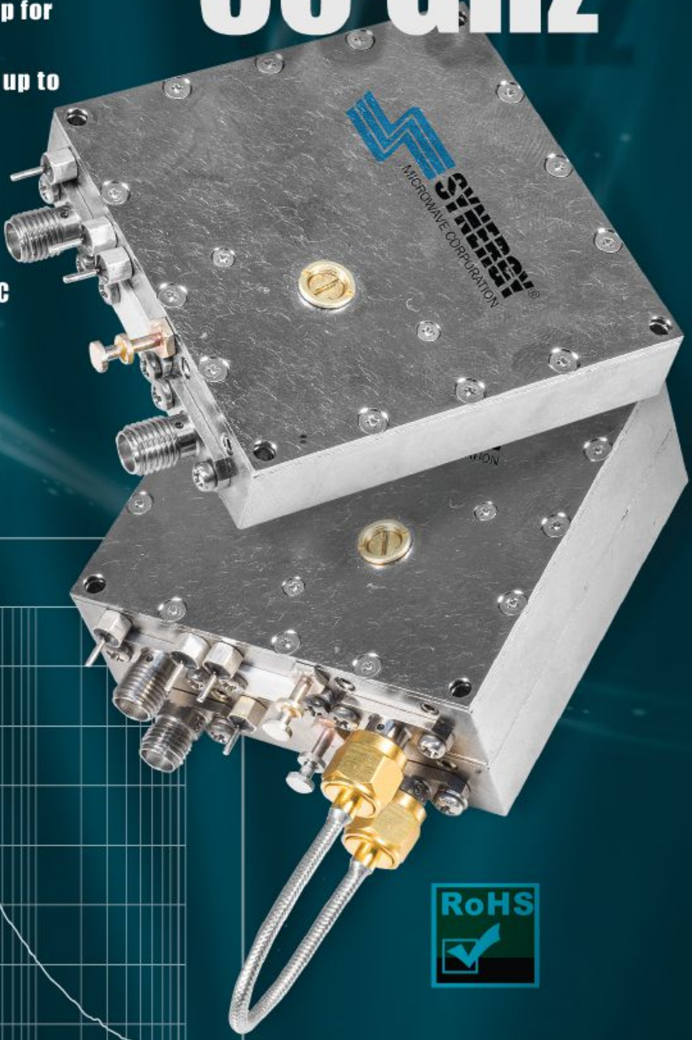

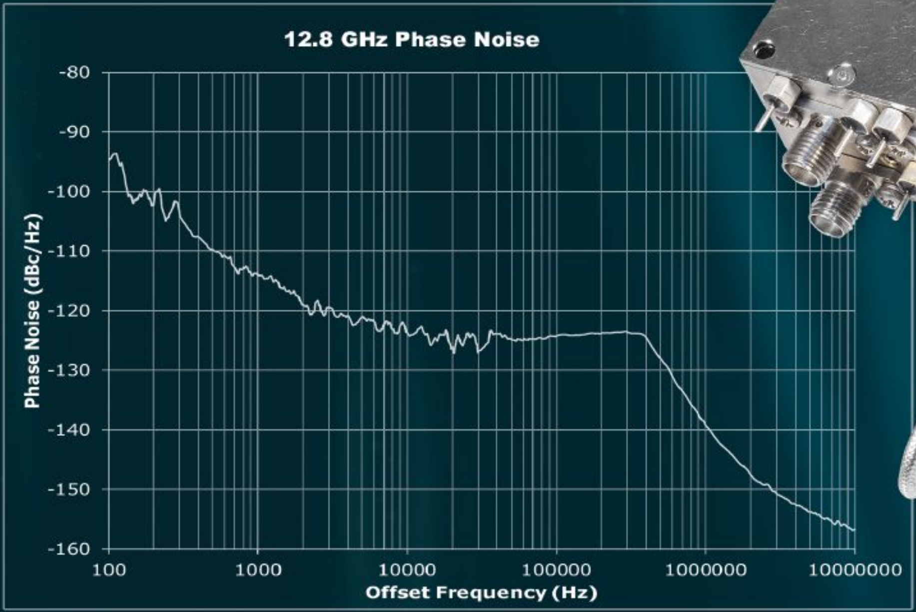

RoHS

Talk To Us About Your Custom Requirements.

SYNERGY®
MICROWAVE CORPORATION

Phone: (973) 881-8800 | Fax: (973) 881-8361
E-mail: sales@synergymwave.com
Web: WWW.SYNERGYMWAVE.COM
Mail: 201 McLean Boulevard, Paterson, NJ 07504

Around the **Circuit**

OQ Technology and **Round Solutions GmbH** signed a strategic partnership to enable the two parties to sell and promote each other's products and services in global satellite standard 3GPP NTN NB-IoT connectivity for machines and devices in remote and rural areas. The two companies will work together to cross-market their products and services, test OQ modules and devices and integrate them into both companies' solutions and promote that in the DACH region, and provide early access to new products and services such as the IO-GATE. OQ Technology is a front runner in providing global LEO 5G narrowband IoT connectivity through its nanosatellite constellation, the group already has eight satellites in orbit, with more to be launched soon.

NEW STARTS

Signal Hound announced it is expanding its physical presence by doubling the footprint at their southwest Washington headquarters by 11,000 square feet. The decision to expand operations is a result of Signal Hound's recent growth and the additional necessity for increased capacity for current and future needs. Earlier this year, Signal Hound officially assumed occupancy of the raw space, which is the other half of the building in which the company currently resides. In 2023, Signal Hound officially added the SP145 14.5 GHz Real-Time Spectrum Analyzer to its high performance line of spectrum analyzers and is planning to launch several new products in the coming years.

ACHIEVEMENTS

Kymeta Corporation announced the U.S. Patent and Trademark Office awarded Kymeta two U.S. patents. The first patent is related to the cooperation of a SD-WAN edge appliance and a satellite terminal, enabling users to engage in concurrent or switched satellite and cellular communications. The second patent is related to an electronically steered array antenna operating across multiple satellite networks in multiple modes (e.g., concurrent mode, switched mode, etc.). These achievements demonstrate Kymeta's continued thought leadership in the marketplace as the satellite communications industry evolves into a multi-orbit, multi-network ecosystem.

CONTRACTS

Mercury Systems Inc. announced that it received a five-year, $243.8 million, indefinite delivery/indefinite quantity contract to deliver rapidly reprogrammable electronic attack training subsystems for the **Naval Air Warfare Center Weapons Division**. These subsystems build on more than 25 years of test and training technology from the Mercury Processing Platform to bring the most advanced, near-peer jamming and electronic warfare capabilities to U.S. pilot training organizations. The most effective way to prepare pilots and aircrews for real-world combat environments is through training scenarios that represent near-peer threat capabilities to the greatest possible extent.

Quantic Wenzel has been selected to engineer and manufacture key electronic assemblies for **Northrop Grumman's AN/SLQ-32(V)7 SEWIP Block 3 Program**. The program is the third in a series of incremental upgrades that adds an electronic attack capability to the AN/SLQ-32 electronic warfare system to defend ships against anti-ship missiles. Northrop Grumman chose Quantic Wenzel for the multi-year program in part because of the company's expertise in high performance solutions.

Planet Labs PBC announced its fully owned subsidiary, **Planet Labs Federal Inc.**, was awarded a seven-figure contract by the **Naval Information Warfare Center** Pacific for vessel detection and monitoring over key areas of interest throughout the Pacific. The project will integrate both Planet's daily, global PlanetScope data and high-resolution SkySat data into the Department of Transportation's SeaVision platform, a web-based maritime situational awareness tool. The contract includes a fusion of technology from SynMax, a longtime Planet partner, who will provide vessel detection using their analytics technology over Planet data.

PEOPLE

▲ *Amit Shrestha*

Reticulate Micro Inc., a defense technology company, appointed **Amit Shrestha** as chief financial officer (CFO), effective March 1. As CFO, Shrestha oversees the company's finance strategy with an emphasis on fiscal discipline and accountability while serving as a strategic advisor on global growth strategy. Shrestha joins Reticulate Micro following a 20-year career at Microsoft Corporation, where he led finance and digital transformation in strategic regions in both Latin America and the Greater China Region, as well as serving as CFO of the company's U.S. Public Sector business.

▲ *Steven Layton*

mmTron Inc., a high performance semiconductor company helping unleash the mmWave frontier, has appointed **Steven Layton** as vice president of sales. With over 30 years' experience in the microwave and mmWave industry, Layton brings a breadth of knowledge and depth of expertise to this role. His career spans iconic companies such as Avantek, Litton and Endwave, with roles ranging from applications to sales. Before joining mmTron, he served for seven years as the chief operating officer (COO) of KG Technologies, where he was responsible for switching solutions for energy management. He rebranded the company and grew revenue and profitability, combining his skills in strategic vision and operations.

Quadsat, a specialist provider of unmanned aerial vehicle-based RF measurement solutions, has appointed **Karina Bergstrøm Larsen** as its new chairman of the board. Larsen joins Quadsat with a rich and proven background in the satellite industry, having founded saetta labs

Boulder, Colorado USA

saettalabs.com

- Thermally Stabilized
- Ext Ref Input (PLL)
- Status Display
- Lock Detect

Sapphire Loaded Cavity Oscillators
X-Band

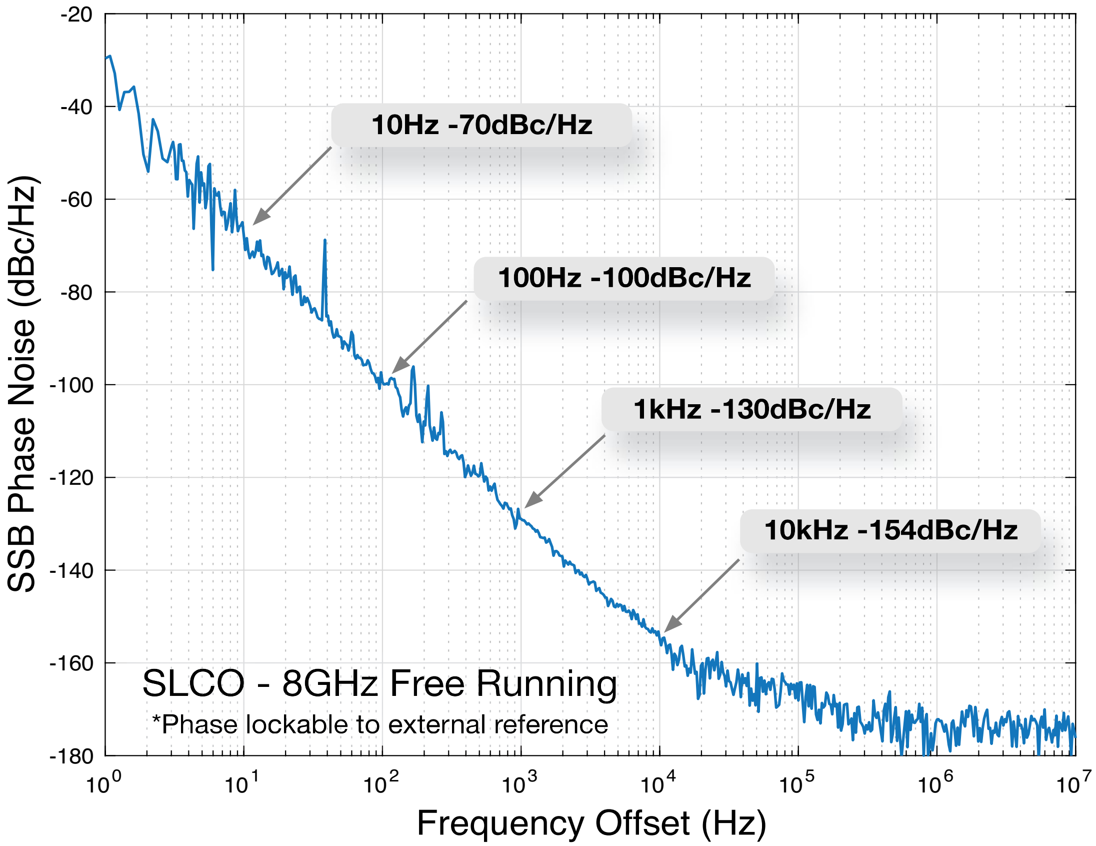

and scaled her own successful company before orchestrating a triumphant exit to Honeywell Aerospace. Larsen is now an independent consultant for satellite and aerospace, as well as putting her time into mentoring and encouraging girls to follow a career in STEM. Larsen's appointment comes as Torben Frigaard Rasmussen transitions from his role as chairman, following his instrumental role in securing a significant Series A funding round of €9 million for Quadsat last year.


▲ **Karina Bergstrøm Larsen**

Sivers Semiconductors AB announced that its subsidiary, Sivers Semiconductors Inc., has appointed **Dr. Bami Bastani** as U.S. executive chairman and has been nominated as the chairman of the board of directors of Sivers Semiconductors AB. Dr. Bastani joined Sivers' team as strategic advisor to the board and the management team in August 2023. He brings over 42 years of semiconductor industry experience, most recently as senior vice president at GlobalFoundries and GlobalFoundries' board member at the Global Semiconductor Alliance. Prior to GlobalFoundries, Dr. Bastani held president, CEO and board member positions at Meru Networks, Trident Microsystems and ANADIGICS. He brings over 20 years of serving on the boards of directors of public and private companies.


▲ **Dr. Bami Bastani**

REP APPOINTMENTS

Insulated Wire Inc. introduced **Altaix Electrónica** as its new representative for Spain and Portugal. Altaix is an ideal addition to Insulated Wire's European sales team, being an engineering focused group with significant experience in RF and microwave design.

Electro Rent announced a distribution agreement with **VIAVI Solutions**. This agreement enables Electro Rent to sell new VIAVI test instruments in North America, including fiber optics, optical transport, antenna and wireless field equipment. Therefore, Electro Rent customers are now able to purchase new VIAVI equipment for their testing needs, in addition to the rental, and used purchase options for VIAVI equipment already available through Electro Rent.

Complete Probe Solutions Inc., a U.S.-based manufacturer of fully automatic wafer probers, announced its appointment as the U.S. distributor for **Gel-Pak's** new Gel-Probe product line. The Gel-Probe product line encompasses enhanced probe tip cleaning and polishing solutions designed for semiconductor wafer test applications. Gel-Pak has reentered the elastomer-based probe tip cleaning market with the full support of CPS. Its enhanced Gel-Probe line currently includes the Gel-Probe ReMove and Gel-Probe ReFine products.

GaAs-Based Q/V/E-Band Solutions from Altum RF

Altum RF's lineup of broadband Q/V/E-band low-noise and medium-power amplifiers enable next-generation technology and high-capacity networks. Applications include test and measurement, SATCOM, and point-to-point wireless communication for 5G and 6G networks. These high-frequency amplifiers use advanced GaAs technology, which delivers low noise figure and linear amplification with less signal distortion at medium power.

Part Number	Frequency Range (GHz)	Gain (dB)	OP1dB (dBm)	NF (dB)	Package
ARF1208	37 – 59	26.5	16.5	2.5	Bare Die
ARF1207	57- 71	24	23	5	Bare Die
ARF1206	71 - 86	20	12	2.5 at 71 GHz 3.5 at 86 GHz	Bare Die
ARF1303	DC - 60	15	21	3.5 at 20 GHz 4.8 at 40 GHz	Bare Die

LEARN MORE AT ALTUMRF.COM

INFO@ALTUMRF.COM | +31 (0) 40 2390 888 | TWINNING CENTER, DE ZAALE 11, 5612 AJ EINDHOVEN, THE NETHERLANDS

INVITED PAPER

A Vibration-Compensated OCXO with Digital PLL & Aging Compensation

Mehran Mossammaparast, Patrick Mullin, Nikki Quinn and Mike Sawicki
Quantic Wenzel, Austin, Texas

Oven controlled crystal oscillators (OCXOs) are deployed in a variety of applications where the g-sensitivity of piezoelectric crystals plays a significant role in the overall system performance. These devices are used in communication, navigation, timing, radar and quantum computing applications to generate high spectral purity and stable primary frequency references. Developing new techniques to mitigate and minimize OCXO frequency source degradation is critical to advancing the state-of-the-art sensitivity and accuracy demanded by rapid technological advancements across scientific, commercial and defense industries. This article will present an oscillator that achieves a significant reduction in the dynamic phase noise of a compact crystal oscillator.

Equipment operating in the aerospace environment can experience any number of challenging dynamic vibration environments with a range of intensities and frequencies. These vibrations have many causes. They may arise from aircraft features like propellers, jet engines or rotors. The vibrations may also be the result of interaction with the atmosphere in response to turbulence and maneuvers. They may also be caused by terrestrial operations like take-off, landing or launch and finally, there may be extra-terrestrial micro vibrations while the platform is in orbit. The phase noise degradation experienced in these environments can range from micro-vibration levels experienced in a spacecraft due to altitude or spin thruster controllers to vibration levels as high as 0.02 g^2/Hz with g_{rms} = 4.4 g. Regardless of the magnitude of the vibration, OCXO degradation can easily cause system degradation.

The effects of vibration are also influenced by the location of the equipment, whether it is inside or outside of the aircraft, along with how the equipment is sheltered. The equipment itself can also contribute to the vibration profile because of its mass, materials or mechanical components, such as cooling fans. Dynamic vibration degradation created by the environments just described will typically manifest in the OCXO output as a frequency shift, elevated spurious signal levels and higher phase noise. As the OCXO performance degrades, radar range resolution, navigation receiver performance or electronic warfare system performance may also degrade.

OCXOs can also provide good short-term stability and clean frequency references for atomic frequency standards, whether the standards use Rb,[1] Cs or Hydrogen maser atomic clocks.[2] By locking the OCXO reference to atomic resonance, the short-term stability of the reference is combined with the long-term stability of the atomic resonance. This stability enables the fundamental laws of physics to be tested in settings that require extreme levels of precision and

Exodus AMP4071P-1KW, 4.0–6.0 GHz, 1KW Pulse

Exodus AMP4071P-1KW Pulse Amp: Designed for Pulse, EMC/EMI Mil-Std 461, Pulse Radar apps. Superb Pulse Fidelity (up to 100usec), duty cycles to 10%, min. 60dB gain. Monitoring: Forward/Reflected power (Watts & dBm), VSWR, voltage, current, temperature. Compact 5U chassis.

Exodus AMP2071A-LC, 80–1000 MHz, 750W, 500W P1

Exodus AMP2071A-LC: 80-1000MHz, >750W, >1000W nominal, >600W P1dB, 60dB gain. Monitoring parameters: Forward/Reflected power, VSWR, voltage, current, temperature. Weight <40kg, dimensions 19”W x 27”L x 8.75"H."

Exodus 40.0-50.0 GHz, 40-Watt SSPA, AMP4076B

Exodus AMP4076B: Rugged SSPA for 40-50GHz. Broadband, class A/AB design, 40W Min, 46dB gain. Superb TWT Replacement, monitoring: Forward/Reflected power, VSWR, voltage/current, temperature. Weight 50kg, compact 8U chassis.

Exodus AMP1146A 2.0 – 8.0GHz, 70W Minimum Solid-State Module

Exodus AMP1146A is a compact 2.0-8.0GHz Module. Produces 70W min, 80-90W nominal, 48dB min power gain, <-20dBc harmonics. Features current & temperature sensing, built-in protection circuits for reliability. Dimensions: 4.3”W x 7.8”L x 1.0”H.

Exodus AMP2070A, 1.0–6.0GHz 150W, 100W P1

Exodus AMP2070A: Ideal for broadband EMI-Lab, Comm. & EW applications. Class A/AB linear design, covers 1.0-6.0GHz, 150W Min, 100W P1dB, 52dB gain. Optional monitoring parameters, compact 3U approx. 25kg.

Exodus 18.0-40.0GHz, 10dBm+ Low Noise Amplifier

Exodus LNA3007-1: 18.0-40.0GHz, 10dBm power, 20dB gain. Small Class A linear design for reliability & ruggedness. Nominal dimensions: 14.95 x 18.8 x 8.9 mm, 2.92 mm K-female connectors.

EXODUS | ADVANCED COMMUNICATIONS

Execution is Everything

Amplifiers
CW & Pulse
Watts to KW

RF & Microwave Amplifiers 10KHz-75GHz

Exodus 18.0 - 40.0 GHz, 25-Watt SSPA AMP2145B-LC

10KHz-250MHz	800MHz-6.0GHz	2.0-8.0GHz	1.0-30.0MHz	2.9-3.5GHz	6.0-18.0GHz
3000 Watts	1000 Watts	500 Watts	500W	1KW Pulse	500W

3674 E. Sunset Road, Suite 100, Las Vegas, Nevada 89120 USA
Tel : 1-702-534-6564 Email : sales@exoduscomm.com

EXODUS ADVANCED COMMUNICATIONS

accuracy.

In the Square Kilometer Array (SKA) and next-generation Very Large Array (ngVLA) radio astronomy science projects, the precise time and frequency distribution is of significant concern. In the SKA project, an H-maser clock needs to be distributed by fiber and then recovered at each dish site to achieve the required frequency stability and phase noise performance. This synchronized frequency signal needs to be distributed to hundreds of receivers in a star-shaped topology. To support astronomical observations, the coherence requirements demand short-term phase stability of better than 1×10^{-12} at $\tau = 1$ sec intervals.[3] High-stability, phase-locked OCXOs are required between H-masers at transmit and receiver sites.

Similarly, autonomous vehicles that use frequency-modulated continuous wave radars present challenges. The frequency accuracy and stability of the reference clocks play essential roles in determining the accuracy and probability of moving target detection.[4] Unless vibration-induced noise caused by road conditions, vehicle acceleration or braking is accounted for, the vibration-induced noise can create OCXO frequency or phase shifts and this will likely degrade the performance of the vehicle's radar receiver.

ACCELERATION-INDUCED CRYSTAL OSCILLATOR PHASE NOISE

It is well-known[5] that when a crystal oscillator of frequency, f_0, is subjected to random acceleration, its resonant frequency shift, Δf, is proportional to the magnitude of acceleration and dependent on the direction of that acceleration. This frequency shift can be written as a vector dot product as shown in Equation 1:

$$\frac{\Delta f}{f_0} = \left(\vec{\Gamma} \cdot \vec{\alpha}\right) \qquad (1)$$

where $\vec{\Gamma}$ and $\vec{\alpha}$ are the acceleration sensitivity and the peak applied acceleration vectors, respectively.

As a result, the associated single sideband (SSB) power spectral density of phase fluctuations, expressed in dB, can be determined as in Equation 2:

$$\mathcal{L}\left(f_a\right) = 20\log\left(\left(\vec{\Gamma} \cdot \vec{\alpha}\right)\right)/2 \cdot \left(f_0 / f_a\right)\Big) \text{ in dBc/Hz} \qquad (2)$$

MITIGATION OF OSCILLATOR VIBRATION

Over the past 40+ years, Quantic Wenzel has developed a variety of methods to counteract vibration-induced signal degradation. Traditional techniques such as crystal selection, passive mechanical isolation and bootstrapping have become mainstays in low phase noise designs for dynamic environments. Quantic Wenzel's latest developments in active vibration compensation, when used alone or in combination with traditional techniques, are enabling further improvement in the state-of-the-art phase noise performance during vibration.

A standard approach to mitigate the effects of vibration-induced phase noise in oscillators is to use passive mechanical dampers or isolators that have a low natural frequency. Examples of this technique include wire rope isolators and compounded elastomeric shock mounts. Depending on the quantity and damping characteristics of the isolators and shock mounts, the size of the oscillator package may increase.

Additionally, the resonant frequency of the vibration-isolated mass can introduce signal degradation. To mitigate this effect, Quantic Wenzel has devised a modular payload system that can adjust this resonance using different combinations of base metals, shock mount configurations and extra masses.

However, active vibration compensation enables real-time detection and compensation of crystal acceleration sensitivity over a wider range of vibration frequencies. Quantic Wenzel has developed analog and digital active compensation techniques to address these active vibration-compensation challenges. These techniques are being implemented across a wide range of induced environmental conditions. They enable the selection of an optimal solution that accommodates size, weight and power considerations.


DC (2.5A MAX)
1625
AC + DC — AC
DC (2.5A MAX)
1623
DC (2.5A MAX)
1626
AC + DC — AC

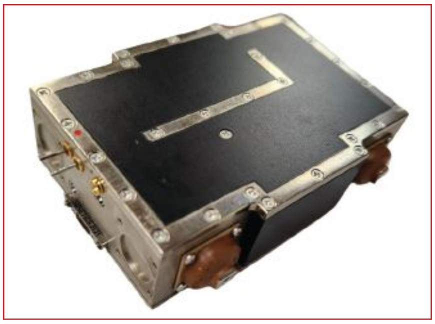

Fig. 1 VXO payload module.

MICROCONTROLLER-BASED VIBRATION COMPENSATION

A recent development at Quantic Wenzel uses a microcontroller-based, vibration-compensated OCXO called a VXO. This VXO combines an active, low phase noise, vibration-compensated ovenized oscillator and a multi-stage multiplier with a sub-Hz digital phase-locked loop that is locked to a high-stability atomic-based reference. This approach includes a low phase noise OCXO and it combines active and passive vibration-compensation techniques in a mixed-signal design to achieve broad frequency range compensation in multiple applications. The microcontroller circuitry consumes less than 150 mA and can accurately estimate the complex conjugate of the vibration-induced phase noise. The circuitry can cancel the noise in real-time, in effect becoming the "brain" of the system. Passive isolators may also be added for improved performance if space permits. The VXO payload may also "learn" its aging characteristics when locked to an Rb or Cs standard. This allows for a long-term holdover time that is useful when the external reference is disconnected or lost. A prototype incorporating this technique is shown in ***Figure 1***. This unit is built and tested using 0.3E-9/g crystal sensitivities, indicating an effective sensitivity per axis of 0.3E-11/g from 8 Hz to 1 kHz.

Figure 2 shows the static (PN) and dynamic (DPN) SSB phase noise results from an OCXO using active vibration-compensation techniques when subjected to a random vibration profile of 0.002 g²/Hz from 8 Hz to 1 kHz. Repeated dynamic phase noise measurements indicate a consistent improvement of 20 dB for all axes from 10 to 100 Hz and greater than 15 dB improvement from 100 to 1000 Hz. When combined with a passive isolation system, this improvement becomes significant even above 100 Hz.

Similarly, ***Figure 3*** shows the Allan Deviation plot of PN and DPN results for an 80 MHz active vibration-compensated VXO that has been subjected to 0.002 g²/Hz random vibration. In this case, the real-time, active vibration-compensation techniques are very effective in reducing

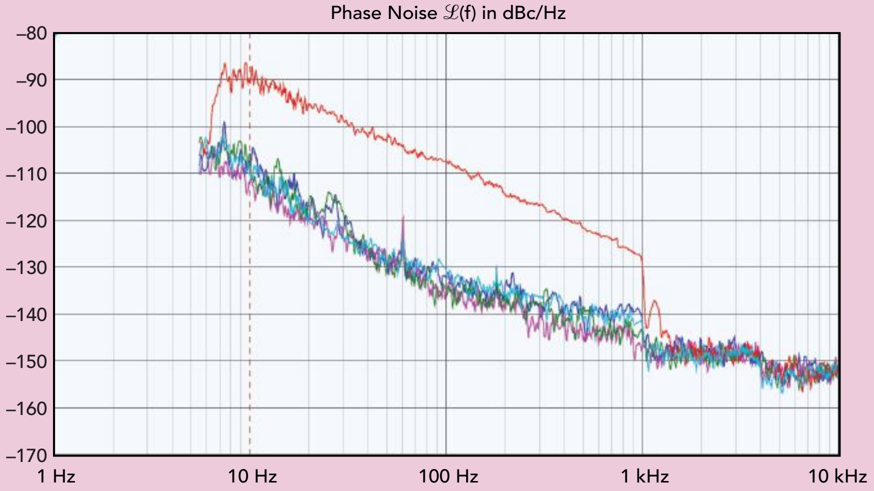

Notes	Input Freq	Input Amplitude	dBc/Hz at 10 Hz	Elapsed	Acquired
VXOM X-Axis DPN	80 MHz	9 dBm	–108.0	2 m 16 s	13629 pts
VXOM Static PN	80 MHz	9 dBm	–111.6	2 m 41 s	16082 pts
VXOM Y-Axis DPN	80 MHz	9 dBm	–106.3	2 m 25 s	14470 pts
VXOM DPN Uncompensated	80 MHz	9 dBm	–90.3	2 m 18 s	13772 pts
VXOM Z-Axis DPN	80 MHz	9 dBm	–110.5	2 m 51 s	17137 pts

Fig. 2 OCXO static and dynamic phase noise with active vibration compensation.

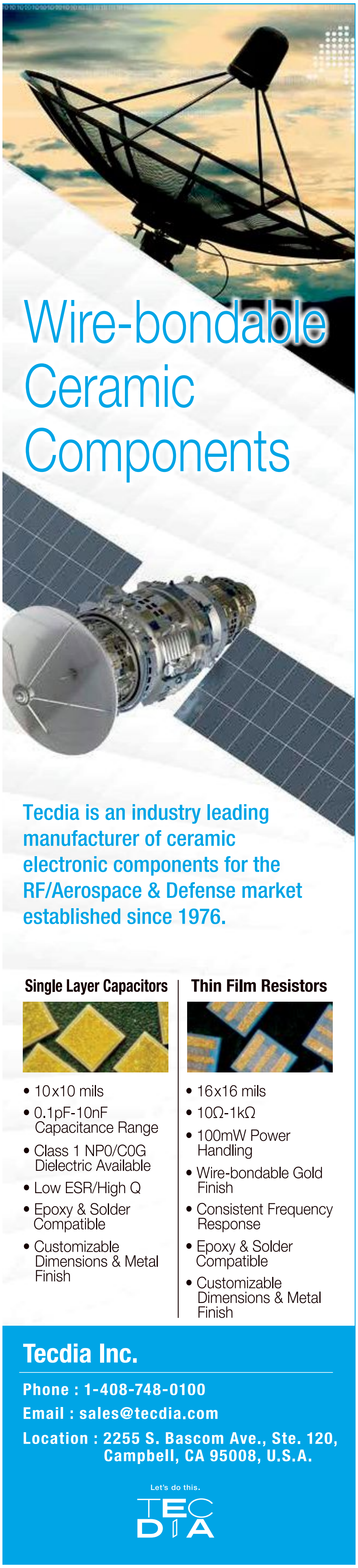

ELEVATE YOUR SIGNALS WITH PRECISION-CRAFTED MILLIMETER WAVE POWER AND LOW NOISE AMPLIFIERS PROUDLY MADE IN THE USA

955 Series
High Power Amplifiers

Frequency- Gains -Pout

27-31 GHz, 31 dB, 20 Watts
26.5-40 GHz, 40 dB, 4.0 Watts
49.5-50 GHz, 40 dB, 25 Watts
49.5-50.5 GHz, 40 dB, 50 Watts
65-70 GHz, 35 dB, 3.0 Watts
71-76 GHz, 25 dB, 5.0 Watts
92-96 GHz, 30 dB, 4.5 Watts

955 Series
Low Noise Amplifiers

Frequency- Gains - Noise Fig

26.5-40 GHz, 20 dB, 3.5 dB
33-50 GHz, 20 dB, 5.5 dB
40-60 GHz, 15 dB, 5 dB
40-60 GHz, 30 dB, 4.5 dB
50-75 GHz, 40 dB, 5 dB
60-90 GHz, 30 dB, 4.5 dB
75-110 GHz, 30 dB, 3 dB

CUSTOM PROJECTS

This a selection of models we've built. Consult with our sales and engineering team for your specific requirements

Millimeter Wave Products, Inc. is an award-winning global provider of millimeter and microwave techology, components, and assemblies.

We offer volume production, individual components, systems, and MORE, in the 7 GHz to 325 GHz spectrum. From standard individual components to custom-designed parts and sub-assemblies, we are your best choice for Millimeter Wave and Microwave Products!

Would you like more information about our components and capabilities? Contact our sales and engineering team today! Apply MiWave's experience, talent, and manufacturing resources to your project for optmized soutions!

MI-WAVE
Millimeter Wave Products Inc.

DIAMOND
SPONSOR
IMS
WASHINGTON, DC
2024

www.miwv.com
sales@miwv.com
727-563-0034

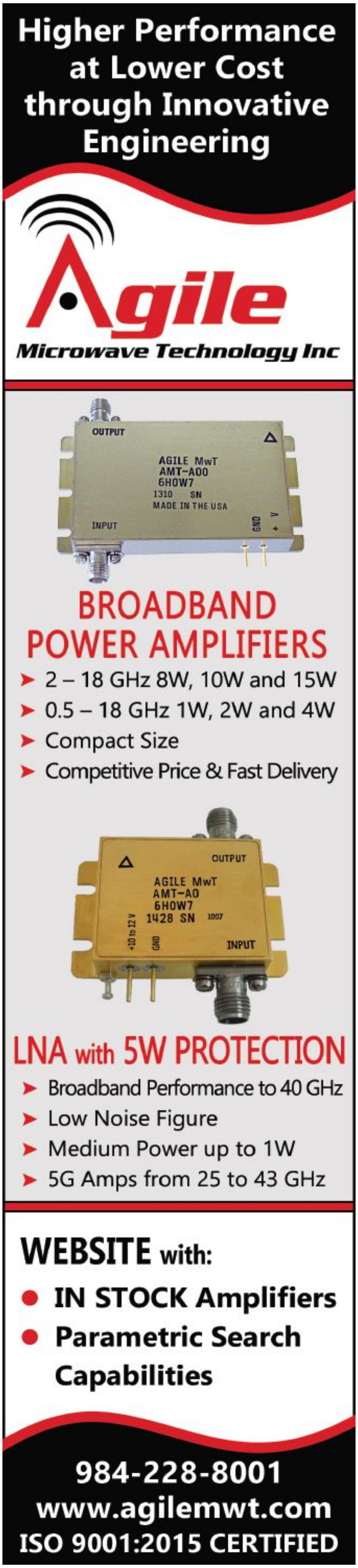

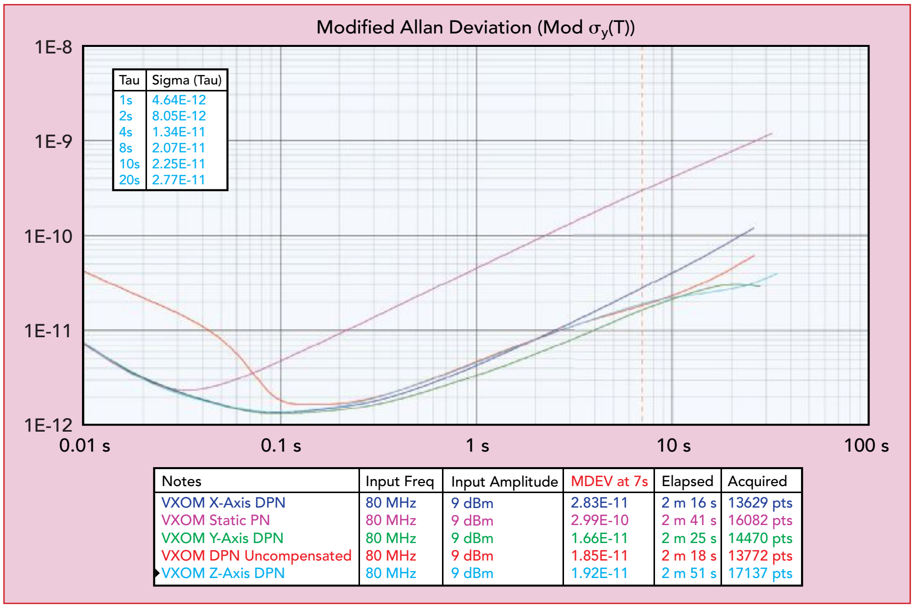

Tau	Sigma (Tau)
1s	4.64E-12
2s	8.05E-12
4s	1.34E-11
8s	2.07E-11
10s	2.25E-11
20s	2.77E-11

Notes	Input Freq	Input Amplitude	MDEV at 7s	Elapsed	Acquired
VXOM X-Axis DPN	80 MHz	9 dBm	2.83E-11	2 m 16 s	13629 pts
VXOM Static PN	80 MHz	9 dBm	2.99E-10	2 m 41 s	16082 pts
VXOM Y-Axis DPN	80 MHz	9 dBm	1.66E-11	2 m 25 s	14470 pts
VXOM DPN Uncompensated	80 MHz	9 dBm	1.85E-11	2 m 18 s	13772 pts
VXOM Z-Axis DPN	80 MHz	9 dBm	1.92E-11	2 m 51 s	17137 pts

Fig. 3 **VXO static and dynamic phase noise with active vibration compensation.**

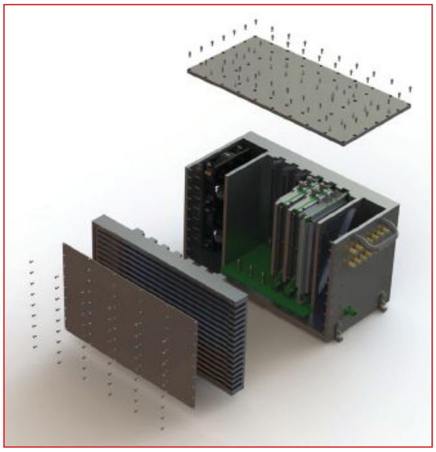

Fig. 4 **Ruggedized conduction-cooled ATR chassis.**

the vibrations in the 0.01 to 1 second range. These techniques can be deployed in a host of systems, providing critical performance improvements in different vibration environments. Tying this all together, the VXO payload has been integrated into a VPX module and into a ruggedized ATR chassis as shown in ***Figure 4***.

CONCLUSION

This paper presented some of the challenges and solutions that led to the development of a compact multiplied crystal oscillator with active and passive vibration compensation. Using these techniques, the crystal sensitivity has been reduced by a factor of 100. The performance improvements achieved are as follows:

- Effective g-sensitivity of less than 0.3E-11/g
- Size of 4 × 3 × 1 in.
- Includes digital PLL, aging compensation and ×30 multipliers
- Automatic calibration of all 3-axes in production
- Vibration compensation of more than 20 dB
- Available in a passively vibration-isolated or hard-mounted single module or a 3U VPX plug-in module with multiple low and high frequency outputs. ■

References

1. Z. Chen et al, "A Low Phase Noise Microwave Source for Atomic Spin Squeezing Experiments in Rb," arXiv:1204–4215, *[physics.atom-ph]*, 2012.
2. M. Ahmed et al, "The Brazilian Time and Frequency Atomic Standards Program," *Annals of the Brazilian Academy of Sciences*, pp. 217–252, 2008, Web: https://doi.org/10.1590/S0001-37652008000200002.
3. B. Wang, et al., "Square Kilometre Array Telescope—Precision Reference Frequency Synchronization via 1f-2f Dissemination," *Sci. Rep. 5*, 13851; doi: 10.1038/srep13851, 2015.
4. F. Hau, F. Baumgärtner and M. Vossiek, "Influence of Vibrations on the Signals of Automotive Integrated Radar Sensors," *IEEE MTT-S International Conference on Microwaves for Intelligent Mobility (ICMIM)*, Nagoya, Japan, 2017, pp. 159–162, doi: 10.1109/ICMIM.2017.7918881.
5. A. Hati, C., Nelson and D. Howe, "Vibration-induced PM Noise in Oscillators and its Suppression," *I-Tech Education and Publishing*, Vienna, AT, 2009, Web: https://tsapps.nist.gov/publication/get_pdf.cfm?pub_id=842 583.

INVITED PAPER

The Sky is The Limit for Open-Field and Live-System RF Testing

Dr. Don Goodeve
SixArms/RadioCode Inc., British Columbia, Canada

Jason Schreiber
SixArms, Queensland, Australia

Testing antenna systems in a realistic deployment environment presents many challenges. While highly-controlled laboratory-based methods remain critical in the design, development and quality control of RF systems, the deployment environment is the ultimate arbiter of performance. In addition, traditional testing approaches can encounter significant constraints when testing large, high-power systems or in installations where there is the potential for complex interference between systems components.

This article discusses the advent of drone-based radio measurement systems. It will explore the challenge of transforming versatile, lightweight drone platforms into high performance radio testing platforms. Their rapid movement and precise 3D positioning can allow open-field and in-situ testing to be utilized where traditional techniques are unavailable and/or cost-prohibitive. A case study exploring the use of practical commercial drone-based measurement technology will be presented, demonstrating the effectiveness of this approach.

The modern environment contains a profusion of radio technologies. Innovation is rapid and the need to be able to evaluate new antenna designs and installations effectively and quickly is pressing. The goal is to accurately characterize the performance of an antenna system that can be expected in a real-world environment.

IDEAL MEASUREMENT ENVIRONMENT

The ideal is to remove all outside influences from the measurement of an antenna system. To perform such measurement requires a shielded environment that is fully impedance-matched with free space, ensuring that all that is measured is the antenna system itself. Once such measurements are obtained, the impact of real-world influences can be superimposed to approximate expected real-world performance.

Open-Field Measurements

An open-field measurement site may provide many of the features required, however proximity to the ground causes coupling, which must either be eliminated or fully accounted for in measurements.[1] A clear advantage of this approach is that measurements may be made at a sufficient distance that far-field performance is measured directly. The addition of suitably designed rotation/translation equipment makes scanning possible, however careful design is required to eliminate the artifacts that make such equipment expensive. Exposure to the elements introduces variability that can be challenging to control and account for, except in stable, hot desert environments.

Chamber-Based Measurements

To address the limitations of open-field testing, controlled environments integrating impedance matching (reflection absorbing) materials to approximate open-field performance, along with the device under test (DUT) and measurement antennas enable high-quality predictive measurements.[2] Limitations of such environments are size and the associated cost of developing and maintaining these resources. The use of smaller, portable chambers begins to address the issues of cost and maintenance. However, the size limit creates additional constraints, such as the need to operate in the near-field, derive the approximate far-field performance and the limited size of the DUT.

Freely-Positioned Measurement Devices

Open-field measurement is an attractive approach. However, a key problem arises when measuring the radiated field if the required measurement scope exceeds the parameters of any purpose-designed measurement range. If it were possible to measure the radiated field at any position, in any orientation and at any distance around an antenna, then a new space of possible measurement approaches would become available.

In-Situ Measurements

The ultimate arbiter of performance is how antennas perform in the application environment, whether they are mounted on a tower, a ship, an airframe or any other application where installation location, installation faults and other interfering equipment will contribute to system performance. These environments are also not ideal, with factors like obstructions, reflections and weather influencing the system behavior.[3] These influences are approximated in system design, but real-world surprises still abound, leading to unexpectedly poor performance. The diagnosis of and solution for these issues requires in-situ measurement. Current techniques for this are limited to utilizing ground-based antennas up to approximately 10 meters above the ground or commercial helicopters with their attendant complexity and cost. Standards for such measurements have been developed.[4]

DRONE-BASED MEASUREMENTS

The remainder of this article addresses the use of modern drone technology to both provide for an expansion of the open-field testing approach and to offer, for the first time, a means to provide high-quality in-situ diagnostic measurements during normal system operation across a wide variety of antenna system applications. The aim is to provide this test capability rapidly and at a low cost.

Fig. 1 **Integrated drone-based measurement platform.**

Enabling Technologies

An ideal, freely-positioned measurement device can be approximated using modern rotor-based drone technology and low-cost, high performance, headless software-controlled radio receivers. An example of this technology is shown in ***Figure 1***.

Drone Platforms

Early drone platforms experimented with several configurations. Typical attributes of modern drone platforms that can be used for this type of operation are:[5-8]

- A quadcopter configuration that is typically 85 to 100 cm in diameter
- 1.5 kg payload capacity
- 20 to 30 W available payload power supply
- 30-minute flight time
- Direct communication from the flight controller to the payload is available
- Automatic waypoint generation and flight control.

Headless Software-Controlled Radio Platforms

Disruption to traditional radio measurement has arisen in the form of high performance headless programmable radio platforms or software-controlled receivers (SCRs). Utilizing modern design techniques, these devices boast performance comparable to high-end integrated measurement equipment. However, they lack a purpose-built user interface because they require the use of a host computer to provide an application solution like traditional spectrum analysis. When first introduced, these platforms had significant sampling speed and frequency range performance constraints, but these limitations have been aggressively addressed in subsequent generations. Current devices offer full traceable calibration and can cover frequency ranges from 9 kHz to 40 GHz, exploiting high speed communications such as USB 3 and gigabit Ethernet to realize performance that directly competes with traditional integrated measurement platforms. A representative sample of offerings is presented in the references.[9-11] Typically, these SCR platforms have a dynamic range better than 90 dB, noise figure better than -154 dBm/Hz, low phase noise and excellent image rejection.[9]

Drone Compatibility

A limitation of drone platforms is the available payload weight and power supply performance. Any measurement mission will require sufficient autonomy to perform the required measurement sweep in a single flight. Fortunately, recent innovations have delivered high performance, low-weight, low-power SCR packages that are compatible with current drone technology.[9,11]

Compute Platforms

Single-board computers based on Intel and ARM architectures are widely available. They are both lightweight and have low power demands, providing sufficient support for suitable SCRs while not exceeding feasible drone payload constraints. Single-board compute platforms can also integrate significant processing through multi-core CPUs and inexpensive low-power, high speed storage using solid-state drive technology such as contemporary M.2-type units with high capacity and excellent write performance.

SOFTWARE

Leveraging these component technologies to provide a complete measurement solution requires the addition of various software components that are briefly outlined below.

Data Capture

The APIs for SCRs are diverse; standards such as VITA49.112 do not enjoy significant support. Despite this apparent limitation, the task of programming data capture, even for diverse device types, is straightforward, as API design has evolved toward ease of use. Most SCR APIs[5,6] provide for both swept spectrum capture and time-domain (IQ) capture with flexible parameter programming utilizing modern host languages like C++ and Python. For both measurement modes, the state-of-the-art capture rates achieved by feasible drone payloads can be extremely high; on the order of 20 GHz/sec scan rate for spectral capture at 10 kHz RBW and up to 40 MHz for continuous IQ capture. The expectation is that these figures will only improve with time.[9-11] These levels of performance imply captured data rates on the order of 100 MB/sec. A single 30-minute flight could theoretically generate on the order of 200 GB of data.

Data Fusion

The SCR and compute platform will provide IQ or swept-spectra radio data correlated with time. The flight control system utilizes referenced GPS and it provides highly accurate position data with centimeter resolution correlated with time.[5-8] Combining these data streams provides the calibrated radio measurement data, accurately positioned in space and time, that are of critical importance.

The required spatial resolution is a constraint that must be accounted for in such a fusion of data. Consideration must be taken for the capture rate for the required data, versus the programmed spatial tracking speed of the drone platform. Once a measurement pattern is determined, software can provide the constraints required for flight path planning. In practice, this does not significantly constrain drone tracking speed.

In-Flight Processing

While it is feasible to capture all the data from a flight, a more sophisticated measurement approach will typically be utilized to maximize efficiency. Where a complex installation is being measured, there may be multiple disjointed bands of interest. A single "tuning" may not capture all the required data and if this occurs, dynamic switching between measurement bands may be required. Multiple antennas may be required to capture all the data and this requires more sophisticated sequencing.

Data compression is another reason for using in-flight processing. While it may be feasible to capture all the data from a flight, transferring that data to a host platform may require considerable time to facilitate post-processing. Instead, a hybrid approach can be used that captures a subset of full-bandwidth data to allow measurement verification, while abstract measurements like channel RSSI, along with pulse rise and fall times can be recorded for the full measurement sequence.

Level Adaption

Signal level optimization is an additional challenge that is normally accounted for by a technician in a controlled measurement environment. Signal capture platforms have a finite, constrained dynamic range. Most SCR platforms provide programmable signal path gain/attenuation to optimize the available dynamic range for the best signal fidelity for the measurement being made. Utilizing dynamic adaption managed during collection by flight software ensures that signal quality is maximized while trading off against capture performance. A versatile approach allows different techniques to be chosen for different measurement tasks to allow exploitation of this trade-off. These techniques include one-off initial calibration, adaptive/tracking or continuous recalibration for rapidly changing or intermittent signals.

Report Generation

Accurate, position-correlated measurement is essential, but it is not sufficient to produce an effective measurement platform. A clear advantage of the headless programmable SCR approach is that all the measurement information is directly available on a general-purpose computing platform where it may be rapidly processed into relevant information for the user. Such processing is even possible during flight, utilizing a telemetry link to deliver early reporting. This reporting demonstrates that the measurement mission is proceeding as intended and it allows real-time operator decisions to optimize the use of flight time. Once a drone has landed, all the data can be rapidly downloaded to a host, facilitating complete report generation. This method realizes an integrated, high-quality, system-measurement solution that does not require a high degree of operator expertise.

CASE STUDY: IN-SITU BROADCAST ANTENNA MEASUREMENT

The ability to measure systems in-situ in normal operation and obtain extensive, accurate diagnostic data at a low cost enables system qualification at installation and proactive ongoing maintenance. This case study utilized a drone platform with radio measurement payload and test antennas, like that shown in ***Figure 2***.

Measurement Setup

To examine the target broadcast system antenna, a standard flight plan[4] was designed to ensure adequate coverage of the expected antenna pattern at the anticipated output power level. Note that in a measurement scenario, a significant amount of calibrated attenuation may need to be added to the signal path from the measurement antenna to ensure the maximum input power of the SCR is not exceeded. Before launch, a suitable test antenna configuration is selected and connected to the in-flight measurement SCR. The antenna and cable setups are calibrated before deployment and on an ongoing basis. The drone platform is then programmed for the required flight plan and the telemetry link from the drone SCR

▲ Fig. 2 **Example drone platform.**

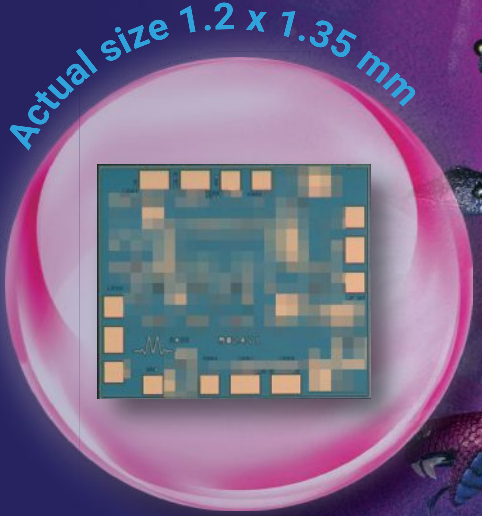
Actual size 1.2 x 1.35 mm

measurement platform is confirmed to be operational. The measurement flight path, showing data collection segments in green and intervening drone transit paths in red, overlayed on a perspective image of the test location is shown in ***Figure 3***.

The flight plan consists of a series of vertical climb/descent sections used to determine the elevation of the main beam of the antenna at a suitable measurement distance. These are then followed by a 360-degree orbital sweep on the measured elevation of the antenna main beam at this radius. During this capture, received signal power is integrated over the bandwidth of one of the active antenna broadcast channels. Note that multiple channels can be measured within a single flight, if required.

Results

This section shows the results from the measurement flight path. ***Figure 4*** shows the elevation pattern for an antenna determined by a vertical scan at the center of the discovered main beam. ***Figure 5*** shows the telem-

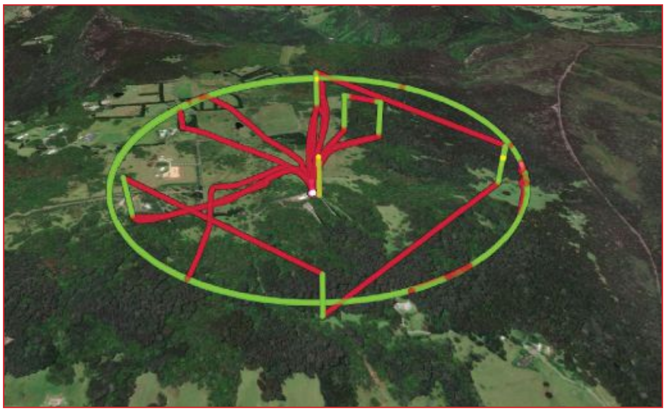

Fig. 3 **Measurement flight path.**

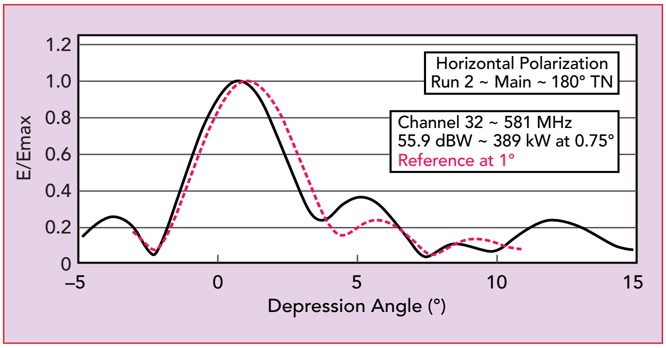

Fig. 4 **Measured elevation pattern.**

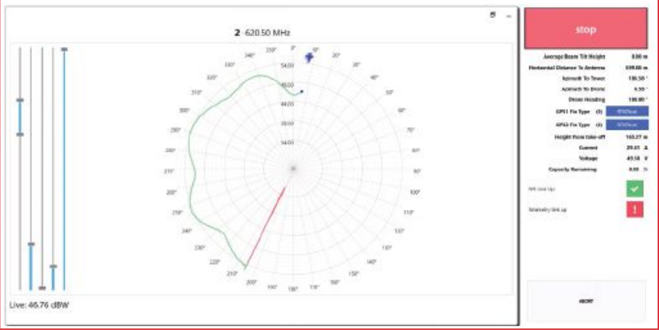

Fig. 5 **Telemetry link to optimize data collection time.**

MiCable

NEW

0.4-8GHz HIGH POWER Directional & Dual-Directional Coupler

- High power handling : up to **600W**
- Low VSWR & insertion loss
- Excellent coupling, flatness and directivity which will significantly improve the signal acquisition accuracy
- Environment conditions meet MIL-STD-202F

P/N	CW Power Max.(W)	Nominal Coupling (dB)	Main Line VSWR	Coupling VSWR	Insertion Loss*	Coupling	Flatness	Directivity Min.(dB)
			Max.(:1)		Max.(dB)			
0.4-8GHz Directional Coupler								
D3002H004080	120	30	1.3	1.3	0.8	30±1.0	±0.8	18
D4002H004080	120	40	1.3	1.3	0.8	40±1.0	±0.8	18
D3005H004080	250	30	1.4	1.4	0.7	30±0.9	±1.3	14
D4005H004080	250	40	1.4	1.4	0.7	40±1.0	±1.4	14
D3008H004080	400	30	1.4	1.4	0.7	30±0.9	±1.3	14
D4008H004080	400	40	1.4	1.4	0.7	40±1.0	±1.4	14
D3012H004080	600	30	1.4	1.4	0.7	30±0.9	±1.3	14
D4012H004080	600	40	1.4	1.4	0.7	40±1.0	±1.4	14
0.4-8GHz Dual-Directional Coupler								
D3002HB004080	120	30	1.3	1.3	0.8	30±1.0	±1.0	18
D4002HB004080	120	40	1.3	1.3	0.8	40±1.0	±1.0	18
D3005HB004080	250	30	1.4	1.4	0.7	30±0.9	±1.5	14
D4005HB004080	250	40	1.4	1.4	0.7	40±1.0	±1.6	14
D3008HB004080	400	30	1.4	1.4	0.7	30±0.9	±1.5	14
D4008HB004080	400	40	1.4	1.4	0.7	40±1.0	±1.6	14
D3012HB004080	600	30	1.4	1.4	0.7	30±0.9	±1.5	14
D4012HB004080	600	40	1.4	1.4	0.7	40±1.0	±1.6	14

*Theoretical I.L. Included

— Test Curve —
D4012H004080

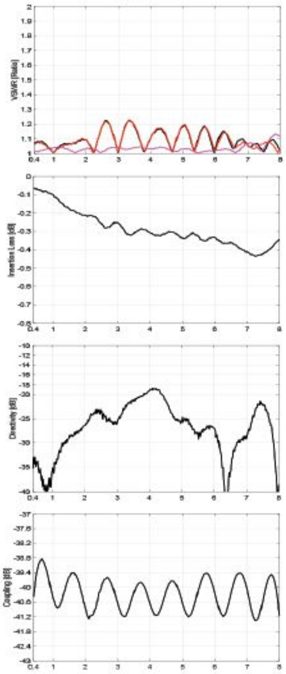

More Information-
Scan the QR Code

MIcable Inc.

www.micable.cn ✉ sales@micable.cn ☎ +86-591-87382856

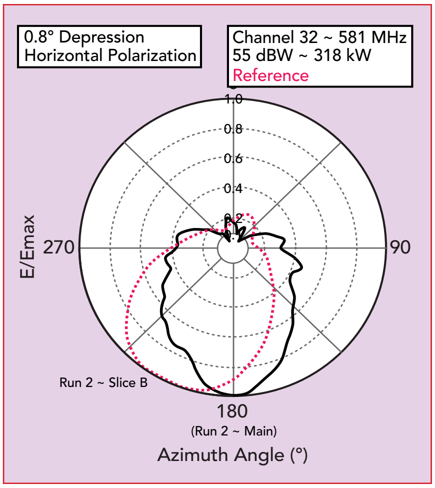

▲ Fig. 6 **Polar plot of signal strength from a 360-degree orbital sweep on antenna main beam.**

etry link that allows real-time display of collected data to validate the in-flight decision-making to optimize collection time.

Figure 6 shows the measured antenna output as a solid line, versus the designed pattern shown in the dashed line. It is clear from this measurement that the antenna output is close to what is expected, but the antenna directional output is approximately 30 degrees off the designed azimuth. This error led to a violation of the broadcast license by the operator and poor system performance in the desired reception area.

Other issues can be identified from similar measurements. ***Figure 7*** illustrates sweep results identifying manufacturing defects and ***Figure 8*** illustrates the effects of complex structural interference with the designed antenna output profile.

Direct measurement of deployed and active antenna systems delivers valuable engineering data. The cost-effectiveness and speed with which standardized drone-based measurements can be performed transform this type of measurement from a reactive diagnostic tool to an installation and proactive maintenance tool for system designers and installers.

FUTURE DIRECTIONS

First-generation systems have provided the ability to measure signal strength in space and provide useful data on fixed antenna systems for broadcast-type applications. This covers a wide application space in terrestrial broadcast, cellular and public safety markets. These systems have largely relied on spectral-type measurements and straightforward signal strength determinations from one or more drone-mounted antennas.

Second-generation systems are integrating more sophisticated abilities to process time-domain signals enabling the evaluation of, for example, pulsed radar systems. The addition of more advanced demodulation software on the flight platform enables deeper characterization of signals. These characterizations include things like the complex impacts of multi-path, fading and signal distortion.

Additional opportunities will arise in applications that value the ability to obtain high-quality, spatially accurate measurements at a low cost. These applications may in-


RF-LAMBDA EUROPE


RF-Lambda
RFSP160TA0020G-S
F:0.05-20GHz
SN:16010600274
J0
TTL

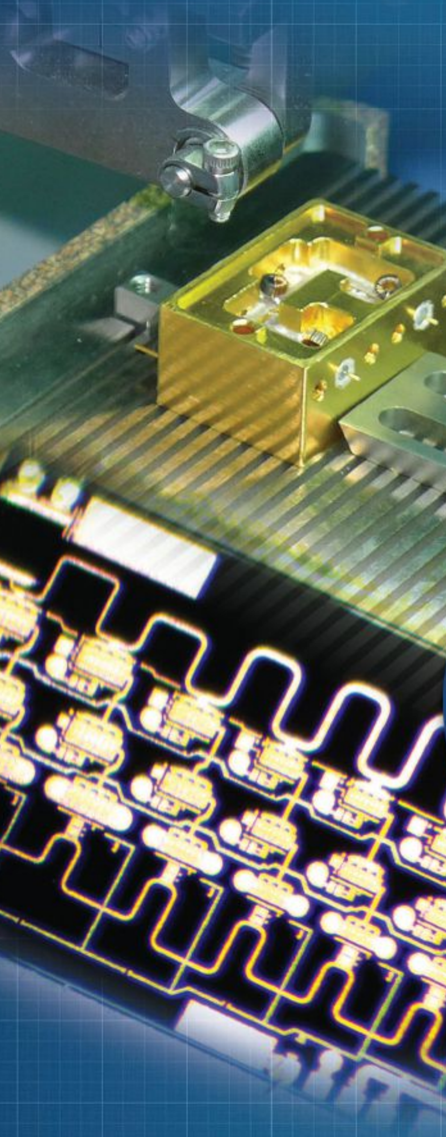


RF-Lambda
RFSP32TA5M43G-S
F:0.5-43.5GHz
SN:16011400065


RF-Lambda
RFSP16TA5M43G-S
F:0.5-43.5GHz
SN:16011400064

clude aviation navigation aids such as Localizer/Glideslope and VOR. For these applications, traditional measurement and characterization approaches are highly time-consuming and expensive.

CONCLUSION

Modern drone platforms combined with evolving high performance programmable receivers combine to open a new range of approaches to antenna systems measurement. The exploitation of this approach is in its infancy as a complement to traditional measurement and system diagnostic techniques. It is exciting to be at the forefront of this innovative approach and to participate in a revolution in radio systems measurement. For the future of radio systems measurement, the sky truly is the limit.

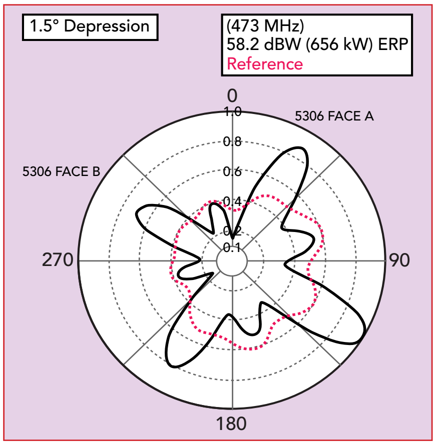

Fig. 7 Manufacturing errors impact omnidirectional radiation pattern.

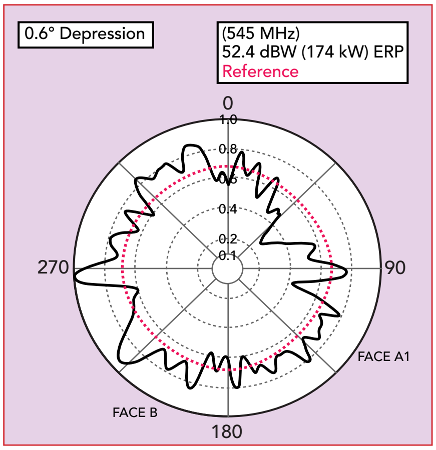

Fig. 8 Complex structural interference impacts omnidirectional radiation pattern.

References

1. J. F. Aubin. "A Brief Tutorial on Antenna Measurements," *Microwave Journal*, Vol. 48, No. 8, August 2005.
2. D. Campbell et al., "Simulating Antenna Measurements in an Anechoic Chamber,"*Microwave Journal*, Vol. 57, No. 5, July 2014.
3. H. L. Bertoni, "Radio Propagation for Modern Wireless Systems," *Pearson Education 1999*.
4. "Airborne Verification of Antenna Patterns of Broadcasting Stations," ITU-R SM.2056-1, 2014.
5. "Freefly Systems Astro RTK," Web: https://freeflysystems.com/astro.
6. "DJI Matrice 300 RTK," Web: https://enterprise.dji.com/matrice-300.
7. "Acecore Zoe," Web: https://acecoretechnologies.com/zoe/.
8. "Aeronavics Navi," Web: https://aeronavics.com/models-of-drones/navi/.
9. "Signal Hound Spectrum Analyzers," Web: https://signalhound.com/.
10. "ThinkRF R5750 real-time spectrum analyzer," Web: https://thinkrf.com/products/Real-time-Spectrum-Analyzers/r5750-real-time-spectrum-analyzers.
11. "Harogic Spectrum Analyzers," Web: https://harogic.eu/.
12. "VITA Radio Link Layer Protocol (VRL) Standard," VITA 49.1, *VMWBUS International Trade Association (VITA)*, 15th Edition, 2021.

KRATOS®
MICROWAVE USA

High-Performance SSPAs with demonstrated reliability

Kratos Microwave USA, formerly CTT, has over 40 years of experience in the design and manufacture of microwave amplifiers, frequency converters and integrated assemblies delivering high-performance solutions for advanced defense platforms.

Since our inception, we have delivered thousands of microwave products for various military applications. Our San Jose, California manufacturing facility supports a mix of both low-volume and high-volume builds based on program specific needs. Design and construction utilize both SMT and hybrid chip and wire manufacturing techniques as necessary for specific products and applications.

Additionally, we offer rapid prototype development, highest packaging density, and a flexible engagement model including build-to-print capabilities.

Kratos has an extensive portfolio of power amplifiers covering 1 to 40 GHz with power levels ranging from 300W CW to 2kW pulsed for aerospace, defense, and instrumentation customers. Our products support various Radar, EW, and Communications applications meeting unique mission specific electrical and environmental requirements.

Kratos amplifier products utilize GaAs and GaN technologies selected to meet SWAP-C challenges. Kratos engineering is constantly evaluating new semiconductor devices to develop market-leading high-density and high-efficiency SSPAs. Amplifiers can be supplied as individual modules, as part of integrated assemblies, or in rack-mount configurations. Options include integrated power supply, heat sink and micro-controller for control and display.

Kratos GaN SSPAs are designed for
☐ Small Form Factor
☐ Decoys & Expendables
☐ SAR, TCDL, UAVs
☐ AESA Radar Systems
☐ EW: ECM, ECCM & ESM

Contact Kratos Microwave USA today for more information.

Narrowband Capability		Broadband Capability	
Band	Output Power	Freq. (GHz)	Output Power
L & S	2000W (Pulse)	1-2, 2-4, 2-6	200W (CW
C & X	1000W (Pulse)	4-8, 6-12	150W (CW)
Ku	100W (CW)	6-18	80W (CW)
Ka	50W (CW)	2-18	40W (CW)

AS9100D
ISO 9001:2015

❖ High Power Amplifiers ❖ Low-Noise Amplifiers ❖ Integrated Microwave Assemblies ❖
❖ Transceiver Modules ❖ Frequency Converters ❖

www.kratosdefense.com
Kratos Microwave USA • 5870 Hellyer Avenue • San Jose • California 95138
Phone: 408-541-0596 • E-mail: microwavesales@kratosdefense.com

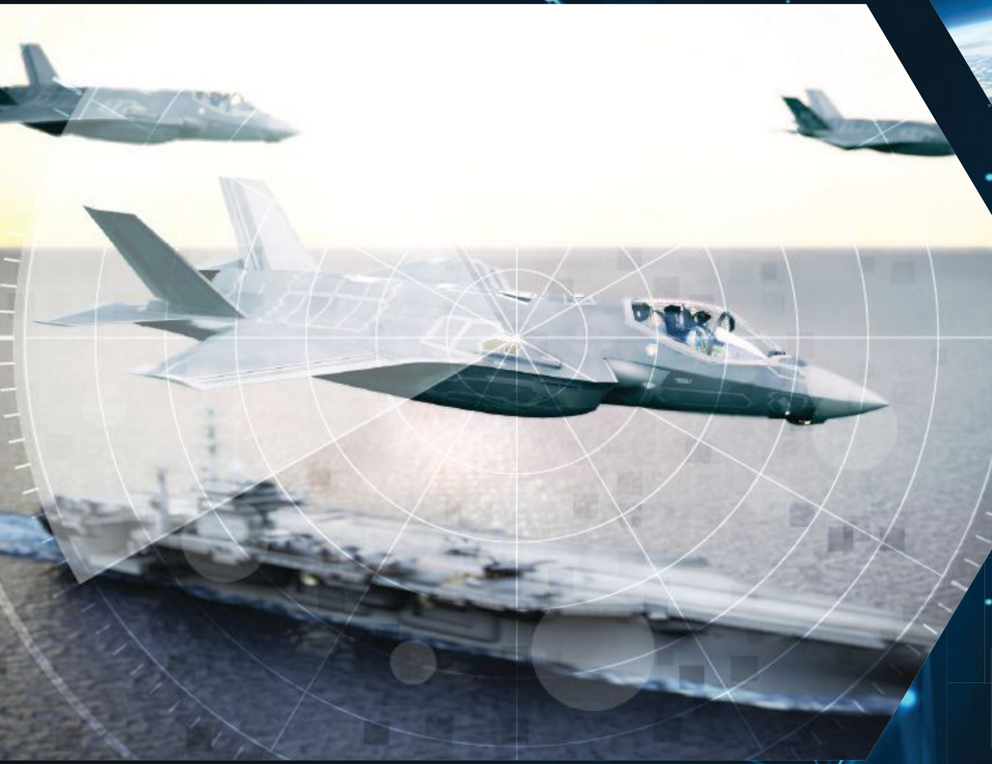

Design of Dual-Layer Curved Cylindrical FSS with Sharp Roll-Off and Flat Bandpass Property

Saptarsika Das, Ramesh Chandra Tiwari and Lourembam Lolit Kumar Singh
Mizoram University, Mizoram, India

Nurnihar Begam, Rahul Mondal and Partha Pratim Sarkar
University of Kalyani, West Bengal, India

Durjoy Roy
Rishi Bankim Chandra College, Naihati, West Bengal, India

The frequency selective surface (FSS) has been the subject of extensive research for the last three decades. An FSS acts like a bandpass or bandstop filter at microwave frequencies. Extensive research has been done on bandwidth enhancement and the decrease of insertion loss, for example, but this work has been done mainly on planar FSSs. Very little work has been done on curved FSSs. The design of a dual-layer curved cylindrical FSS with the sharp roll-off and flat bandpass properties described here can reduce interference and increase channel capacity in a communication system.

The FSS is a spatial filter in the radio frequency range. It comprises a periodic arrangement of identical elements in a 1D or 2D array. Patch and aperture are two fundamental types. A vast amount of research has been done on planar FSSs because a unit cell of an infinite array can be used for the analysis and comprehensive study of the entire structure. The same approach cannot be taken for a curved structure as its extrapolation from a single unit cell is not possible because, for certain incident fields, element currents and scattering from the edges of the curved surface diverge significantly.[1] Hence, the curved FSS is a mathematically complex structure and is difficult to analyze.

While wide bandwidth is the basic requirement for high speed communications, roll-off plays an important role in reducing noise and interference during the transition from the passband to the stopband. Good roll-off has been documented with aperture-type planar FSSs having Archimedean spiral and annular ring elements.[2-4] Wideband and multiband aperture-type planar FSSs have been reported. A flat passband response with high roll-off has been achieved.[5,6]

A bandpass planar FSS with a square slot exhibited 2.7 GHz bandwidth with left and right roll-offs of 7.33 dB/GHz and 30 dB/GHz, respectively.[7] A polarization-insensitive FSS was designed using a square unit cell loaded with two pairs of ring slots and one split-ring slot pair.[8] The structure demonstrated good transmission characteristics within the passband with a steep roll-off. These planar structures are excellent candidates for high performance passband FSSs and can be designed easily. The task of achieving high performance with sharp roll-off, wide bandwidth and low insertion loss, however, is not easy to realize in a curved structure, as the nature of the transmission

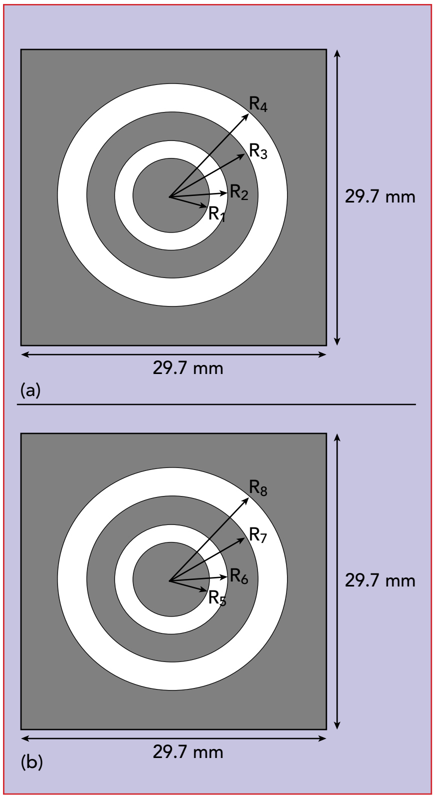

Fig. 1 **FSS unit cells: Layer 1 [R_1 = 5.5, R_2 = 8.75, R_3 = 10 and R_4 = 14 mm] (a), Layer 2 [R_5 = 6, R_6 = 8.25, R_7 = 10 and R_8 = 14 mm] (b).**

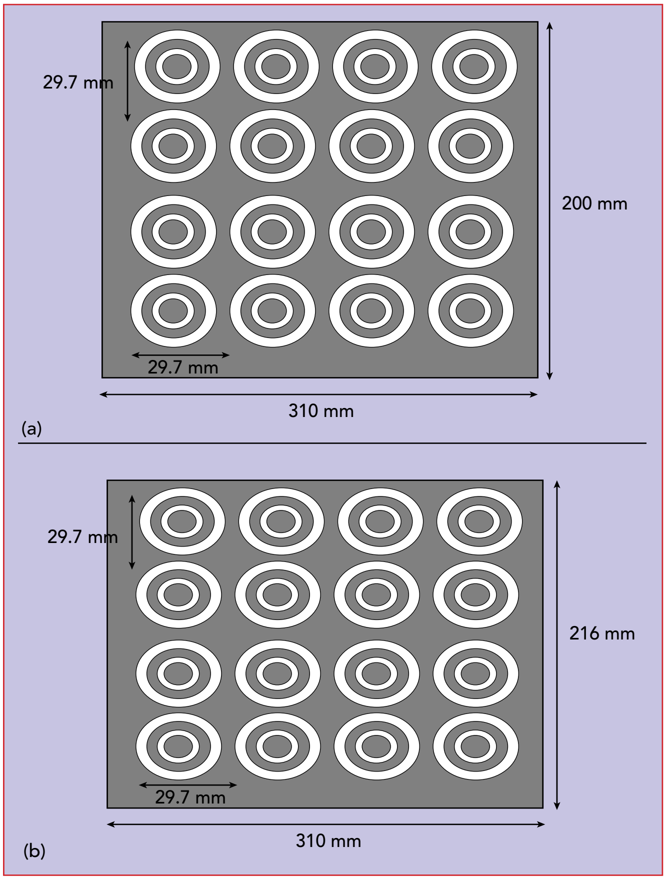

Fig. 2 **FSS layers: Layer 1 (a) and Layer 2 (b).**

curve entirely depends on the FSS element, the lattice and the degree of surface curvature.

The properties of curved FSSs have been studied using basic elemental structures like tripoles, circles and others.[9-11] A design with a tripole element,[9] resulted in reduced bandwidth for a curved structure as compared to a planar FSS. A sandwich radome wall investigation was carried out using a double square loop FSS structure.[12] The conformal FSS resulted in enhanced bandwidth and high roll-off, however, no experimental validation was provided.

A spherical dome-shaped FSS with a radius of 50 mm demonstrated wideband performance but with a poor roll-off.[13] The study of a single-layer hemispherical FSS with a novel-shaped element demonstrated a wide band response with an approximate roll-off of 9 dB/GHz,[14] while a double-layer ring slot planar and curved FSS exhibited a good bandpass response over a large angle of incidence.[15]

This article describes the design, simulation and measurement of a dual-layer semi-cylindrical curved FSS with concentric annular ring elements. The structure provides a wide passband response in X-Band. It can be used as a bandpass filter with 45 percent bandwidth which is almost the same for planar and curved structures. It demonstrates that an FSS can be designed to work on a curved surface and achieve a wide bandwidth, low insertion loss and sharp roll-offs at both band edges.

DESIGN

Figure 1 shows the unit cell of a dual-layer aperture-type planar FSS. Two concentric annular rings of different radii are periodically arranged in a metallic screen to configure both layers of the aperture. Aluminum foil paper is used as a metallic sheet and air is the dielectric. The periodicity of the FSS is 29 mm in both vertical and horizontal directions. An air gap of 7.6 mm between the two layers is determined to be optimum. The structure is simulated using Ansys HFSS. The two planar layers of the composite FSS are shown in ***Figure 2***.

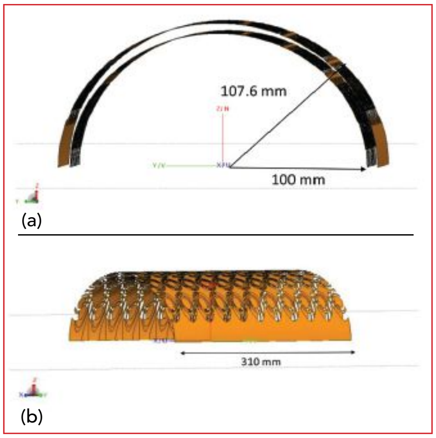

Fig. 3 **Semi-cylindrical FSS: front view (a) and side view (b).**

The dual-layer semi-cylindrical aperture-type FSS is designed, keeping the dimensions of the elements and periodicity like that of the designed planar structures. The radii of the inner layer and outer lay-

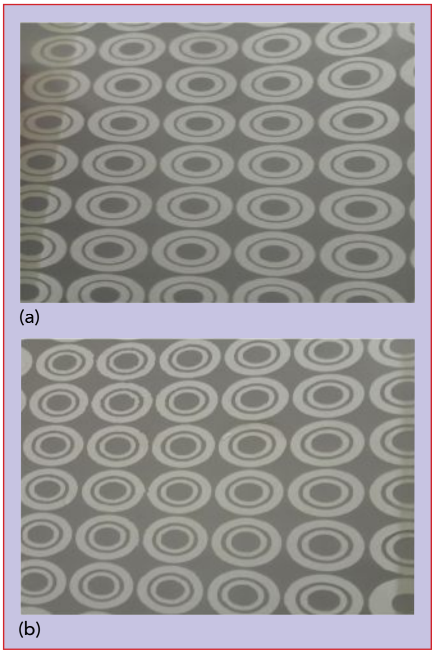

Fig. 4 **Fabricated FSS layers: Layer 1 (a) and Layer 2 (b).**

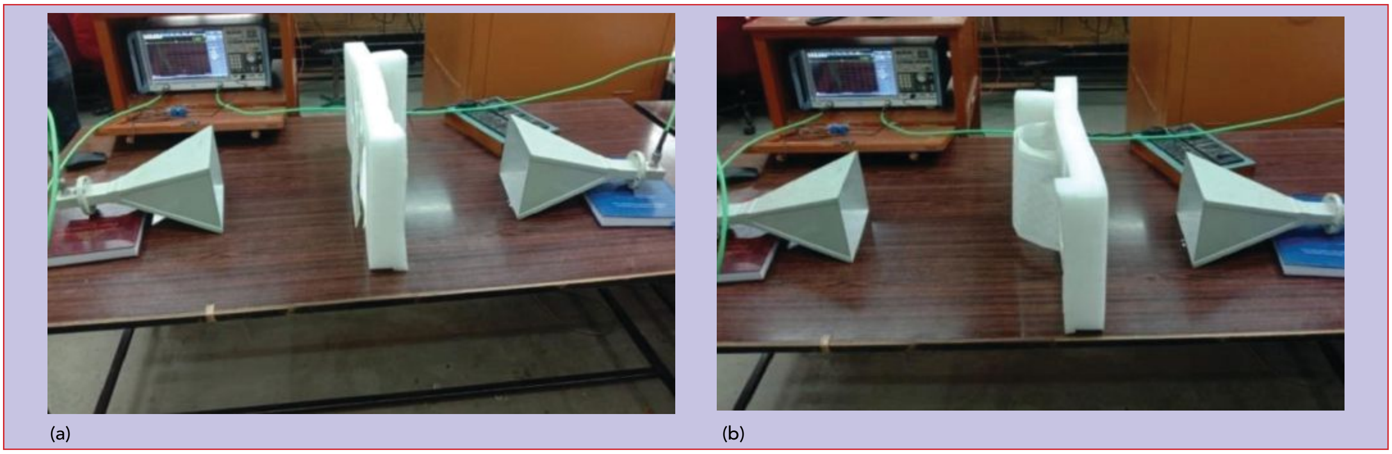
(a) (b)

Fig. 5 **Measurement setup: planar FSS (a) and curved FSS (b).**

TABLE 1

PLANAR FSS PARAMETRIC STUDY RESULTS

Air Gap Between FSS Layers (mm)	Left Roll-Off (dB/GHz)	Insertion Loss (dB)	Right Roll-Off (dB/GHz)
6	39	0.7	16.67
7.6	45	0.3	73.33
8	49.02	0.9	35.05

er of the semi-cylinder are 100 and 107.6 mm, respectively, maintaining the optimized planar air gap of 7.6 mm. The length of the semi-cylinder is 310 mm. The dimensions of the semi-cylinder are limited, as simulation of the curved FSS requires high computational resources.

Two views of the final dual-layer semi-cylindrical curved FSS design are shown in ***Figure 3***. The design and simulation are done in Altair CADFEKO simulation software. The fabricated FSSs are shown in ***Figure 4***. The measurement of both the planar and curved structures is done using a standard microwave test bench (see ***Figure 5***).

RESULT AND DISCUSSION

A parametric study of the planar structure varies the air gap between the two layers (see ***Table 1***). The simulated optimal value of insertion loss is about 0.3 dB for the 7.6 mm air gap. Hence, further study is done using 7.6 mm. The transmission characteristic of dual-layer planar structure with that air gap is shown in ***Figure 6***.

Good bandpass performance is demonstrated experimentally for the planar FSS in the frequency range of 6.7 to 10.7 GHz. Insertion loss is low with a -10 dB bandwidth of 4 GHz (45.96 percent). The planar structure exhibits a sharp roll-off of 45 dB/GHz (left) and 73.33 dB/GHz (right). The experimental result is in good agreement with the simulation. A comparison of the planar structure's performance with other reported work is shown in ***Table 2***. It exhibits a wider bandwidth and sharper roll-offs on both band edges.

Results for the dual-layer semi-


MRFCP6762

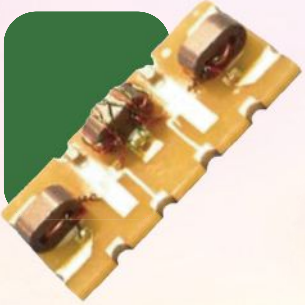

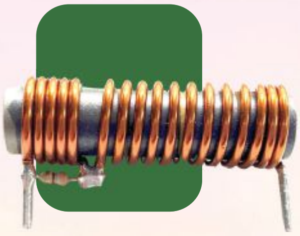

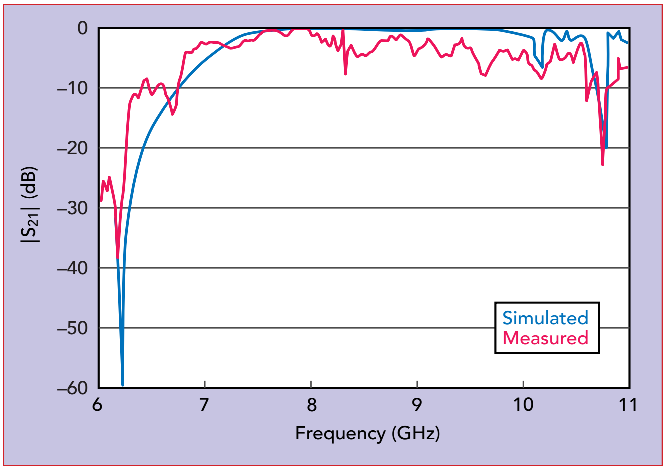

Fig. 6 Planar FSS $|S_{21}|$.

TABLE 2
PLANAR FSS PERFORMANCE COMPARISON WITH OTHER REPORTED WORK

Reference	-10 dB Bandwidth (GHz)	Left Roll-Off (dB/GHz)	Right Roll-Off (dB/GHz)
2	1.9	9.05	14.20
5	3	4.8	43
6	2.7	7.33	30
8	-	24.54	17.5
15	-	3.66	9.2
This Work	4	45	73.33

cylindrical finite curve structure are shown in ***Figure 7***. The two layers of semi-cylindrical curved FSSs are assembled with an air gap of 7.6 mm. Measurements of the structure demonstrate a wide passband of 4.2 GHz for a 45.16 percent bandwidth. It has a good bandpass property with a low insertion loss. Roll-off at the lower band edge is 16.66 dB/GHz and roll-off at the higher band edge is 32.09 dB/GHz. The sharp roll-off achieved by the curved structure increases its selectivity. Good agreement between simulated and measured results is observed. A comparison with recent results reported for curved FSSs is shown in ***Table 3***, demonstrating the highest percentage bandwidth and the sharpest roll-offs.

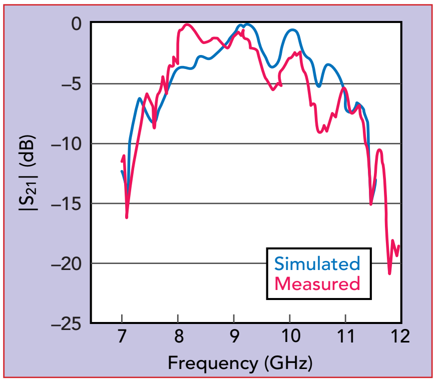

Fig. 7 Curved FSS $|S_{21}|$.

CONCLUSION

Performance of the dual-layer semi-cylindrical aperture-type curved FSS described here is shown to be better than other recent work, while also being near-

TABLE 3

CURVED FSS PERFORMANCE COMPARISON WITH OTHER REPORTED WORK

Reference	Bandwidth (Percent)	Left Roll-Off (dB/GHz)	Right Roll-Off (dB/GHz)
9	32.55	8.5	10
13	23.74	4.37	2.5
14	-	8.98	-
This Work	45.16	16.66	32.09

ly the same as the planar structure.[9,12,13] Achieving a wideband performance with low passband insertion loss and sharp roll-offs in a curved structure is the key accomplishment of this work. Because its conformal structure is easily integrated onto complex surfaces, such as ogives, it is suitable for use in the design of subreflectors and radomes. ■

References

1. B. A. Munk, *Frequency Selective Surfaces: Theory and Design*, Chapter 1, Wiley, New York Wiley, 2005.
2. S. Peddakrishna, T. Khan, B. K. Kanaujia and N. Nasimuddin, "Study of Pass Band Resonance Characteristics of Aperture Type FSS," *AEU International Journal of Electronics and Communications*, Vol. 83, January 2018, pp. 479–483.
3. P. Samaddar, S. Sarkar, S. De, D. C. Sarkar and P. P. Sarkar, "Design of Double Layer Frequency Selective Surface with Almost Flat Pass Band and Sharp Roll Off," *International Journal of Electronic Engineering Research*, Vol. 9, No. 1, 2017.
4. S. Balta and M. Kartal, "A Novel Double-layer Low-profile Multiband Frequency Selective Surface for 4G Mobile Communication System," *ACES Journal*, Vol. 37, No. 4, April 2022.
5. N. Xu, J. Gao, J. Zhao and X. Feng, "A Novel Wideband Low-Profile and Second Order Miniaturized Bandpass FSS," *AIP Advances*, July 2015.
6. G. Shan, C. Y. Gao, H. B. Pu and C. L. Chen, "A Tri-Band Second Order Frequency Selective Surface Designing and Analysis," *E3S Web of Conferences*, Vol. 275, No. 17, January 2021.
7. C. Singh, K. R. Jha, S. K. Sharma, Z. A. Pandit Jibran and G. Singh, "Design of a Wideband Square Slot Bandpass Frequency Selective Surface Using Phase Range Analysis," *Engineering Reports*, Vol. 2, No. 1, January 2020.
8. W. Wu, X. Liu, K. Cui, Y. Ma and Y. Yuan, "An Ultrathin and Polarization-Insensitive Frequency Selective Surface at Ka-Band," *IEEE Antennas and Wireless Propagation Letters*, Vol. 17, No. 1, January 2018, pp. 74–77.
9. P. Samaddar, S. Sarkar, P. P. Sarkar, et al., "Bandpass Planar and Hemispherical FSS Comprising of Tripole Element," *Journal of Physical Sciences*, Vol. 18, 2014, pp. 14–18.
10. N. Begam, S. Saha, P. Sammadar, P. P Sarkar and D. Sarkar, "Design of Curved FSS Providing Stable Response with Variation of Incident Angles," *International Journal of Scientific and Engineering Research*, Vol. 8, No. 3, March 2017.
11. N. Begam, P. Sammadar, S. Saha, S. Sarkar, D. Chanda (Sarkar) and P. P. Sarkar, "Design of Curved Frequency Selective Surface with High Roll-Off," *Microwave and Optical Technology Letters*, Vol. 59, No. 10, October 2017, pp. 2660–2664.
12. R. A. Pandhare, F. L. Lohar, C. Dhote and Y. Solunke, "Design of FSS Based Radome Wall for Airborne Radar Application," *Journal of Microwaves, Optoelectronics and Electromagnetic Applications*, Vol. 20, No. 4, December 2021, pp. 855–869.
13. H. F. Alvarez, D. A. Cadman, A. Goulas, M. E. de Cos Gómez, D. S. Engstrøm, J. C. Vardaxoglou and Shiyu Zhang, "3D Conformal Bandpass Millimeter-Wave Frequency Selective Surface with Improved Fields of View," *Scientific Reports*, Vol. 11, June 2021.
14. N. Begam, S. Saha, P. Sammadar, P. P. Sarkar and D. Sarkar, "Design of a Broadband Hemispherical Frequency Selective Surface with Incident Angle Independent Transmission Characteristics and High Roll-Off," *International Journal of Electronics Engineering Research*, Vol. 9, No. 1, 2017, pp. 9–13.
15. B. Liu, H. Zhao and I. Wang, "Transmission/Scattering Characteristics of Curved Frequency Selective Surface with Double Layer of Ring Slots," *International Conference on Microwave and Millimeter Wave Technology*, May 2021.

MiCable

New

2~6GHz 100W

GaN Power Amplifier

$21,599 (1-4 pcs)

In Stock

- ☑ **High Power** Psat 49/50 dBm
  P1dB 46/47 dBm (Min/Typ.)
- ☑ **High OIP3** 50/53 dBm (Min/Typ.)
- ☑ **Low Harmonic(2nd/3rd)** -20/-25 dBc (Typ.)
- ☑ **Low Spurious** -70 dBc (Typ.)
- ☑ **Low VSWR** 1.5:1 (Typ.)
- ☑ **High Efficiency** 20% (Typ.)

MPAR-020060S50 is a 2~6GHz 100W GaN amplifier with state-of-the-art GaN design technology. It has higher saturation output power while keeping higher P1dB and better linearity.

The built-in control, monitoring and protection functions are offered. It is designed for high power CW & pulse system applications, such as 5G, LTE, WIFI and other related system module & EMC test.

★ Custom designs are available

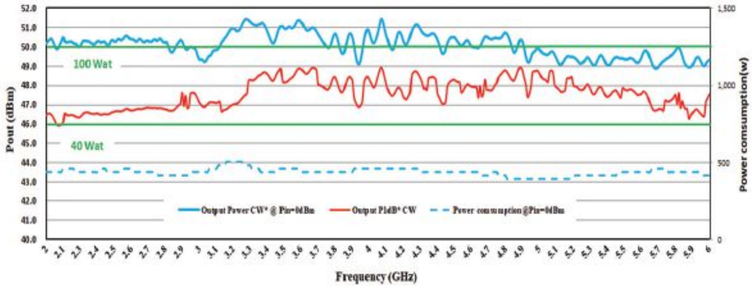

Pout@ Pin=0dBm & P1dB (CW, Load VSWR≤1.2, 25℃)

More Information-
Scan the QR Code

MIcable Inc.

www.micable.cn ✉ sales@micable.cn ☎+86-591-87382856

INVITED PAPER

Capitalize on Full-Wave Electromagnetic Simulations with 3D EM Component Models

Chris DeMartino
Modelithics Inc., Tampa, Fla.

To meet the needs of applications that require small form factors, it may be necessary to build circuits with surface-mount components that are densely packed onto a printed circuit board. In these scenarios, an additional challenge is that components located close to one another may also interact with each other. Unfortunately, these coupling interactions cannot be captured by simulations that include equivalent-circuit models for the components. However, it is possible to capture these coupling interactions by using 3D models in a full-wave 3D electromagnetic (EM) simulation.

This article explains the benefit of using 3D EM simulations combined with 3D models for designs where components are located close to each other. Performing such a simulation allows for a more accurate prediction of the actual performance of these designs. To illustrate this point, two case studies are presented: a design in which components are separated by a considerable distance and another design in which components are located close together. The analysis is carried out by performing planar EM/circuit co-simulations using Ansys® Electronics Desktop and 3D EM simulations using Ansys® HFSS™. All component models used in the examples are included in the Modelithics® COMPLETE+3D Library.

MODELITHICS MICROWAVE GLOBAL MODELS, 3D GEOMETRY MODELS AND 3D BRICK MODELS

The Modelithics COMPLETE+3D Library is a collection of models for components from many popular vendors. Included in this library are Microwave Global Models™, which are measurement-based equivalent-circuit models for capacitors, inductors and resistors.[1] These models capture parasitic effects and scale for part values, substrates and solder-pad dimensions.

The Modelithics COMPLETE+3D Library also includes a collection of 3D Geometry Models for components like inductors, capacitors, filters and packages.[2] These models are based on physical dimensions and material properties and are intended for use in full-wave EM simulations. The benefit of these 3D models is that they enable designers to predict the effects of coupling that may arise when components are located close to other components or objects.

Finally, the Modelithics COMPLETE+3D Library also includes what are known as 3D Brick Models™ for multi-layer ceramic capacitors (MLCCs).[3] A 3D Brick Model is a simplified approximation of a capacitor's physical geometry. However, these models alone do not account

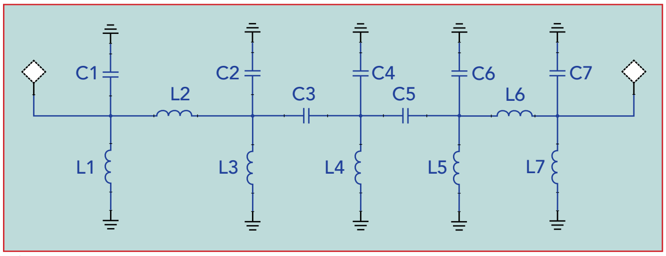

Fig. 1 Simplified bandpass filter schematic.

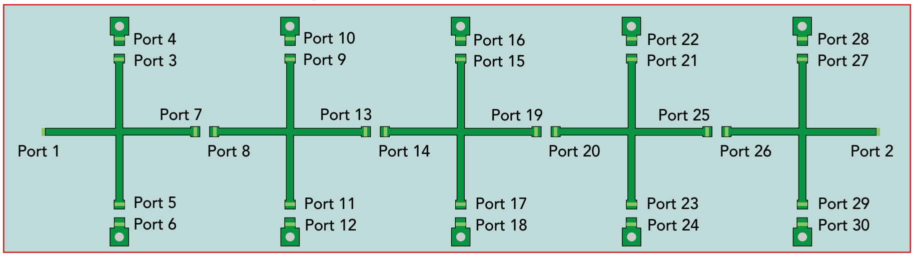

Fig. 2 Bandpass filter layout where components have ample spacing.

TABLE 1

PARTS LIST FOR THE BANDPASS FILTER OF FIGURE 2

Component	Part Value	Manufacturer	Part Number
C1, C7	1.8 pF	Passive Plus	0201N1R8AW500
C2, C6	1.4 pF	Passive Plus	0201N1R4AW500
C3,C5	1.1 pF	Passive Plus	0201N1R1AW500
C4	3.6 pF	Passive Plus	0201N3R6AW500
L1, L7	4.2 nH	TDK	MLG0603P4N2BT000
L2, L6	6.2 nH	TDK	MLG0603P6N2ST000
L3, L5	3.7 nH	TDK	MLG0603P3N7BT000
L4	0.9 nH	TDK	MLG0603P0N9BT000

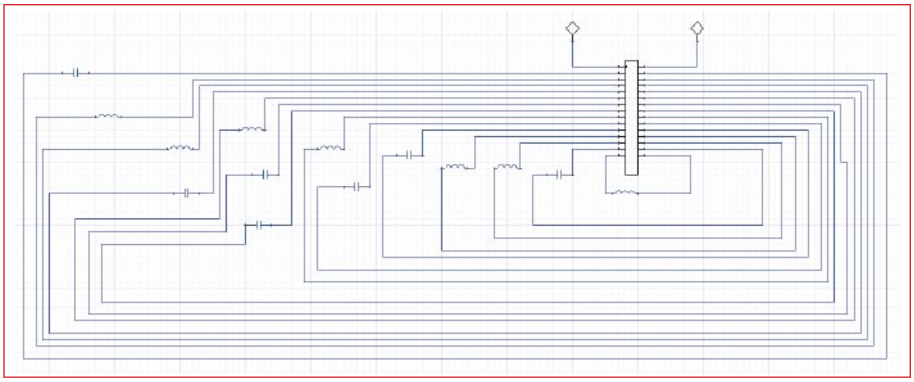

Fig. 3 **Filter layout planar EM data connected to the Microwave Global Models.**

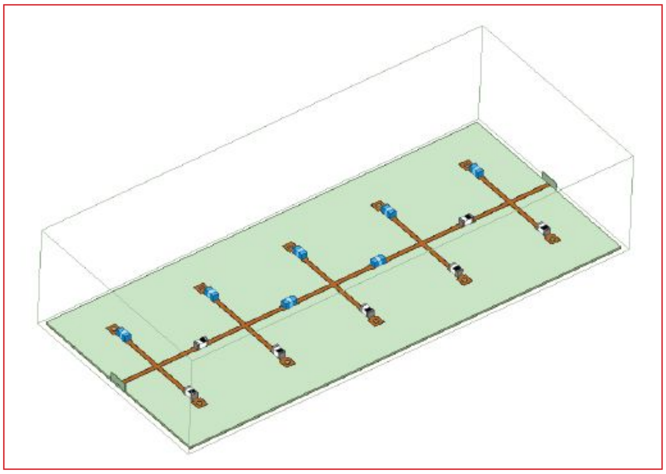

Fig. 4 **HFSS bandpass filter design with 3D Geometry Models and 3D Brick Models.**

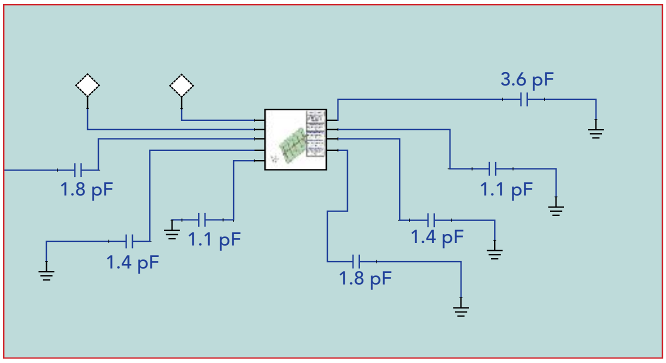

Fig. 5 **Schematic used for the 3D co-simulation of the bandpass filter.**

for internal device parasitics. Therefore, when using 3D Brick Models, the complete simulation process involves first performing a 3D EM simulation that includes all 3D Brick Models along with all 3D Geometry Models, if the design also includes 3D Geometry Models. This 3D EM simulation captures any coupling interactions that may exist between components. The next step is to perform a 3D co-simulation in a circuit schematic. This 3D co-simulation incorporates the 3D EM simulation data and combines it with the Microwave Global Model(s) for the corresponding capacitor(s) to allow for a complete 3D EM simulation.

Case Study 1: Filter Without Component Spacing Constraints

For the following analysis, lumped-element bandpass filter designs will be examined. The topology used for the filter designs shown here is known as the equal shunt legs topology. This topology is available as a selection in Ansys NuHertz® FilterSolutions (ANFS), which is a tool that enables users to synthesize various types of filters.[4] In the case of lumped-element filters, FilterSolutions lets users choose from different topologies, including classical, equal inductors, equal shunt legs, high/lowpass and others.

Figure 1 shows a simplified schematic of the filters that will be presented in this case study. The first example considers the case where there is a considerable amount of space between components. ***Figure 2*** shows the layout of the filter with a total length of about 0.929 in. Note that the substrate used is 0.004 in. thick Rogers RO4350B material. The TDK MLG0603P series and the Passive Plus 0201N series, both of which come in a 0201 size, are used for all inductors and capacitors, respectively. Modelithics offers Microwave Global Models for both part series. Finally, ***Table 1*** lists the values of all the inductors and capacitors. For this example, the targeted center frequency is about 1.5 GHz.

The analysis begins by performing a planar EM/circuit co-simulation using Ansys' 2.5D Method of Moments (MoM) EM solver to simulate the layout shown in Figure 2. A schematic must then be created that includes the planar EM data properly connected to the Microwave Global Models for the MLG0603P inductors and 0201N capacitors. This schematic is shown in ***Figure 3***. Simulating this schematic produces the final planar EM/circuit co-simulation results.

Having discussed the planar EM/circuit co-simulation method, the focus turns to the 3D EM simulation. The planar EM/circuit co-simulation schematic shown in Figure 3 includes Microwave Global Models for the

TDK MLG0603P inductors and Passive Plus 0201N capacitors. For the TDK MLG0603P inductor series, Modelithics also offers 3D Geometry Models for inductors ranging from 0.6 to 120 nH. Modelithics also offers a 3D Brick Model for the Passive Plus 0201N capacitor series. ***Figure 4*** shows the bandpass filter of Figure 2, populated with the components of Table 1 in Ansys HFSS with 3D Geometry Models for the TDK inductors and 3D Brick Models for the Passive Plus capacitors.

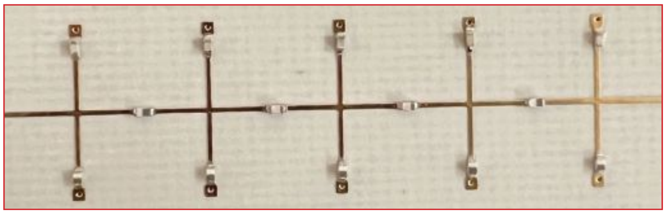

Fig. 6 **One of the (compact) bandpass filters that was built and measured.**

Now, a complete 3D EM simulation is possible by first completing a 3D EM simulation in HFSS of the design shown in Figure 4. The next step is to perform a 3D co-simulation that includes the data from the 3D EM simulation properly connected to the Microwave Global Models for the capacitors. The schematic for this model is shown in ***Figure 5***. It includes the 3D EM simulation data, as the center element, connected to the Microwave Global Models for the capacitors. Simulating this schematic produces the final 3D EM simulation results.

To confirm the measured versus modeled results, the bandpass filter was built and measured. ***Figure 6*** shows the assembled filter including the same inductors and capacitors from the simulations. ***Figure 7*** shows the results obtained from the planar EM/circuit co-simulation and the 3D EM simulation along with the measured data of the filter. The solid red trace represents the planar EM/circuit co-simulation results, while the solid blue trace corresponds to the 3D EM simulation results. The dashed traces represent the measured data of three filters.

Figure 7 reveals that the planar EM/circuit co-simulation and 3D EM simulation produce similar results. A slight difference does exist, as the planar EM/circuit co-simulation produces a frequency response that is shifted roughly 40 MHz lower than that produced by the 3D EM simulation. Figure 7 also shows how the measured data follows the 3D EM simulation results more closely than the planar EM/circuit co-simulation results. Since both simulations produce similar results, coupling interactions do not appear to be significant. While the 3D EM simulation provides a good prediction of actual performance, the planar EM/circuit co-simulation still adequately predicts actual performance.

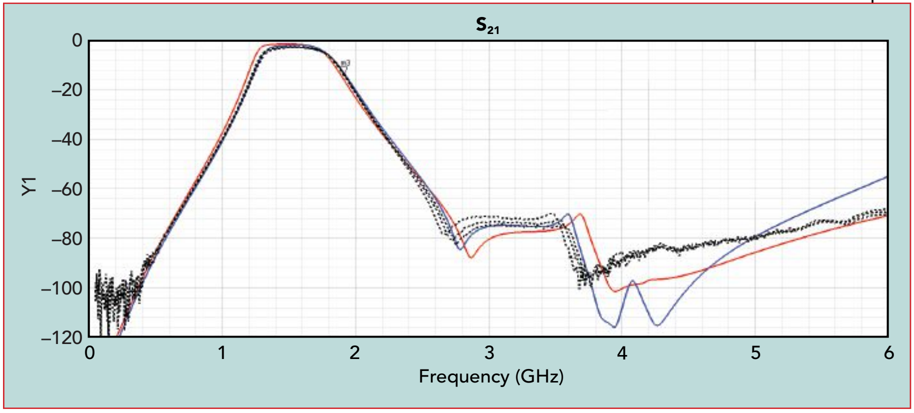

Fig. 7 **Simulated and measured S_{21} of the bandpass filter.**

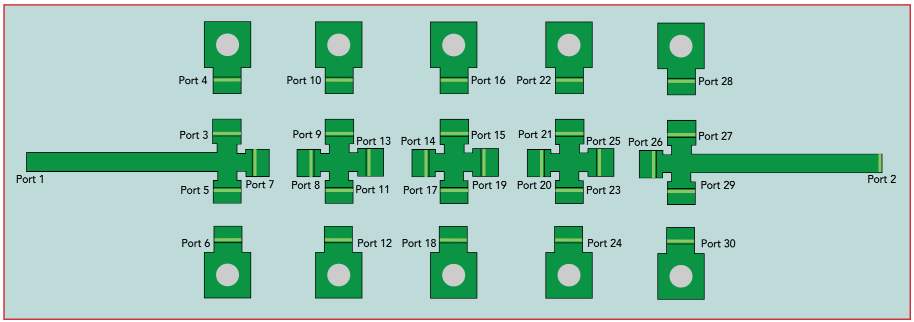

Fig. 8 **Bandpass filter layout with densely packed components.**

TABLE 2

PARTS LIST FOR THE BANDPASS FILTER LAYOUT OF FIGURE 8

Component	Part Value	Manufacturer	Part Number
C1, C7	2.7 pF	Passive Plus	0201N2R7AW500
C2, C6	2.0 pF	Passive Plus	0201N2R0AW500
C3, C5	1.3 pF	Passive Plus	0201N1R3AW500
C4	6.8 pF	Passive Plus	0201N6R8BW500
L1, L7	4.2 nH	TDK	MLG0603P4N2BT000
L2, L6	8.2 nH	TDK	MLG0603P8N2HT000
L3, L5	4.7 nH	TDK	MLG0603P4N7ST000
L4	1.0 nH	TDK	MLG0603P1N0BT000

Case Study 2: Filter With Densely Packed Components

The next case study analyzes a similar bandpass filter. The major difference between this filter and the one analyzed previously is that the components are located very close to each other in this design. ***Figure 8*** shows the layout of this filter. In this case, the total length is only about 0.361 in. Note that the same 0.004 in. thick Rogers RO4350B substrate is used for this design. While this design offers the benefit of smaller size, it also comes with the challenge of greater coupling interactions between components.

The target center frequency for this design is 1.46 GHz. ***Table 2*** lists the part values of the inductors and capacitors. Again, the TDK

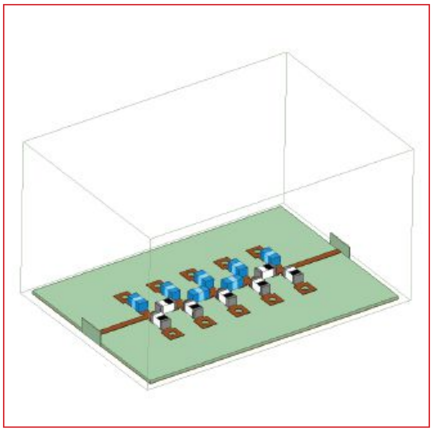

Fig. 9 HFSS compact bandpass filter design with 3D Geometry Models and 3D Brick Models.

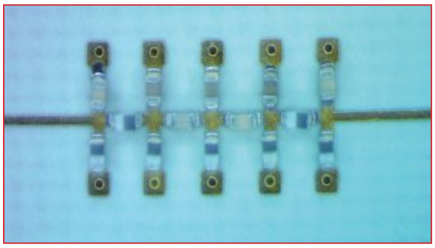

Fig. 10 One of the (compact) bandpass filters that was built and measured.

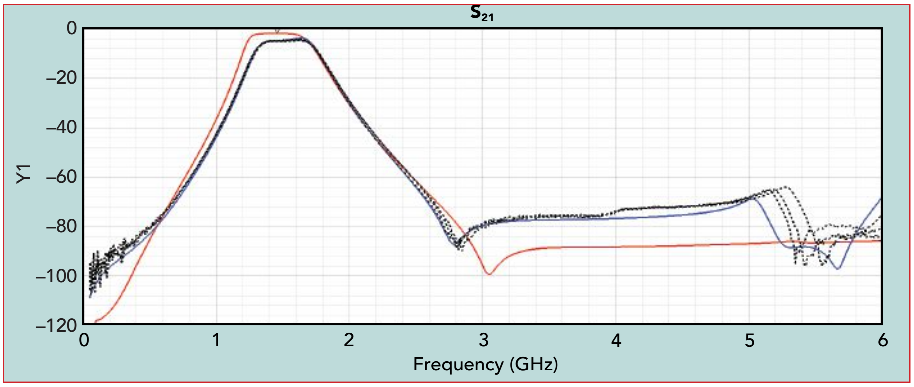

Fig. 11 Simulated and measured S_{21} of the compact bandpass filter.

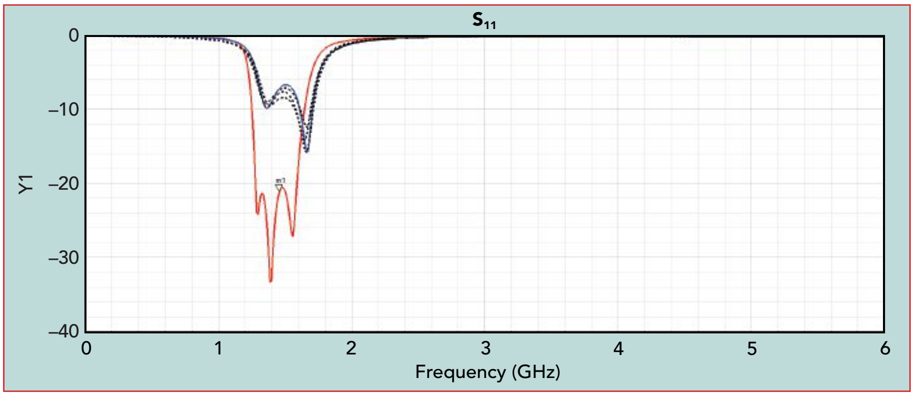

Fig. 12 Simulated and measured S_{11} of the compact bandpass filter.

MLG0603P series and the Passive Plus 0201N series are used for all inductors and capacitors, respectively.

The analysis for this case study is the same as the previous design example. Both a planar EM/circuit co-simulation and a 3D EM simulation are performed as described earlier. ***Figure 9*** shows the bandpass filter in HFSS with 3D Geometry Models for the inductors and 3D Brick Models for the capacitors.

Figure 10 shows the assembled filter including the inductors and capacitors from the simulations. ***Figure 11*** shows the simulated and measured S_{21} of this compact bandpass filter. Again, the solid red trace represents the planar EM/circuit co-simulation results, the solid blue trace corresponds to the 3D EM simulation results and the dashed traces represent the measured data of three filters. ***Figure 12*** shows the simulated and measured S_{11} of the compact bandpass filter over a DC to 6 GHz frequency range and ***Figure 13*** shows the simulated and measured S_{21} of the bandpass filter over the narrower, 0.5 to 3.5 GHz frequency band. In both figures, the solid red trace represents the planar


Pack Your Bags!
IMS
16-21 June 2024
Washington, DC
ims-ieee.org
WASHINGTON DC 2024
CAPITALIZING ACROSS THE SPECTRUM


Pack Your Bags!
See You in D.C. 2024
IMS

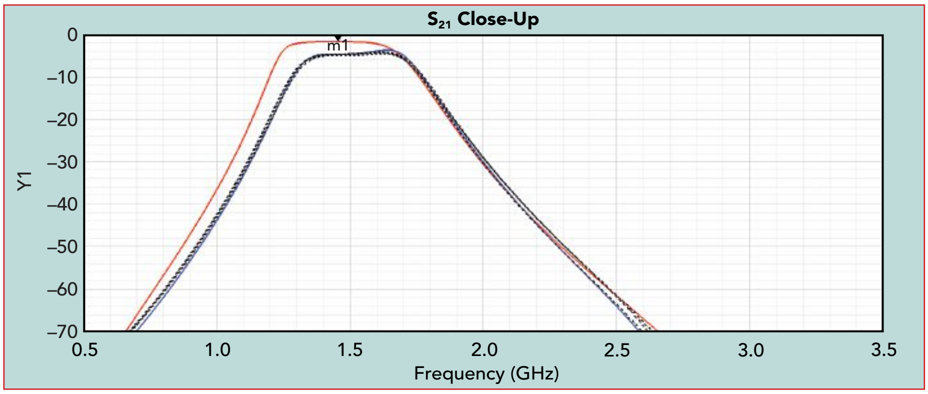

Fig. 13 Narrower band simulated and measured S_{21} of the compact bandpass filter.

TABLE 3

PARTS LIST FOR THE TUNED COMPACT BANDPASS FILTER

Component	Part Value	Manufacturer	Part Number
C1, C7	3.3 pF	Johanson	QLCD250Q3R3B1GV001B
C2, C6	1.6 pF	Passive Plus	0201N1R6AW500
C3,C5	1.8 pF	Passive Plus	0201N1R8AW500
C4	8.2 pF	Passive Plus	0201N8R2BW500
L1, L7	4.2 nH	TDK	MLG0603P4N2BT000
L2, L6	8.2 nH	TDK	MLG0603P8N2HT000
L3, L5	4.7 nH	TDK	MLG0603P4N7ST000
L4	1.0 nH	TDK	MLG0603P1N0BT000

EM/circuit co-simulation results, the solid blue trace corresponds to the 3D EM simulation results and the dashed traces represent measured data of three filters.

Initially, the targeted center frequency of this filter was set at 1.46 GHz. This goal is met considering only the planar EM/circuit co-simulation results. If this were the only verification result, the designer would conclude that the filter design met the requirements and no further action is needed. However, as already shown, the measured data is noticeably different than what the planar EM/circuit co-simulation is predicting. Specifically, in comparison to the planar EM/circuit co-simulation results, the measured data exhibits a reduced bandwidth and higher loss throughout much of the passband. At the desired center frequency of 1.46 GHz, indicated by the m1 marker in the plot, the measured data exhibits poor S_{11} performance.

This analysis demonstrates how a designer may be unpleasantly surprised when only relying on a planar EM/circuit co-simulation to predict the actual performance of a densely packed design such as this one. On a positive note, the 3D EM simulation results do agree very well with the measured data. These results demonstrate the need for and advantage of using 3D models in a 3D EM simulation for designs in which components are densely packed.

In practice, since the design goal is not being met, the filter would be tuned to achieve the desired performance. This task can be accomplished within the 3D co-simulation schematic from Figure 5. Recall how the 3D co-simulation schematic includes the 3D EM simulation data connected to the Microwave Global Models for the capacitors. Therefore, it is possible to tune the filter by simply adjusting the values of the capacitor models within the circuit schematic. Since the 3D EM simulation data is already incorporated into the schematic, there is no need to perform multiple time-consuming EM simulations.

In this case, the filter can be tuned to achieve the desired performance by adjusting all the capacitor values. ***Table 3*** lists the compo-

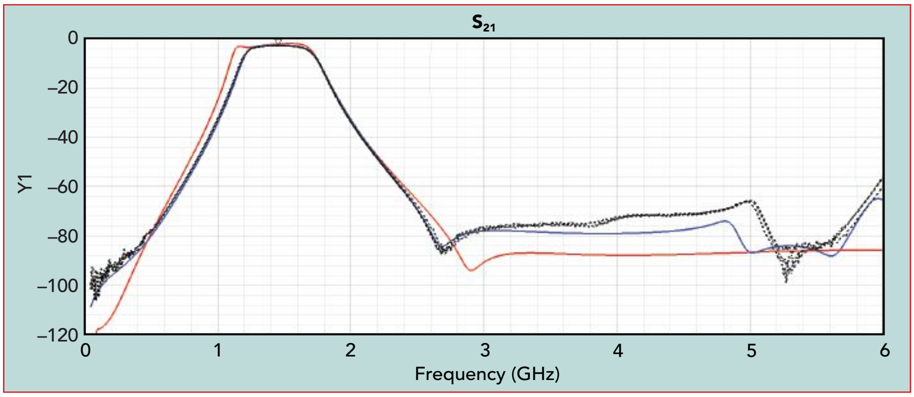

▲ **Fig. 14** **Simulated and measured S_{21} of the tuned compact bandpass filter.**

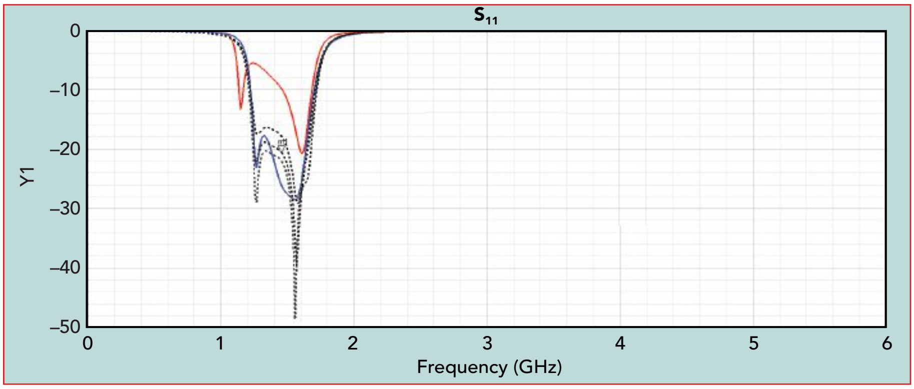

▲ **Fig. 15** **Simulated and measured S_{11} of the tuned compact bandpass filter.**

nents used in this tuned version of the compact filter design. ***Figure 14*** shows the simulated and measured S_{21} of the tuned compact bandpass filter. ***Figure 15*** shows the simulated and measured S_{11} of the tuned compact bandpass filter over the DC to 6 GHz range and ***Figure 16*** shows the simulated and measured S_{21} of the tuned bandpass filter over the narrower 0.5 to 3.5 GHz frequency band. Once again, the legend for the curves is the same. The solid red trace represents the planar EM/circuit co-simulation results, the solid blue trace corresponds to the 3D EM simulation results and the dashed traces represent measured data of three filters.

The performance curves in Figures 14, 15 and 16 illustrate how the 3D EM simulation accurately predicts the actual performance. This time, the design goal is being achieved with the measured data showing a center frequency of 1.46 GHz. At 1.46 GHz, the measured S_{11} is lower than -20 dB. The planar EM/circuit co-simulation results

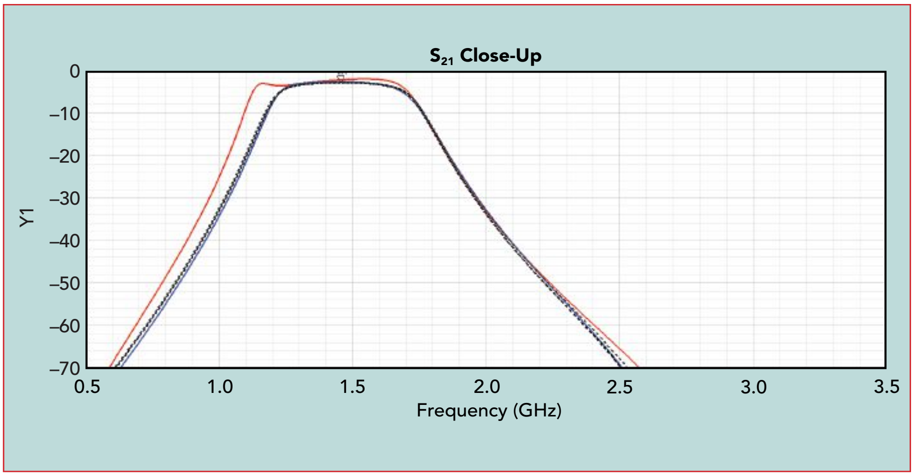

Fig. 16 Narrower band simulated and measured S_{21} of the tuned compact bandpass filter.

again deviate from the measured data. Specifically, compared to the measured data, the planar EM/circuit co-simulation produces a wider frequency response with poor S_{11} at the low end of the passband.

CONCLUSION

The analysis presented here further emphasizes how 3D EM simulations with 3D models are effective for compact designs. Keep in mind that 3D models are not intended to completely replace equivalent-circuit models. Modelithics equivalent-circuit models like Microwave Global Models are very effective in terms of predicting actual performance when coupling interactions are not playing a major role. For densely packed designs where the effects of coupling may be present, 3D models would be the preferred choice. ■

References

1. C. DeMartino, "Application Note 79: Filter Design Flow in Ansys Electronics Desktop with Modelithics Substrate Scalable Models," *Modelithics*, Web: www.modelithics.com/Literature/AppNote.
2. I. Bedford, E. Valentino and L. Dunleavy, "Application Note 63: Introduction to Modelithics 3D Models in HFSS," *Modelithics*, Web: www.modelithics.com/Literature/AppNote.
3. I. Bedford, "Application Note 78: Using 3D Brick Models™ for Full-wave EM/Circuit Model Co-simulation of MLCC Capacitors in Ansys HFSS," *Modelithics* Web: www.modelithics.com/Literature/AppNote.
4. C. DeMartino, "Streamline Filter Design with Ansys NuHertz FilterSolutions and Modelithics Models." *Modelithics*, Blog Post, September 2022.

ACKNOWLEDGMENTS

The author would like to thank the Modelithics lab team, notably Brendan Thompson and Keerthi Padmaraju, for performing the lab measurements for these design examples.

E LEARNING CENTER

Presented by: Microwave Journal

NEW WEBINARS

5/1

BAW Filter Mastery for All: Exploring XBAW and New XP3F Technology, Leveraging Foundry Services from 2 to 20 GHz

Sponsored by: RFMW AKOUSTIS

Now On Demand

Solution to Impedance and Insertion Loss Simulation Errors in PCB Transmission Lines

Sponsored by:

Avishtech

microwavejournal.com/events/2263

Will Flat Panel Beamsteering Arrays Meet the SATCOM Challenge?

Sponsored by:

Anritsu, Anokiwave is now Qorvo, ARA, Inc. and AnTrust

microwavejournal.com/events/2265

Register to attend at mwjournal.com/webinars

ONLINE PANEL SERIES

6/25 New Innovations in Power Amplifiers

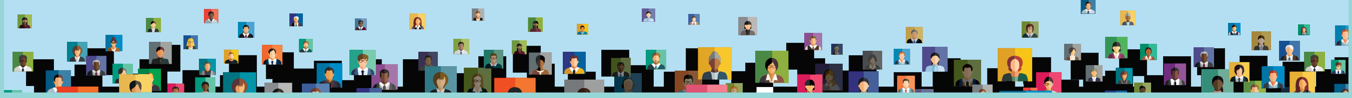

FEATURED eBooks

mwjournal.com/ebooks

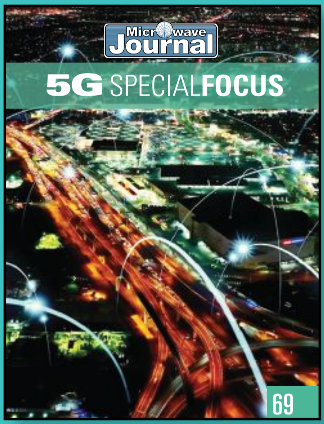

MIMO Needs FinFET: Key Changes for Analog Designers

Gabriele Devita
EnSilica, Oxfordshire, U.K.

5G terrestrial and satellite communications have already begun to use bands in frequency range 2 (FR2), with these frequencies ranging from 28 to 32 GHz. The signal propagation characteristics and short signal wavelengths in these high frequency bands limit the range of wireless communications. RF transceivers operating in these bands often rely on the integration of MIMO antenna systems to meet the link budget requirements and mitigate interference. For the ASIC designer, this means more channels, more radios and more digital signal processing.

Fin field-effect transistor (FinFET) device technology is becoming important for large MIMO systems. This transistor technology provides a high degree of flexibility while enabling digital radio solutions that can be based on RF analog-to-digital converters (ADCs) and digital-to-analog converters (DACs) that support multiple standards. ***Figure 1*** shows a typical FinFET architecture.

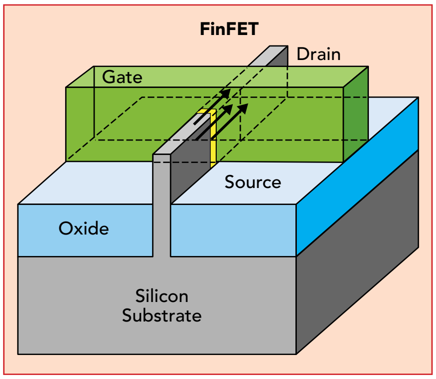

Fig. 1 **FinFET construction. *Source:* Synopsis.**

FinFET construction results in a non-planar, 3D FET device. It gets the name "FinFET" because the source/drain region on the silicon surface resembles a fin. In this architecture, the gate structure is placed on the sides or wrapped around the fin. The advantage of this architecture is that the gate wraps around the vertical channel and conduction occurs on three sides as opposed to traditional planar structures where conduction occurs only at the surface of the channel. The increased surface area between the gate and channel provides better control and reduces leakage compared to planar FETs. Using the FinFET architecture results in better electrical characteristics than planar FETs, like faster switching times and higher current densities.

Despite the advantages, there are drawbacks to devices that implement this architecture. One of the more important drawbacks is power consumption. ***Figure 2*** plots the energy/conversion-step figure of merit for high-resolution ADCs published in the last decade. It shows that the energy-per-conversion increases exponentially when operating above 1 GHz. As an example, increasing the sampling frequency from 1 to 5 GHz increases the converter power by more than 20×.

Significant power can be saved by designing an RF analog front-end. The benefit of this technique is that it allows the multi-GHz RF signal to be down-converted to a lower intermediate frequency (IF) signal, typically below 500 MHz. The transition to the digital domain is from these lower IF frequencies and this relaxes the constraints on the sampling frequency of the data converters.

Using FinFET architectures for analog design introduces other benefits. The architecture enables compact devices, and it has a high Gm and R_{out}. The subthreshold slope of the device is practically ideal, characterized by lower leakage and the high frequency perfor-

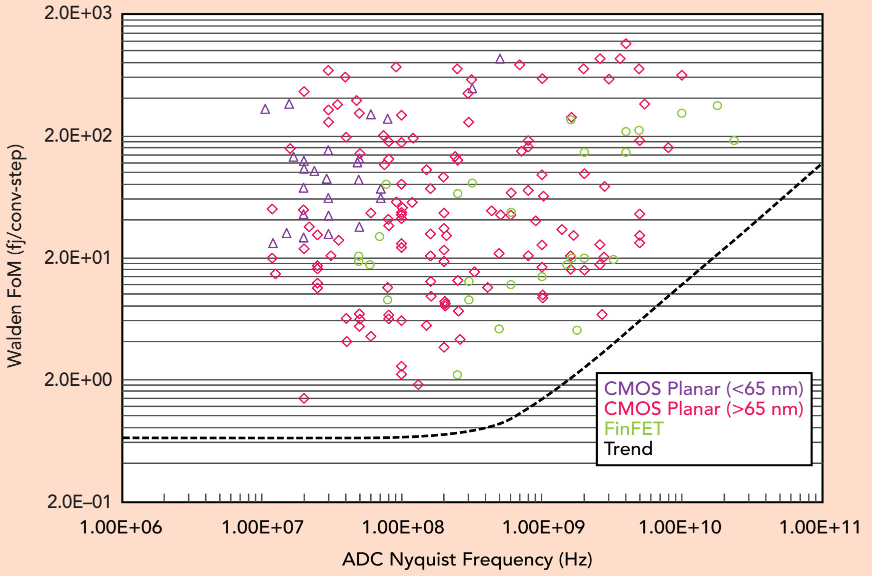

Fig. 2 **Walden fJ/conversion-step FoM as a function of the ADC frequency.**

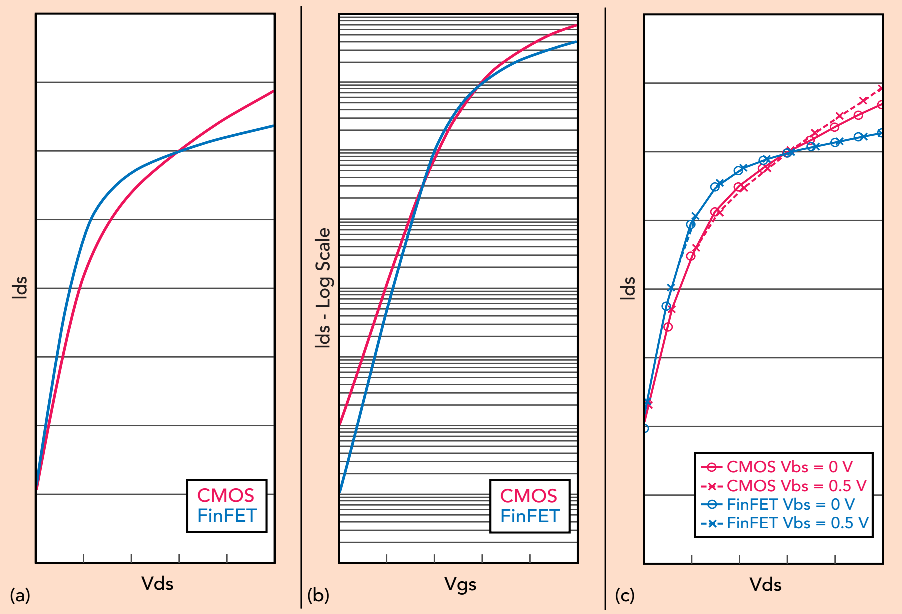

Fig. 3 **(a) R_{out} performance. (b) Threshold current performance. (c) Body bias performance.**

mance is excellent, with peak fT values of 600 GHz. The PMOS versus NMOS β ratio is near a value of one and the threshold of the transistor is nearly unaffected by the body bias. ***Figure 3a*** shows a comparison of R_{out} performance for a FinFET device and a 40 nm planar CMOS device. ***Figure 3b*** shows subthreshold current comparisons for the same two devices and ***Figure 3c*** shows the body bias effect for the FinFET and CMOS devices.

Another drawback to this approach is manufacturing cost and complexity. This architecture requires 2x to 3x as many masks as planar devices require. This makes the analog layout complicated and slow, due to the large number of design rules and process steps. This also makes the technology better suited for digital place and route techniques. These drawbacks complicate the analog layout flow, especially when application performance demands 7 nm, or smaller, topologies. So, what can be done to minimize these challenges?

Here are some guidelines to

make the process of designing analog FinFET ICs easier.

DO NOT MIX DEVICES THAT HAVE DIFFERENT DIMENSIONS

To make the chip modular, the analog designers should agree to a limited set of transistor widths and lengths to use for all the circuits. To maximize RF performance, these unit devices generally implement short channel lengths. Whenever longer geometries are required, in op-amps and mirrors, for example, variations on these geometries shall be generated via series combinations.

This approach reduces the freedom of analog designers, but makes the layout more compact. FinFET rules discourage mixing devices with different width and length values in the layout because this forces the layout engineer to group devices having the same dimensions in a single area. Devices with different sizes cannot be placed nearby and the long interconnects are likely to introduce parasitics that will limit performance.

USE REPEATABLE PATTERNS

It is easier to deal with the complex FinFET DRC rules if the layout engineer keeps the density constant and all the devices are laid out with fixed patterns that are interrupted with dedicated cut layers. Layout regularity ensures predictable analog circuit characteristics. An irregular layout may cause the manufactured devices to deviate from the model.

Figure 4 illustrates how these concepts can be applied to size power-down circuits in a current mirror. In planar geometry, the designer may use minimum-length devices for the power-down transistors and logic, along with longer devices for the mirror. Using the same approach with FinFET devices creates irregular patterns for critical mask layers, like poly and active area. The layout engineer is also forced to satisfy additional rules controlling the spacing of devices with different lengths. If the power-down transistors use the same device length for the mirrors, the layout becomes regular. This maximizes layout efficiency and keeps the density of critical layers constant. This allows the layout engineer to create templates that can be reused for multiple analog blocks.

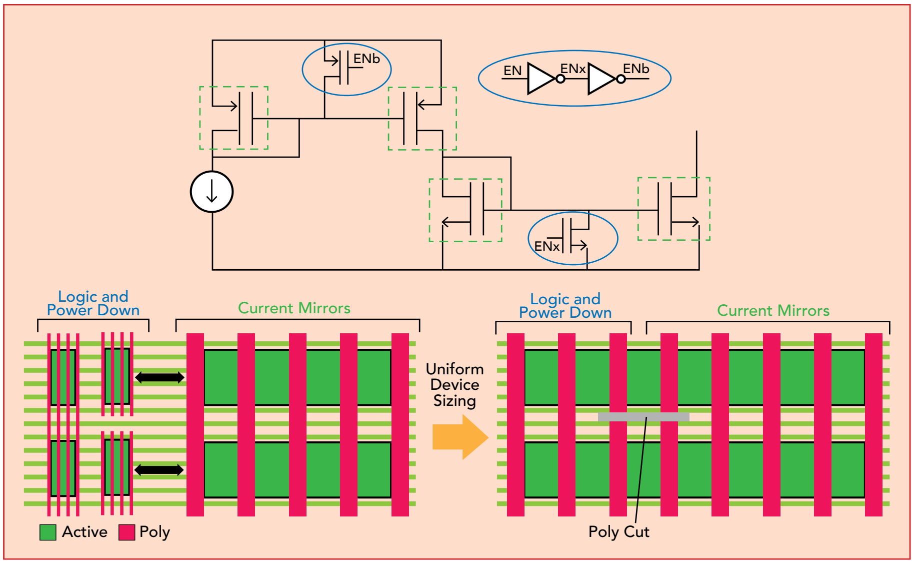

Fig. 4 **Benefits of uniform device sizing.**

ESTIMATE INTERCONNECT PARASITICS FROM THE START

Analog designers generally introduce parasitic extraction only at a later stage of the design. They are included in schematic simulations only for high speed circuits and are limited to sensitive nets because resistance is rarely a problem. This approach does not work with FinFETs. Wiring and RC layout-related parasitics are, in many ways, the limiting factor for performance and these parasitics must be considered from a very early stage. Metal and via resistance are higher, making them more dominant factors than in a planar geometry. Running parasitic-extracted simulations that do not estimate resistance can give optimistic results and may result in a pointless exercise.

As analog blocks tend to use a limited number of transistor geometries, it is recommended to build a library of layouts for these devices. This library should include low-level vias and interconnects. After RC extraction, the resulting sub-cells can be used to design analog blocks. This will ensure that their RC components are included in the simulations from the start.

USE DIGITAL CALIBRATION TO CORRECT ANALOG ERRORS

FinFET lithography is extremely accurate, which should enable better component matching. However, the area of the components tends to be smaller than in planar geometries. Since device matching is inversely proportional to the square root of the device area, this can result in a large offset in comparators or a mismatch in mirrors.

Trying to address this problem by modifying device dimensions may be difficult, if not completely unsuccessful. FinFET logic gates are small and have low power. Wherever possible, it is prudent and much cheaper to resort to digital calibrations to remove matching errors.

CURRENT DENSITY LIMITS THE TRANSMITTER OUTPUT POWER

Designers have already faced this challenge when working on sub-40 nm planar geometries. However, FinFET skinny metal layers and small vias impose even more stringent limitations on the maximum current density. These layers and vias have limited current carrying capability. This may force power amplifier (PA) designers to use wider wires and increase the transistor width to accommodate the required vias and contacts. Depending on the voltage levels, designers may also need to increase the wire spacing.

Longer wires and larger gate areas introduce parasitics, making in-

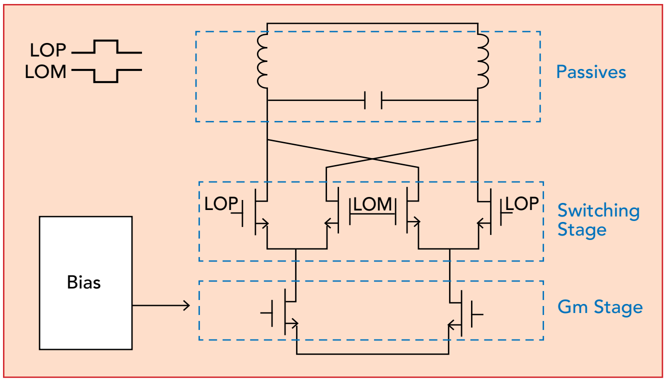

Fig. 5 Hierarchy of a Gilbert cell mixer optimized for FinFET simulation.

terconnects one of the limiting factors in PA design. The effects of interconnects must be considered in conjunction with the usual efficiency and linearity trade-offs. Surprises can be avoided by floor planning the amplifier early in the design phase, even when the desired output power is relatively modest and on the order of just a few milliwatts.

HIGH FLICKER NOISE CORNER FREQUENCY

Flicker noise in FinFET devices is a bigger issue than in planar geometries and the corner frequency in this architecture can be as high as 100 MHz. The impact on noise-sensitive circuits like VCOs, PLLs and receiver amplifiers can be very significant. The obvious solution to this issue is to increase the size of the devices. This will reduce the noise, but this improvement comes at the expense of RF performance. Alternatively, some of these issues can be resolved at the system level. For example, careful receiver frequency planning can ensure baseband operation at frequencies above the flicker corner and relax the associated block-level specifications.

SIMULATIONS ARE SLOW

FinFET models are complex, which leads to slow simulations. In addition, since the parasitic resistance cannot be ignored, most of the simulations will be performed with an extracted netlist that includes thousands of components. This can result in a brute-force approach that relies on big servers and multi-core simulators to thoroughly evaluate and verify the design. However, a better recommendation is to adapt the simulation strategy to this challenge and increase the hierarchical levels in the design. As an example of this methodology, ***Figure 5*** proposes a more structured hierarchy for a simple Gilbert cell mixer. Given the limited number of components, the whole circuit could be drawn flat. However, after layout extraction, this choice leads to a large, flat netlist, with limited simulation and debugging options.

On the other hand, a more granular hierarchy like the one shown in Figure 5 separates the different sections of the design based on their functionality. Depending on the simulation, this gives the designer flexibility to use accurate, fully extracted views for critical sub-blocks while using coarser models for the other sections. As a rule of thumb, most block-level simulation times should be kept under one hour in duration. This limits the brute-force tests to the final verification stage.

CONCLUSION

FinFET device architectures have many advantages for large MIMO antenna-based RF systems. The architecture enables small, high speed digital signal processing to integrate into flexible digital radios. However, the expansion of RF applications into higher frequency bands means that the power consumption performance of RF ADC/DAC-based solutions becomes a serious challenge. One approach to minimize this challenge is to design low-power RF analog front-ends to convert the high frequency RF signal to a lower frequency IF signal. Realizing high performance, cost-effective approaches for this conversion process and circuitry will be of paramount importance to the success of these systems. Moving to FinFET technology represents a drastic change for analog designers, but this article has presented seven recommendations to smooth this transition and facilitate high performance FinFET analog circuit design. ■

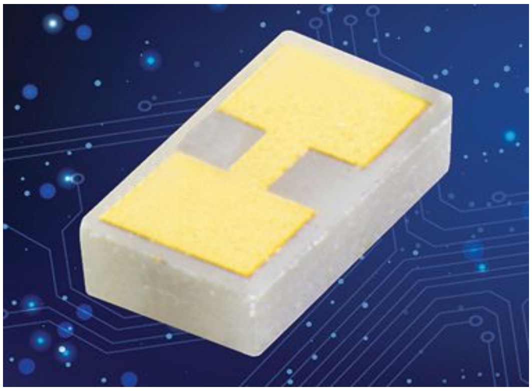

Microwave and Millimeter Wave Gain Slope Equalizers

Dielectric Laboratories, Inc.
A Knowles Precision Devices Brand
Cazenovia, N.Y.

PHYSICAL CONSTRAINTS FOR BROADBAND OPERATION

Most microwave hardware engineers have had the sobering experience of testing a new design and not having it look like the model. This is particularly true as more applications require wideband, high frequency modules. These broadband, high frequency modules usually have gain roll-off at the high end of the band from a combination of inductive and capacitive parasitics in the components and packages. These parasitic elements create gain roll-off and VSWR mismatch losses while interconnecting transmission lines and other passive components have loss characteristics that increase with frequency.

GAIN EQUALIZERS: THE HISTORICAL APPROACH

This issue is typically addressed with a gain equalizer. The loss characteristic of these devices is positive versus frequency, meaning they have more loss at lower frequencies. The overall module will have more loss, but more amplifier gain can compensate for this loss. The positive loss slope of the gain equalizer is designed to flatten the loss characteristic over the entire band. Historically, passive gain equalizers have utilized a stacked combination of surface-mount chip resistors and chip capacitors. The resulting parallel RC circuit is mounted in series across a gap in the microstrip line. Stacking the chips minimizes the circuit footprint, which helps minimize reflection losses.

Pre-assembled RC circuits work well with pick-and-place assembly and reflow methods. However, typical SMT chip termination materials make it difficult to pre-attach the resistor and capacitor chips without the connection reflowing and possibly disassembling during the board attachment process. The RC chip stack needs to be small, usually in 0201 or up to 0402 case sizes, to maintain good VSWR performance across electronic warfare (EW) bandwidths. Even with all these precautions, the actual performance of a stacked chip gain equalizer may not be as close to ideal performance as a designer would like.

A NEW BREED OF GAIN EQUALIZER

Knowles' Dielectric Laboratories, Inc. (DLI) brand gain equalizers employ monolithic construction with precision thin film conductor and resistor films and proprietary high dielectric constant ceramics for superior RF performance repeatability. Integrated R and C values are realized to produce the desired gain slope. The AEQ series of equalizers pro-

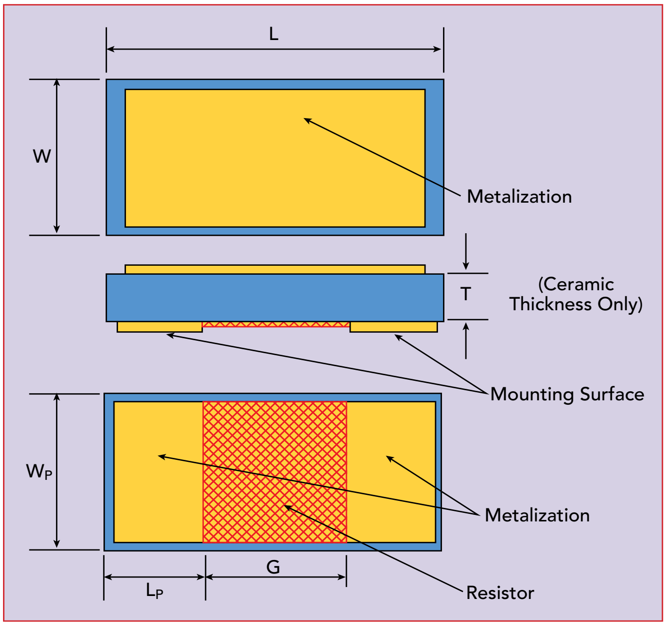

Fig. 1 **Gain equalizer physical layout.**

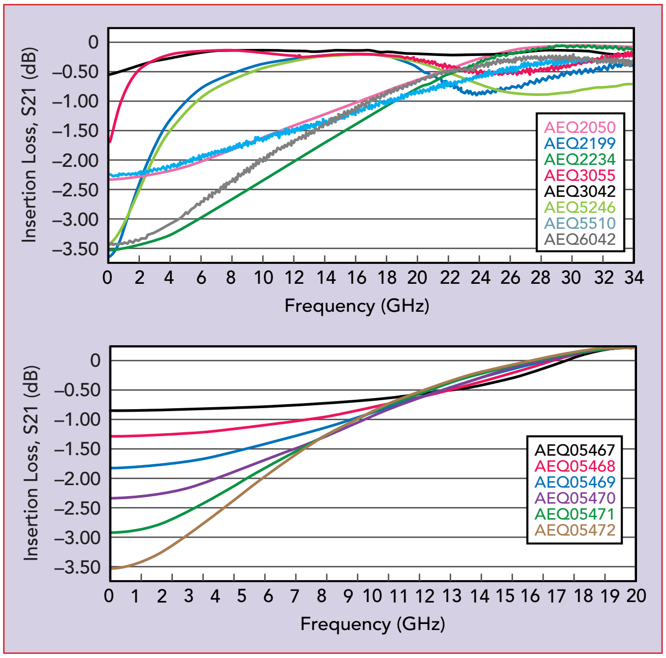

Fig. 2 **Gain equalizer measured performance.**

TABLE 1

KNOWLES' DLI BRAND MONOLITHIC GAIN EQUALIZERS

Part Number		All Dimensions are in mils						Nominal Slope (dB)
Epoxy	Solderable	L	W	T	Lp	Wp	G	
AEQ2050	AEQ05510	30 ± 2	18 ± 2	5 ± 1	9 ± 1	14 ± 1	8 ± 1	2.25
AEQ2199	AEQ05246	28 ± 2	16 ± 2	7 ± 1	7 ± 1	14 ± 1	12 ± 1	3.5
AEQ2234	AEQ06042	32 ± 2	16 ± 2	5 ± 1	8 ± 1	12 ± 1	12 ± 1	3.25
AEQ3042	AEQ3042	40 ± 2	20 ± 2	6 ± 1	17.5 ± 1	17.5 ± 1	3 ± 1	0.6
AEQ3055	AEQ3055	40 ± 2	20 ± 2	6 ± 1	15.4 ± 1	18.4 ± 1	7.2 ± 1	1.5
AEQ05467	AEQ05467	28 ± 1	16 ± 1	7 ± 1	7 min.	14 ± 1	10	1.0
AEQ05468	AEQ05468	28 ± 1	16 ± 1	7 ± 1	7 min.	14 ± 1	10	1.5
AEQ05469	AEQ05469	28 ± 1	16 ± 1	7 ± 1	7 min.	14 ± 1	10	2.0
AEQ05470	AEQ05470	28 ± 1	16 ± 1	7 ± 1	7 min.	14 ± 1	10	2.5
AEQ05471	AEQ05471	28 ± 1	16 ± 1	7 ± 1	7 min.	14 ± 1	10	3.0
AEQ05472	AEQ05472	28 ± 1	16 ± 1	7 ± 1	7 min.	14 ± 1	10	3.5

vides solutions for applications ranging from 6 to over 40 GHz. The gain equalizers have terminations compatible with standard SMT or conductive epoxy attachment. This series targets EW applications and the gain equalizers come in a variety of sizes, as shown in ***Table 1***. The physical dimensions of the equalizers are defined in ***Figure 1***.

Figure 2 illustrates the typical measured performance of the series. The AEQ54xx-series operates from 50 MHz to 20 GHz, with slopes ranging from 1.0 to 3.5 dB. The other entries in Table 1 are typically a little bigger and these gain equalizers operate from 50 MHz to 34 GHz, with slopes ranging from 0.6 dB to 3.5 dB. The gain equalizers are intended to be used in small-signal applications. Thermal dissipation is a limitation because of the small size of the equalizer and the low thermal conductivity of printed circuit board materials. The dissipated power will be greater for lower frequency signals since the insertion loss is lower in higher frequency ranges.

CONCLUSION

If you have gain slope issues in microwave modules, you should consider gain equalizers. Knowles' DLI brand gain equalizers are designed as a small, low-cost solution to gain slope challenges. These equalizer designs employ a monolithic construction with precision thin film conductors and resistor films with proprietary high dielectric constant ceramics for superior RF performance and repeatability. Components are well suited for use with pick-and-place equipment. They are available in tape-and-reel packaging for high volume applications.

Dielectric Laboratories, Inc.
A Knowles Precision Devices Brand
Cazenovia, N.Y.
www.knowlescapacitors.com/Products/Microwave-Products/Gain-Equalizers

Passive Components Reach 110 GHz

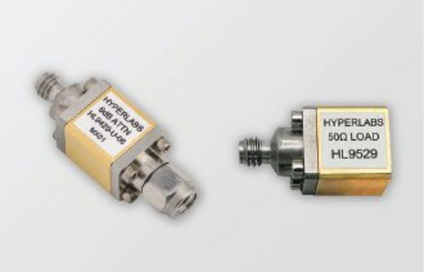

HYPERLABS INC. is expanding its 110 GHz component offerings by introducing a range of new broadband attenuator values and a new 50 Ω termination. The HL9429 attenuator is available in values of 3 dB, 6 dB and 10 dB. These attenuators exhibit flat frequency response with bandwidth from DC to more than 110 GHz, making them an excellent choice for attenuating a wide range of broadband pulsed waveforms in applications like ultra-wideband, noise-like pulses, radar and PAM-4, accommodating high speed serial data signals up to and beyond 224 Gbps. Each attenuator value is available in matched pairs, ensuring excellent amplitude and phase match for use in differential systems. The maximum input power is 20 dBm.

The HL9529 is a 50 Ω termination targeting a wide range of applications. It exhibits good return loss from DC to more than 110 GHz. The HL9529 is useful for terminating unused ports in high bandwidth systems and for metrology applications.

Both products feature 1.0 mm connectors and a square body design compatible with a standard 0.375 in. open-end wrench. The HL9429 attenuator housing with connectors measures 1.141 x 0.377 x 0.377 in. The HL9529 termination housing with connectors measures 0.737 x 0.377 x 0.377 in.

HYPERLABS also offers a 67 GHz version of both products. The HL9427 attenuator and HL9527 termination feature 1.85 mm connectors. Alternate connector configurations and connector series are available upon request.

Founded in 1992 and privately owned, HYPERLABS sells an array of broadband components including baluns, bias tees, DC blocks, power splitters/dividers, attenuators, transition time converters and pick-off tees, operating up to and above 100 GHz. HYPERLABS' instrumentation line includes pulse generators, TDRs/TDTs, controlled impedance analyzers, signal path analyzers, cable skew testers and samplers/harmonic downconverters.

HYPERLABS INC.
Beaverton, Ore.
www.hyperlabs.com

Oscillators Target New Space Applications

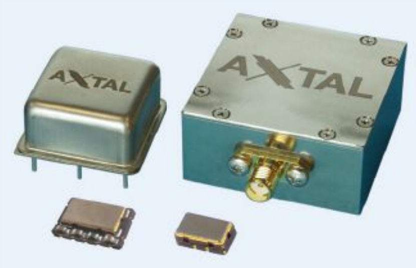

In today's dynamic space environment, where precision and reliability are paramount, AXTAL GmbH introduces its state-of-the-art temperature-compensated crystal oscillators (TCXOs) and oven-controlled crystal oscillators (OCXOs). These devices have been designed to meet the demanding mission-critical requirements of space. They provide outstanding radiation immunity and frequency stability for LEO applications and pave the way for lower-cost, high performance space solutions.

TCXOS

AXTAL's TCXOs set new standards with their compact design and exceptional stability. The AXLE7050S and AXLE5032S series fulfill this requirement at frequencies from 10 to 50 MHz with stabilities up to ±1 ppm. They are designed and tested to withstand radiation levels of up to 40 kRad(Si) TID and are immune to single-event latch-ups up to 120 MeV-cm²/mg. With typical phase noise levels of -67 dBc/Hz at 1 Hz and a floor of -160 dBc/Hz (20 MHz), they guarantee precise timing for critical space missions. The AXLE7050S and AXLE5032S are packaged in hermetically sealed, surface-mount ceramic enclosures measuring 7 x 5 mm and 5 x 3.2 mm, respectively, offering versatility without compromise.

OCXOS

For applications requiring higher stability, AXTAL's OCXOs operate flawlessly in high-radiation environments and offer precision in every aspect. The AXIOM70SL, AXIOM75SL, AXIOM3838S (10 MHz) and AXIOM75SH (100 MHz) series set new standards with their ±10 ppb (10 MHz) stability and robust construction. With typical phase noise levels of -135 dBc/Hz at 100 Hz and a floor of -180 dBc/Hz (100 MHz), they ensure uncompromising performance. These OCXOs are available in various sizes and configurations from 25 x 25 mm THD/SMD to 38 x 38 mm connectorized and offer unrivaled flexibility for various space applications.

With its continued commitment to innovation and quality, AXTAL pushes the boundaries of space technology to ensure the success of future space projects.

AXTAL GmbH
www.axtal.com
+49.6261.939834

4-Channel Frequency Counter/Analyzer Simplifies Measurements

The CNT-104S multi-channel instrument combines the functionalities of a high performance universal frequency counter and time-interval analyzer into a single device. This compact benchtop unit measures frequency, phase or time across four input channels simultaneously, presenting the parallel results on a large color display. The instrument provides < 7 ps time resolution and 13 digits/s frequency resolution with a measuring speed of up to 20 million measurements/s. Pendulum Instruments claims the CNT-104S outperforms any current timer/counter/analyzer on the market. The single-shot resolution delivers faster phase comparison results between clocks, allowing the capture of tiny time and phase changes in real-time.

All four channels offer parallel, independent and gap-free time-stamping of the input signals. Previously, this has only been possible using multiple instruments. Designers can compare the phases of four atomic clocks without a switch. Multi-stop, time-interval measurements benefit those conducting time-of-flight measurements in physical research applications.

A touchscreen and an intuitive menu structure facilitate simple navigation and instrument setup. Alternatively, a wireless mouse can be connected to the unit to make measurement settings. A built-in web server allows the unit to be operated remotely from almost anywhere. Gigabit Ethernet or Wi-Fi connectivity provides flexible remote-control capability.

Intelligent AUTO SET helps configure the best settings for each measurement to avoid mistakes. Results are presented in both numerical and graphical formats. A toggle function allows test data to be viewed in numerical, statistics, distribution and timeline modes.

For over 60 years, Pendulum Instruments, a global expert in time and frequency measurement, analysis and calibration has addressed aerospace and defense, telecom, metrology and R&D applications. Learn how the CNT-104S can be configured to meet your specific needs and/or budget demands.

Pendulum Instruments
Redwood City, Calif.
pendulum-instruments.com

MAKING WAVES

Cloud & Intelligent Edge: Shaping the Future of 4IR

During MWC 2024, ADI's Martin Cotter took the stage with Schneider Electric's CTO and SVP Aurelien Le Sant to discuss the future of industrial networking.

Analog Devices, Inc.

www.youtube.com/watch?v=JTAJ_E2DyXo&t=5s

Rural Broadband Installation and Testing Challenges and How to Overcome Them

As network operators strive to optimize broadband services in rural regions, proper test procedures and solutions become crucial.

Anritsu

bit.ly/3R51mwS

A New Look Catalog from Insulated Wire Inc. for 2024!

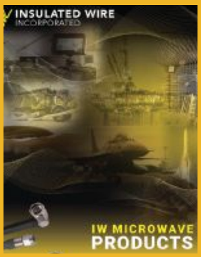

The latest edition provides specifications for our extremely low loss/phase stable products from 0341 to 7506 (0.034 to 0.750 in. diameters), Re-Flex hand-formable range, semi-rigid and 75 Ohm coaxial cables. The 2024 catalog also includes connector outlines, back by customer request!

Insulated Wire Inc.

https://insulatedwire.com

The Basics of OFDM

Understanding orthogonal frequency division multiplexing (OFDM) is essential to the foundations of modern communications technologies. Mini-Circuits' latest blog post defines what orthogonal is and explains why that matters.

Mini-Circuits

https://hubs.ly/Q021Xvh80

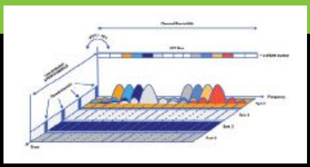

Accelerating Large-scale Semiconductor Parametric Testing Using a Multi-bus Switch Matrix

In this guide, Pickering discusses large-scale parallel parametric testing, scan-list sequencing and triggering, relay failure and maintainability and more.

Pickering Interfaces

https://rb.gy/9iy50q

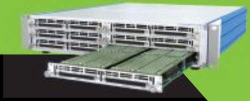

Signal Microwave's Marketplace now on Digi-Key

Signal Microwave announced the launch of its Marketplace store on Digi-Key. Signal Microwave's Supplier Center on the Digi-Key website is now live. This will give customers easy access to view or buy any of their products and content available through Digi-Key.

Signal Microwave

https://shorturl.at/rFR08

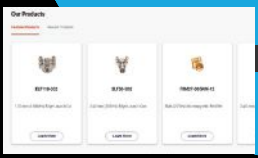

NEW PRODUCTS

FOR MORE NEW PRODUCTS, VISIT WWW.MWJOURNAL.COM/BUYERSGUIDE
FEATURING VENDORVIEW STOREFRONTS

DEVICES/COMPONENTS/MODULES

5G Mitigation Filter for C-Band

A1 Microwave has expanded their range of C-Band receive filters for satellite ground installations to include off-the-shelf components that are fully compliant with the RED and BLUE spectrum masks. In addition to the close-in 5G rejection, they also feature transmit band rejection as well as X-Band radar for use in naval applications. This includes a recent trial for the UK Royal Navy as well as hundreds of installations on cruise ships and terrestrial news-gathering equipment.

A1 Microwave
www.a1microwave.com

High-Power RF Fixed Attenuators

VENDORVIEW

Fairview Microwave has announced the release of its RF fixed attenuators with 2.4 mm connectors, boasting high-power ratings of up to 5 watts (CW) and a frequency range of up to 50 GHz. The new RF fixed attenuators with 2.4 mm connectors are designed to meet the evolving needs of RF professionals and engineers, offering unparalleled performance and versatility. They are the ideal solution for those seeking precision control over RF signals while ensuring stability and reliability in demanding applications.

Fairview Microwave
www.fairviewmicrowave.com

2-Way Power Divider

VENDORVIEW

KRYTAR Inc announced a new two-way power divider offering high performance over the ultra-broadband frequency range of 4 to 40 GHz (C- through Ka-Bands) in a compact package. The new power divider offers the ultimate solution for emerging designs and test and measurement applications, including mmWave, 5G, radar, satellite communications and more. KRYTAR's technological advances provide excellent operating performance of this new two-way unit.

KRYTAR Inc.
www.krytar.com

Ultra-Wideband 16-Way Power Divider/Combiner

VENDORVIEW

The MIcable 6 to 40 GHz ultra-wideband 16-way power divider/combiner P16N060400 can accept a 6 to 40 GHz signal and deliver 16 output signals with extremely good amplitude unbalance (±0.3 dB typical) and phase unbalance (±6 degrees typical). Due to wide bandwidth, excellent VSWR (< 1.3:1 typical), insertion loss (> 5 dB typical) and isolation (> 18 dB typical), it can be widely applied in 5G, testing, instruments and other related fields that need wideband high performance signal distribution network.

MIcable Inc.
www.micable.cn

Power Splitter

VENDORVIEW

Mini-Circuits' model SPL-2G42G50W4+ is a coaxial active power splitter with more than 360 degrees and a phase-shift range from 2.4 to 2.5 GHz. With an I2C control interface, it tunes phase with 1 degrees resolution, with 165 degrees of the range continuously variable. The active power splitter adjusts attenuation in 0.5 dB steps over a minimum 30 dB range. The active power splitter is equipped with MCX female connectors and exhibits 1 dB typical insertion loss. It draws 650 mA typical current from a +5 VDC supply.

Mini-Circuits
www.minicircuits.com

High Q Low ESR Capacitors

Passive Plus' product offering includes traditional high Q low ESR 1111 (0.110 × 0.110 in.) multi-layer ceramic capacitors for ultra-high frequency/microwave RF power amplifiers, mixers, oscillators, filter networks, low noise amplifiers, timing circuits and delay lines. These capacitors are available in two dielectrics (P90 or NP0); three different terminations: magnetic (100% Sn - solder over nickel plating), non-magnetic (100% Sn - solder over copper plating) and tin/lead (90% Sn 10% Pb - solder over nickel plating) and are designed and manufactured to meet the requirements for MIL-PRF-55681 and MIL-PRF-123.

Passive Plus
www.passiveplus.com

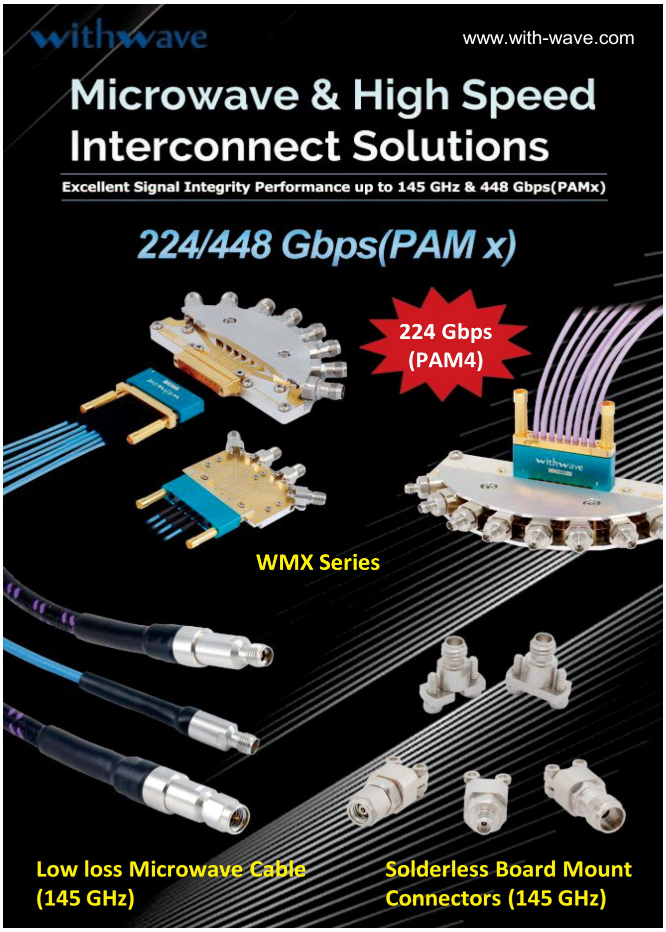

NewProducts

Analog Phase Shifter

VENDORVIEW

Quantic PMI model number PS-5G18G-400-A-SFF is a 5 to 18 GHz, low phase noise, analog phase shifter with capability for phase shifting from 0 to 400 degrees. The unit operates from a single positive control voltage of 0 to +10 VDC with a phase voltage sensitivity of 40 degrees per volt. This model offers a typical modulation bandwidth of 50 MHz and is supplied in a PE2 housing measuring only 1.08 × 0.71 × 0.29 in. and can be used with the SMA connectors or in a surface-mount configuration.

Quantic PMI
www.quanticpmi.com

Lowpass Filters

VENDORVIEW

Richardson RFPD Inc., an Arrow Electronics company, announced the availability and full design support capabilities for two families of lowpass filters from CTS Corporation. The RLF and XLF series are optimized to support 3GPP standards that require harmonic suppression through fifth-order harmonics. Both series provide complete solutions for harmonic rejection for wireless infrastructure applications. The RLF family offers extremely low insertion loss (3 to 5 dB, maximum) and superior close-in rejection and attenuation. They are suitable for up to 20 W of average power and 200 W of peak modulated power.

Richardson RFPD Inc.
www.richardsonrfpd.com

Power Divider

VENDORVIEW

The Marki Microwave MPDW-0670CSP2 is an mmWave two-way Wilkinson power divider delivering wideband operation from 6 to 70 GHz. Designed using Marki's innovative, second-generation chip scale packaging, its compact 2.5 × 2.5 mm design enables extreme miniaturization of SMT footprint while providing die-level performance. The MPDW-0670CSP2 is ideal for applications prioritizing low size, weight and power.

RFMW
www.rfmw.com

CABLES & CONNECTORS

Cable Connector

Southwest Microwave's latest SMI product offering is 54070-001B, a direct solder .047 SC flex cable connector with a built-in bullet. It combines the SSBB cable receptacle with the bullet interface, creating a single-pc cable bullet. The frequency range is DC to 67+ GHz. As a standalone connector on a cable, it serves as a manual test probe. It also can be ganged together in a multipin configuration and thereby serve as the heart of the SSBB multipin cable harness.

Southwest Microwave
www.southwestmicrowave.com

AMPLIFIERS

10 GHz, 100 W Amplifier

VENDORVIEW

Exodus AMP2053A-1LC is a rugged solid-state power amplifier incorporating advanced technology for 6 to 10 GHz applications. Class A/AB design for all industry standards, 100 W minimum with 50 dB gain. Excellent power/gain flatness, forward/reflected power monitoring in both dBm and watts, VSWR, voltage, current and temperature sensing for superb reliability and ruggedness. Nominal weight is 45 lbs in a compact 3U chassis, 5.25× 19 × 27 in.

Exodus Advanced Communications
www.exoduscomm.com

Single-Ended RF Amplifier IC

VENDORVIEW

The QPL7425 is a GaAs pHEMT single-ended RF amplifier IC featuring 25 dB of flat gain and low noise. This IC is designed to support HFC and fiber to the home applications from 5 to 1218 MHz using a single supply operating from 3 V to 8 V. QPL7425 offers low noise and distortion plus high gain in a 3×3 QFN package for convenient layout and design in set top and infrastructure projects for 75 Ω CATV and satellite applications.

Qorvo
www.qorvo.com

S-Band Low Noise Amplifier

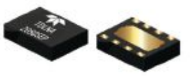

Teledyne e2v HiRel announced the availability of a rad-tolerant S-Band low noise amplifier (LNA), model TDLNA2050SEP, that is ideal for use in demanding high reliability, space and radar applications where low noise figure, minimal power consumption and small package footprint are critical to mission success. This new LNA, developed on a 90 nm enhancement-mode pseudomorphic high electron mobility transistor (pHEMT) process, is available in an 8-pin dual-flat no-lead 2 × 2 × 0.75 mm plastic surface-mount package, and is qualified per MIL-PRF 38534 Class K.

Teledyne e2v HiRel
www.teledynedefenseelectronics.com

SEMICONDUCTORS

Low-Cost RF Module

Sivers Semiconductors AB announced the commercial launch of its state-of-the-art new low-cost RF module BFM02803, covering the 5G frequency range 2 mmWave bands N257, N258 and N261 (from 24.25 to 29.5 GHz). Module BFM02803, presented at the Mobile World Congress 2024, is optimized for high performance, high-power fixed wireless access (FWA) applications and enables differentiation and meet the requirements of large-scale manufacturing of FWA products. It is designed to interface with leading baseband modems.

Sivers Semiconductors AB
www.sivers-semiconductors.com

ANTENNAS

Dual Polarized Antenna

VENDORVIEW

Model SAY-3735135302-22-S1-DP-WR is a dual polarized Cassegrain antenna assembly for Q-Band satellite communication ground stations. With a reflector diameter of 96 in., the antenna includes separate WR-22 ports for left- and right-hand circular polarizations. Typical isolation between ports is 40 dB and the half-power beamwidth is 0.2 degrees. Frequency coverage is 37 to 42 GHz for the receive channel and 46 to 51 GHz for the transmit channel. Integrated bandpass filters are included.

Eravant
www.eravant.com

Gain Horn Antenna Radome Covers

VENDORVIEW

Pasternack, an Infinite Electronics brand, announced the release of its innovative standard gain horn antenna radome covers. Meticulously designed, they protect a wide array of waveguide horn antennas, ensuring optimal functionality and resilience in outdoor settings. The standard gain horn antenna radome covers stand out due to their exceptional features. They are outdoor-rated and weatherproof, crafted to withstand the rigors of external conditions and protect waveguide horns from environmental factors.

Pasternack
www.pasternack.com

TEST & MEASUREMENT

4×4 Butler Matrix

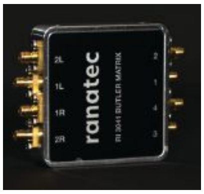

Ranatec announced that it has extended its product portfolio to include the Ranatec RI 3041 4×4 butler matrix. Targeted for testing at frequencies from 2.4 to 8.0 GHz, the next generation butler matrix 4×4 delivers the widest operational bandwidth available on the global market. Addressing the needs of an evolving electronics market, the next generation RI 3041 4×4 provides a compact design that is smaller in size, lighter, larger operating bandwidth, provides increased accuracy and amplitude accuracy, plus lower insertion loss.

Ranatec
www.ranatec.com

Oscilloscopes

SIGLENT unveiled three new series of oscilloscopes designed to improve signal fidelity, visualization and analysis. These latest additions complete Siglent's lineup of oscilloscopes, each equipped with advanced 12-bit analog-to-digital converters and designed for signal quality. With bandwidths ranging from 70 MHz to 4 GHz, Siglent's high-resolution oscilloscopes now provide outstanding signal fidelity for a wide range of applications, including power, EMI, frequency analysis, embedded design and failure analysis.

Siglent
www.siglentna.com

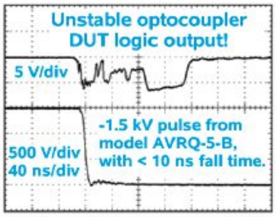

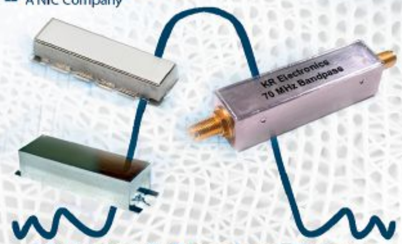

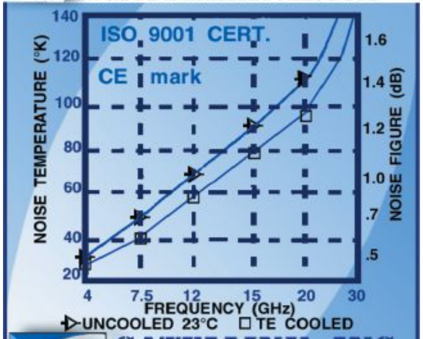

Reviewed by: Katerina Galitskaya

Bookend

Adaptive Radar Detection: Model-Based, Data-Driven and Hybrid Approaches

Angelo Coluccia

Angelo Coluccia's "Adaptive Radar Detection: Model-Based, Data-Driven and Hybrid Approaches" dives deep into radar technology, machine learning and data-driven approaches. This comprehensive work is a great resource for radar professionals and researchers seeking to explore the intersection of traditional radar theory and modern data-driven techniques. The book's strength lies in its ability to seamlessly integrate insights from diverse fields, including radar, statistical signal processing, machine learning and artificial intelligence. This multidisciplinary approach is enhanced by original contributions, diagrams and figures based on experimental data. It serves as both a reference guide and a springboard into the world of adaptive radar detection.

The author starts by laying a solid foundation, offering an insightful overview of radar fundamentals and classical adaptive radar detectors. Readers are guided through classical model-based tools, showcasing their pros and cons. Chapters 2 and 3 introduce essential theoretical elements and algorithmic tools from machine learning, providing engineers in the radar community with a practical understanding of classification problems. Readers are given a reference to popular machine learning algorithms, facilitating the application of data-driven techniques to radar detection. One of the book's highlights is Chapter 4, which delves into hybridization between model-based and data-driven concepts. Techniques for data-driven constant false alarm rate detection are discussed, addressing the challenge of bridging traditional model-based approaches with modern data-driven methods. This chapter brings up the need for robust detectors that can adapt to signal variations and reject unwanted interference.

In conclusion, "Adaptive Radar Detection: Model-Based, Data-Driven and Hybrid Approaches" by Angelo Coluccia is a thoughtfully constructed and comprehensive resource. It blends traditional radar theory with contemporary data-driven approaches, paving the way for a new frontier in radar technology. Whether you are an experienced radar professional or an engineering student seeking to stay abreast of this dynamic field, this book provides a good roadmap to navigate the world of radar detection.

ISBN: 9781630819002
Pages: 350
To order this book contact:
Artech House (2022)
us.artechhouse.com


Microwave Journal
Spring Into Action...
Subscribe/Renew Today!!
mwjournal.com

Advertising**Index**

Sales Representatives

Eastern and Central Time Zones
Carl Sheffres
Group Director
(New England, New York, Eastern Canada)
Tel: (781) 619-1949
Cell: (781) 363-0554
csheffres@horizonhouse.com

Michael Hallman
Associate Publisher
(NJ, Mid-Atlantic, Southeast, Midwest, TX)
Tel: (301) 371-8830
Cell: (781) 363-0338
mhallman@mwjournal.com

Pacific and Mountain Time Zones
Brian Landy
Western Reg. Sales Mgr.
(CA, AZ, OR, WA, ID, NV, UT, NM, CO, WY, MT, ND, SD, NE & Western Canada)
Tel: (831) 426-4143
Cell: (831) 713-9085
blandy@mwjournal.com

Submitting ad material?
Visit: www.adshuttle.com/mwj
(866) 774-5784
outside the U.S. call
+1-414-566-6940

Ed Kiessling
(781) 619-1963
ekiessling@mwjournal.com

International Sales
Richard Vaughan
International Sales Manager
Tel: +44 207 596 8742
rvaughan@horizonhouse.co.uk

Zena Coupé
Tel: + 44 207 1506737
Cell: +44 7887 874074
zena@expomedia.biz

Germany, Austria, and Switzerland (German-speaking)
Brigitte Beranek
Tel: +49 7125 407 31 18
bberanek@horizonhouse.com

France
Gaston Traboulsi
Tel: +44 207 596 8742
gtraboulsi@horizonhouse.com

Korea
Jaeho Chinn
JES MEDIA, INC.
Tel: +82 2 481-3411
corres1@jesmedia.com

China
Shanghai
Linda Li
ACT International
Tel: +86 136 7154 0807
lindal@actintl.com.hk

Wuhan
Phoebe Yin
ACT International
Tel: +86 134 7707 0600
phoebey@actintl.com.hk

Shenzhen
Annie Liu
ACT International
Tel: +135 9024 6961
anniel@actintl.com.hk

Beijing
Cecily Bian
ACT International
Tel: +86 135 5262 1310
cecilyb@actintl.com.hk

Hong Kong
Floyd Chun
ACT International
Tel: +852 28386298
floydc@actintl.com.hk

Taiwan, Singapore
Simon Lee
ACT International
Tel: +852 2838 6298
simonlee@actintl.com.hk

Japan
Katsuhiro Ishii
Ace Media Service Inc.
Tel: +81 3 5691 3335
amskatsu@dream.com

Corporate Headquarters: 685 Canton Street, Norwood, MA 02062 • Tel: (781) 769-9750

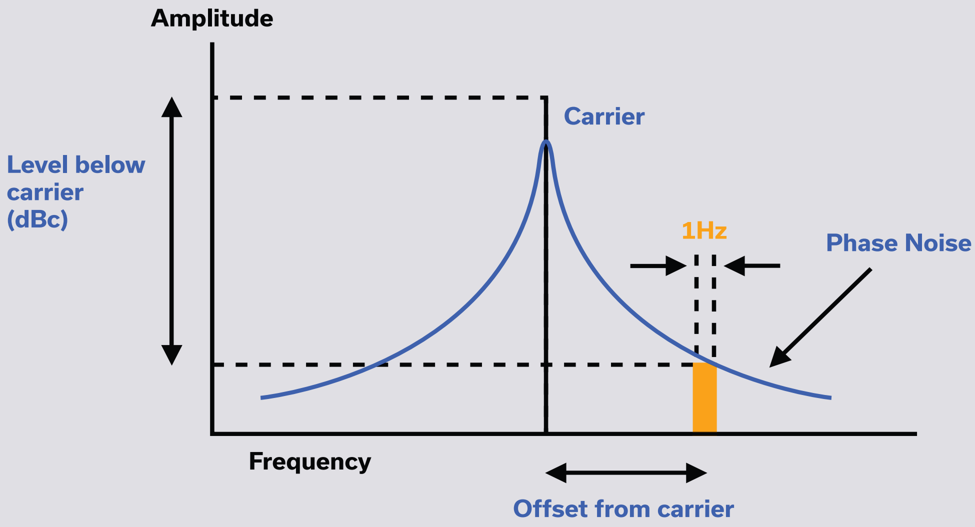

INDUSTRY-LEADING PERFORMANCE

Low Phase Noise Amplifiers

For Sensitive Transceiver Systems

- Additive phase noise as low as -173 dBc/Hz @ 10 kHz Offset
- Ideal for radar, test instrumentation and more
- Wide selection in stock for the most demanding requirements
- State-of-the-art measurement capability in house

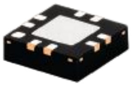

NEW RELEASE

LVA-273PN+

- Wideband, 0.01 to 26.5 GHz
- -172 dBc/Hz additive phase noise @ 10 kHz offset
- +18 dBm P1dB

VIEW PHASE NOISE SPECS

Mini-Circuits®

Nuvotronics: Small Solutions for Big Problems

Nuvotronics was founded in Virginia in 2008. The company origins came from efforts to commercialize PolyStrata®, a new packaging technology that was being funded primarily by DARPA's 3D micro-electrical-RF-systems (3D-MERFS) and disruptive manufacturing technologies (DMT) programs at Rohm and Haas. The business assets and IP surrounding PolyStrata were purchased from Rohm and Haas and these assets became the foundational basis for Nuvotronics. Since its founding in 2008, Nuvotronics has been refining the techniques and expanding the applications of the PolyStrata technology.

PolyStrata is a microfabrication process that allows precision patterned layers of both metals and polymers to be deposited on a flat substrate, resulting in sophisticated miniature devices with features ranging from a few microns to several centimeters. The 3D-MERFS program was focused on developing mmWave phased arrays for satellite communications and the DMT program addressed broadband GaN-based hybrid microwave amplifiers.

The PolyStrata technology is based on integrated circuit manufacturing techniques, so large numbers of devices can be fabricated on a single substrate. As Nuvotronics commercialized and increased volume, they pushed to larger substrates. In 2014, with investment and adoption from customers, the wafer manufacturing capability grew from six-inch to eight-inch substrates and the company moved to its current location in Durham, N.C.

The growth of the manufacturing capabilities continued. In 2019, Nuvotronics was acquired by Cubic Corporation, a leader in edge computing and networking, expeditionary communications and assured datalink solutions. Nuvotronics became the advanced microelectronics group within Cubic and the eight-inch wafer manufacturing line was expanded. In 2021, the company began constructing a 14-inch x 14-inch panel manufacturing line to augment the capacity in response to an increase in demand for components in LEO satellites. The 14-inch panel line became operational at the end of 2023.

As a result of these activities, the Cubic Nuvotronics facility in Durham, N. C., has grown to a 60,000 sq. ft. factory. This facility offers full design, fabrication, assembly and test of circuits and packaged die in one secure location for shorter lead times and greater cost savings. On the existing eight-inch production line, Nuvotronics has a capacity of 500 wafers per year, but the 14-inch panel expansion increases output by 23x. The expectation is that this will accelerate the affordable production of multi-use RF and mmWave packages, components and subsystems.

The advantages of the PolyStrata technology have dramatically expanded the product portfolio. Nuvotronics now touts a wide range of standard and custom passive components, subassemblies and antenna arrays, along with packaging and multi-chip module capabilities to 175 GHz and beyond. These components and capabilities target 5G/6G wireless, space, test and measurement, defense and dual-use applications. Nuvotronics is proud to be a vertically integrated company that can offer new solutions to optimize performance and SWaP-C considerations from design through manufacturing and testing as the company pivots toward standard products. For Nuvotronics, big problems require small solutions.

Nuvotronics
www.cubic.com/nuvotronics


ECO-18
AARONIA AG
ECO 100XA-18
REAL-TIME SPECTRUM ANALYZER
9kHz – 18G
PM
Rx1
Input 50Ω
PEAK +20 dBm
Input 50Ω
+25 dBm / 16 VDC